ANNUAL PROGRESS REPORT

1974

BONE MINERAL LABORATORY

UNIVERSITY OF WISCONSIN

MADISON, WISCONSIN

PROGRESS REPORT

NASA Grant No. Y-NGR-50-002-051

"SKELETAL STATUS AND SOFT TISSUE

COMPOSITION IN ASTRONAUTS"

AND

NASA Grant No. Y-NGR-50-002-183

"TISSUE AND FLUID CHANGES BY

RADIONUCLIDE ABSORPTIOMETRY IN VIVO"

August 1, 1974

John R. Cameron
Richard B. Mazess
Charles R. Wilson

Department of Radiology
University of Wisconsin Medical Center
Madison, Wisconsin 53706

FOREWORD

This progress report is a summary of research on the measurement of bone mineral content and body composition, _in vivo_, at the University of Wisconsin from July 15, 1973 through July 15, 1974. Research support for our laboratories comes from the National Aeronautics and Space Administration through Grant Y-NGR-50-002-051 and Y-NGR-50-002-183 and the University of Wisconsin. The research work represents primarily the efforts of the following: Dr. Mark Mueller, Dr. Everett L. Smith, Robert M. Witt, John M. Sandrik, Kianpour Kianian, William Kan, James Hanson, Mark Madsen, Ralph Mathisen, Howie Gollup, Norbert Pelc, and Clifford E. Vought. We wish to express appreciation for their efforts.

We would like to thank Randie Wealton for her secretarial help in preparing these reports and Stephanie Wurdinger, Kim Smith and Quentin Verdier for assembling these reports. We would also like to thank Orland Canto for the illustrations.

Certain parts of this report represent work in progress which will be continued during the coming year, and work which resulted from previous support through AEC Contract No. AT-(11-1)-1422.

John R. Cameron   Richard B. Mazess   Charles R. Wilson

ANNUAL PROGRESS REPORT ON AEC CONTRACT AT-(11-1)-1422

Table of Contents

BONE MINERAL CONTENT IN NORMAL U.S. WHITES

Richard B. Mazess and John R. Cameron

Department of Radiology (Medical Physics),
University of Wisconsin Hospitals, Madison,
Wisconsin

ABSTRACT

Photon absorptiometry with ^{125}I was used to measure
the bone mineral content and the bone width on 763
children between the ages of 5 and 19 years, on 538
adults between the ages of 20 and 49 years, and on 550
adults over the age of 50 years. Measurements were made
on the midshaft and the distal end of the radius and the
ulna, and on the humerus midshaft. This has permitted
analysis of annual bone growth in children, and the rate
of change in elderly adults per decade.

Male and female children grew at about the same
rate (8% per year) until adolescence. After adolescence
females grew at a slow rate until the mid-twenties, while
males reached adult mineralization by age 20. Males
remained relatively constant until the fifties, and
declined slowly (4% per decade) thereafter. Females
began their decline in the forties, and between age 45
and 75 they lost bone at 10% per decade; after age 75
the loss was reduced to 4% per decade.

Age is really of greatest import in assessing bone
mass only in children and in females between 45 and 75
years; bone and body size is of greater import for
normalization of data for other age-sex groupings.

Key Words: Absorptiometry - Aging - Bone Mineral Content -
Growth - Normal Values.

INTRODUCTION

Since the introduction of single photon absorptiometry a decade ago,
there has been a widespread acceptance of this method of bone mineral
measurement. In order to assess abnormality of bone mineral standards of
normal bone mineral content are needed. There have been some attempts to
provide these standards (Johnston and Goldsmith, 1971; Smith et al., 1972).
The present report provides a compilation of data collected by the University
of Wisconsin Bone Mineral Laboratory.

Over the past five years a large number of apparently normal U.S. white subjects have been measured. The adult sample was derived from several sources: a) hospital or laboratory visitors, b) homes for the elderly, and c) scientific meetings. The children's sample was derived from: a) hospital and laboratory visitors, b) a survey of school age children between ages 6 and 14, and c) a study of little league baseball players between 8 and 19 years of age. None of the subjects had a history of spontaneous fractures, renal disease, or immobilization.

METHODS

Bone mineral content was measured with both digital and direct readout analog systems. Over this period of data collection calibration was routinely checked against ashed bone sections, and various standards; long term precision over this period has been on the order of 1% for standards simulating the forearm bones.

RESULTS

Adults

The heights and weights of the adults by decades are given in Table 1. There was a decrease of stature by about 2 cm per decade in females, and 1 cm per decade in males, after the thirties. This may be a secular trend, but was also no doubt a reflection of vertebral collapse and height loss. The mineral content, bone width, and the mineral-width ratio for the radius shaft, distal radius, ulna, and humerus are given in Tables 2, 3, 4, and 5. In females the bone mineral content and mineral-width ratio were relatively constant through the thirties and into the early forties. This was followed by a period of relatively rapid bone loss between the mid-forties and mid-seventies, with a somewhat slower decrease thereafter. In males the bone mineral content and mineral-width ratio stayed relatively constant through the fifties with bone loss progressing from the sixties on. In both sexes the bone widths did not change with age appreciably; the apparent decrease of the bone width of the distal radius in later life may actually be an artifact of the edge criterion used to start and stop a scan. The distal radius width is critically dependent on the edge criterion, especially in the elderly. An 85% edge criterion, rather than the usual 70% edge, should probably be used for ^{125}I scans of the distal radius in demineralized subjects.

| | | HEIGHT (cm) | | | WEIGHT (kg) | | |
AGE GROUP	N	X̄	SD	CV	X̄	SD	CV
MALES							
20-29*	102	178.9	7.6	4.2	76.3	11.3	14.8
30-39+	117	179.6	7.1	4.0	79.8	12.4	15.5
40-49+	117	177.0	8.4	4.7	78.8	10.5	13.3
50-59+	46	177.5	6.0	3.4	79.5	8.2	10.3
60-69*	40	175.2	8.8	5.0	75.9	15.5	20.4
70-79*	50	174.8	8.0	4.6	74.1	12.6	17.1
80-89*	3	163.4	2.9	1.8	61.5	5.9	9.6
FEMALES							
20-39*	123	163.6	6.6	4.0	58.1	10.4	17.9
30-39*	29	164.9	6.4	3.9	65.2	10.6	16.2
40-49*	42	160.3	8.3	5.2	63.8	10.6	16.6
50-59*	60	161.0	5.6	3.5	63.8	11.9	18.6
60-69*	78	159.1	6.9	4.3	62.8	11.3	18.0
70-79*	100	158.2	6.9	4.4	62.6	11.3	18.0
80-89*	74	155.4	7.4	4.8	56.8	9.4	16.6
90-99*	16	152.7	8.4	5.5	55.4	10.3	18.6

SOURCES: * from mid-radius data
+ from humerus data

Table 1: Heights and weights of adult male and female groups by decades.

| AGE GROUP | N | AGE | MINERAL(mg/cm) | | | WIDTH(mm x10⁻⁵) | | | MINERAL/WIDTH | | |
			X̄	SD	CV	X̄	SD	CV	X̄	SD	CV
MALES											
20-29	105	24.6	1307	173	13.2	1476	144	9.7	.825	.078	8.8
30-39	72	34.0	1322	138	10.5	1479	125	8.5	.895	.070	7.6
40-49	64	44.2	1304	146	11.2	1485	147	9.9	.880	.077	8.7
50-59	31	54.7	1313	159	12.1	1489	116	7.8	.880	.064	7.3
60-69	46	64.1	1226	229	18.7	1569	297	18.9	.790	.122	15.4
70-79	22	74.2	1256	188	15.0	1553	148	9.5	.811	.110	13.6
80-89	16	84.1	1182	219	18.5	1577	177	11.2	.751	.110	14.6
FEMALES											
20-29	126	22.0	952	108	11.3	1230	109	8.8	.774	.055	7.1
30-39	29	33.7	1000	121	12.1	1304	156	12.0	.769	.064	8.3
40-49	42	44.4	977	95	9.7	1298	240	18.6	.763	.074	9.8
50-59	63	55.0	885	136	15.3	1252	119	9.5	.706	.078	11.0
60-69	93	64.6	769	142	18.5	1259	125	9.9	.610	.086	14.1
70-79	134	72.2	722	126	17.4	1255	112	8.9	.575	.085	14.7
80-89	121	83.8	681	143	21.1	1271	156	12.2	.538	.104	19.5
90-99	29	92.2	675	129	19.2	1295	112	8.6	.521	.084	16.2

Table 2: Absorptiometric measurements on the distal third of the radius shaft in adult males and females by decades.

AGE GROUP	N	AGE	MINERAL (mg/cm)			WIDTH (mx10^{-5})			MINERAL/WIDTH		
			$\bar{X}$	SD	CV	$\bar{X}$	SD	CV	$\bar{X}$	SD	CV
MALES											
20-29	27	24.3	1386	204	14.7	2342	413	17.6	.600	.079	13.3
30-39	19	33.8	1317	186	14.1	2283	364	15.9	.588	.106	18.0
40-49	12	43.8	1298	154	11.9	2162	339	15.7	.608	.076	12.5
50-59	10	55.5	1330	177	13.3	2201	352	16.0	.614	.108	17.7
60-69	30	64.9	1191	288	24.2	2362	435	18.4	.516	.134	26.0
70-79	14	74.3	1187	279	23.5	2330	550	23.6	.536	.183	34.1
80-89	14	84.5	1134	282	24.9	1989	456	22.9	.578	.116	20.1
FEMALES											
20-29	54	23.2	984	126	12.8	1857	267	14.4	.539	.092	17.0
30-39	6	32.7	955	84	8.8	1635	195	12.0	.564	.091	16.2
40-49	11	45.9	933	174	18.7	1953	462	23.6	.494	.114	23.0
50-59	37	55.5	886	146	16.5	1855	255	13.7	.482	.080	16.7
60-69	71	64.6	742	116	15.7	1902	364	19.1	.402	.088	21.9
70-79	96	75.1	718	175	24.4	1820	316	17.4	.402	.103	25.6
80-89	87	83.7	645	144	22.4	1724	370	21.5	.388	.111	28.6
90-99	18	92.5	668	173	25.9	1775	343	19.3	.392	.127	32.5

Table 3: Absorptiometric measurements on the distal radius in adult males and females by decades.

MIDSHAFT ULNA

AGE GROUP	N	AGE	MINERAL (mg/cm)			WIDTH (mx10^{-5})			MINERAL/WIDTH		
			$\bar{X}$	SD	CV	$\bar{X}$	SD	CV	$\bar{X}$	SD	CV
FEMALES											
20-29	22	23.2	843	121	14.3	1074	179	16.7	.791	.094	11.8
30-49	6	39.7	868	95	11.0	1108	138	12.5	.794	.135	17.0
50-59	18	54.9	804	126	15.7	1105	131	11.8	.728	.078	10.8
60-69	24	63.8	702	106	15.1	1109	119	10.7	.625	.093	14.9
70-79	38	75.4	615	121	19.6	1103	108	9.8	.562	.120	21.4
80-89	30	83.7	590	116	19.7	1130	128	11.3	.525	.105	20.1
90-99	7	92.7	560	86	15.4	1126	115	10.2	.499	.069	13.8

DISTAL ULNA

AGE GROUP	N	AGE	MINERAL (mg/cm)			WIDTH (mx10^{-5})			MINERAL/WIDTH		
			$\bar{X}$	SD	CV	$\bar{X}$	SD	CV	$\bar{X}$	SD	CV
FEMALES											
20-29	20	23.2	511	154	30.0	999	183	18.3	.511	.112	22.0
30-49	6	39.7	510	86	16.9	1013	141	13.9	.513	.114	22.3
50-59	17	55.1	452	89	19.7	971	134	13.8	.469	.086	18.3
60-69	22	64.0	364	60	16.4	1000	127	12.7	.366	.059	16.1
70-79	38	75.4	330	96	29.1	1038	134	12.9	.318	.090	28.4
80-89	29	83.7	303	78	25.8	1026	116	11.4	.296	.068	23.1
90-99	7	92.7	287	113	39.4	1029	102	9.9	.274	.082	29.9

Table 4: Absorptiometric measurements on the shaft and on the distal end of the ulna in adult females by decades. (Only a few males in each of the decade groups were measured.)

AGE GROUP	N	AGE	MINERAL (mg/cm)			WIDTH (mx10^{-5})			MINERAL/WIDTH		
			$\bar{X}$	SD	CV	$\bar{X}$	SD	CV	$\bar{X}$	SD	CV
MALES											
20-29	100	25.9	2766	333	12.0	2305	215	9.3	1.200	.093	7.7
30-39	118	34.6	2732	383	14.0	2300	226	9.8	1.188	.113	9.5
40-49	118	44.3	2731	340	12.5	2315	198	8.5	1.181	.114	9.6
50-59	49	54.6	2779	335	12.1	2343	183	7.8	1.189	.137	11.5
60-69	28	63.6	2579	408	15.8	2300	193	8.4	1.122	.157	14.0
70-79	16	74.4	2622	415	15.8	2348	135	5.7	1.114	.143	12.8
80-89	18	85.6	2287	456	20.0	2337	181	7.8	.980	.186	18.9
FEMALES											
20-29	31	23.0	2098	243	11.6	1987	176	8.8	1.056	.079	7.5
30-39	11	34.7	2117	260	12.3	1969	169	8.6	1.074	.074	6.9
40-49	19	42.7	2081	240	11.5	2013	132	6.6	1.033	.089	8.6
50-59	12	55.6	1811	307	17.0	1940	219	11.3	.943	.183	19.4
60-69	22	65.9	1539	464	30.2	2070	521	25.2	.748	.160	21.4
70-79	47	74.8	1384	300	21.7	1964	207	10.6	.707	.140	19.8
80-89	39	84.1	1296	211	16.3	2012	168	8.3	.644	.089	13.8
90-99	10	92.5	1271	227	17.9	2000	168	8.4	.639	.116	18.1

Table 5:   Absorptiometric measurements on the midshaft of the humerus in adult males and females by decades.

The coefficients of variation differed with age and measurement site. Relatively high mineral variation was evident for the distal radius and ulna; in the younger adults it was 15 to 20% while the variation in older adults was even larger (20 to 30%). This variation may reflect the difficulties of measuring the distal bone sites, rather than a real biological pattern. The variation was not reduced by using the mineral-width ratio. At the other measurement sites the variation was only 10 to 15% for younger adults and 15 to 20% for the elderly groups; in general the variation of the mineral-width ratio was a few percent lower than that of the mineral content itself.

Children

The heights and weights of the children are given in Table 6; the Wisconsin children were somewhat taller and heavier than those examined by others (McCammon, 1970). Skeletal ages of a sub-sample of these children were entirely normal (Mazess and Cameron, 1971). The bone mineral, width, and mineral-width ratio for the midshaft of the radius, ulna and humerus are given in Tables 7, 8, and 9. There was insufficient data on the distal ulna and radius in children to warrant compilation.

Table 6

AGE GROUP	N	HEIGHT (cm)			WEIGHT (kg)		
		X	SD	CV	X	SD	CV
MALES							
6*	15	121.1	5.0	4.2	23.0	2.6	11.2
7*	27	127.8	5.2	4.0	25.9	3.9	14.9
8*	39	135.5	6.2	4.6	29.2	5.5	18.9
9+	42	140.3	6.3	4.5	33.0	6.3	19.0
10*	50	144.2	5.9	4.1	35.4	7.1	20.0
11+	44	149.2	6.4	4.3	38.3	5.9	15.3
12*	37	154.5	7.7	5.0	44.8	8.4	18.8
13*	35	158.8	9.6	6.0	47.4	9.8	20.6
14*	35	168.9	6.0	3.6	58.5	6.7	11.6
15*	43	175.2	7.2	4.1	66.5	10.8	16.2
16*	36	176.3	7.3	4.1	68.3	7.4	10.8
17*	39	179.4	6.2	3.5	73.6	9.5	12.9
18*	31	180.6	6.1	3.4	77.4	10.0	12.9
19*	19	181.3	8.9	4.9	79.4	10.3	12.9
FEMALES							
6*	14	123.6	6.3	5.1	22.9	3.8	16.7
7+	20	128.9	6.2	4.8	25.3	3.9	15.4
8*	18	134.5	9.0	6.7	27.2	4.4	16.0
9*	20	137.7	7.5	5.5	31.3	6.4	20.3
10*	24	143.0	6.2	4.3	34.0	6.3	18.6
11*	20	150.4	5.9	3.9	41.0	9.5	23.1
12*	15	160.4	7.7	4.8	45.5	8.2	18.0
13*	18	160.9	5.6	3.5	46.5	7.7	16.5
14*	28	165.2	8.2	5.0	52.9	7.7	14.6
15*	25	165.7	6.6	4.0	55.7	5.9	10.6
16*	13	167.8	5.3	3.2	56.7	6.7	11.9
17*	22	167.9	6.5	3.8	55.9	6.9	12.3
18*	16	164.3	7.3	4.4	58.6	8.6	14.7
19*	32	164.2	8.6	5.3	60.0	10.3	17.2

SOURCES: * from midshaft radius data
+ from humerus data

Table 6: Heights and weights of male and female children by year.

Table 7

AGE GROUP	N	MINERAL (mg/cm)			WIDTH $(mx10^{-5})$			MINERAL/WIDTH		
		X	SD	CV	X	SD	CV	X	SD	CV
MALES										
6	16	472	59	12.4	954	97	10.1	.495	.040	8.0
7	27	509	73	14.3	1000	87	8.7	.508	.042	8.2
8	38	565	71	12.6	1033	89	8.6	.546	.042	7.6
9	39	592	70	11.8	1059	95	9.0	.559	.044	7.9
10	52	640	78	12.2	1112	98	8.8	.577	.062	10.8
11	43	702	107	15.3	1146	119	10.4	.610	.051	8.4
12	39	746	95	12.8	1200	103	8.5	.620	.050	8.1
13	39	813	112	13.8	1268	115	9.1	.640	.049	7.7
14	35	898	126	14.1	1301	101	7.8	.688	.065	9.5
15	43	1048	146	10.3	1420	146	10.3	.738	.064	8.7
16	36	1154	143	12.4	1468	146	9.9	.787	.064	8.1
17	39	1196	130	10.9	1447	99	6.8	.826	.068	8.3
18	31	1247	116	9.3	1480	123	8.3	.843	.051	6.0
19	19	1296	187	14.4	1542	256	16.6	.845	.073	8.6
FEMALES										
6	14	434	79	8.2	911	115	12.6	.474	.044	9.3
7	20	452	63	13.8	912	90	9.8	.497	.141	10.2
8	18	485	66	13.6	924	96	10.4	.525	.049	9.4
9	20	548	70	12.7	972	104	10.8	.564	.125	7.1
10	24	564	93	16.5	999	106	10.6	.563	.163	9.2
11	22	653	125	19.1	1074	106	9.9	.607	.194	15.5
12	15	745	114	15.4	1145	163	14.3	.655	.150	12.2
13	18	738	93	12.6	1144	121	10.6	.646	.128	7.6
14	28	844	112	13.3	1185	119	10.1	.710	.138	5.4
15	25	869	76	8.7	1191	86	7.2	.730	.089	6.2
16	13	882	86	9.8	1214	85	7.0	.727	.101	7.7
17	22	893	99	11.0	1223	89	7.3	.730	.108	7.1
18	16	911	134	14.7	1214	138	11.4	.749	.153	8.4
19	32	937	107	11.4	1228	121	9.8	.764	.115	7.0

Table 7: Absorptiometric measurements the distal third of the radius shaft in male and female children by year.

Table 8

AGE GROUP	N	MINERAL (mg/cm)			WIDTH(mmx10⁻⁵)			MINERAL/WIDTH		
		X	SD	CV	X	SD	CV	X	SD	CV
MALES										
6	4	355	30	8.5	830	50	6.0	.428	.037	8.7
7	14	418	56	13.5	864	109	12.6	.485	.043	8.9
8	26	474	51	10.7	941	51	10.7	.506	.051	10.0
9	29	480	66	13.8	921	86	9.4	.521	.055	10.6
10	30	532	59	11.1	938	66	7.0	.567	.056	9.8
11	29	578	66	11.4	986	82	8.3	.587	.058	9.9
12	24	588	48	8.1	992	55	5.6	.593	.043	7.2
13	20	670	77	11.5	1022	65	6.4	.655	.055	8.3
14	17	746	106	14.2	1107	77	6.9	.672	.065	9.6
15	18	879	127	14.4	1174	90	7.7	.748	.085	11.4
16	17	959	102	10.7	1229	92	7.5	.782	.080	10.3
17	18	978	196	20.0	1257	158	12.6	.790	.176	22.3
18	15	1024	183	17.9	1269	100	7.9	.810	.149	18.3
19	15	1111	147	13.3	1255	103	8.2	.888	.115	12.9
FEMALES										
6	5	354	57	16.0	760	54	7.1	.466	.070	15.0
7	12	374	52	13.8	818	73	8.9	.459	.056	12.3
8	8	413	70	16.9	879	82	9.4	.472	.082	17.4
9	8	481	43	9.0	841	108	12.9	.575	.040	6.9
10	14	473	76	16.0	865	108	12.5	.546	.052	9.5
11	11	540	141	26.1	964	112	11.7	.551	.088	16.0

Table 8: Absorptiometric measurements on the distal third of the ulna shaft in male and female children by year. (Only a few females above age 11 have been scanned.)

Table 9

AGE GROUP	N	MINERAL(mg/cm)			WIDTH(mmx10⁻⁵)			MINERAL/WIDTH		
		X	SD	CV	X	SD	CV	X	SD	CV
MALES										
6	14	1009	128	12.7	1421	172	12.1	.712	.055	7.8
7	27	1112	168	15.1	1472	212	14.4	.757	.055	7.3
8	39	1268	137	10.8	1574	155	9.9	.806	.051	6.3
9	42	1311	155	11.8	1608	137	8.5	.817	.086	10.5
10	47	1470	178	12.1	1719	151	8.8	.855	.071	8.2
11	44	1531	198	12.9	1772	157	8.9	.863	.073	8.4
12	37	1684	191	11.4	1877	148	7.9	.897	.066	7.4
13	34	1786	264	14.8	1906	176	9.2	.936	.102	10.9
14	28	2070	312	15.1	2040	156	7.7	1.012	.110	10.9
15	45	2311	299	12.9	2148	149	6.9	1.074	.106	9.8
16	30	2672	400	15.0	2273	182	8.0	1.172	.120	10.2
17	35	2754	372	13.5	2212	173	7.8	1.242	.113	9.1
18	30	2948	363	12.3	2314	160	6.9	1.272	.118	9.3
19	16	3161	258	8.2	2430	156	6.4	1.301	.077	5.9
FEMALES										
6	11	943	107	11.4	1350	179	13.2	.702	.069	9.9
7	20	1004	121	12.0	1442	119	8.3	.695	.042	6.1
8	15	1125	165	14.6	1494	141	9.4	.751	.062	8.3
9	22	1215	137	11.3	1581	149	9.4	.769	.059	7.6
10	24	1181	203	17.2	1548	164	10.6	.760	.095	12.5
11	20	1368	247	18.0	1662	174	10.5	.820	.095	11.6
12	13	1533	238	15.5	1738	199	11.4	.881	.079	8.9
13	15	1661	280	16.9	1841	187	10.2	.900	.094	10.4
14	14	1818	154	8.5	1885	93	4.9	.964	.061	6.3
15	24	1896	174	9.2	1861	118	6.3	1.019	.074	7.3
16	10	1898	164	8.6	1908	176	9.2	.998	.081	8.1
17	18	1948	265	13.6	1877	151	8.0	1.037	.098	9.4
18	6	2102	292	13.9	1902	169	8.9	1.107	.140	12.6
19	3	1940	236	12.2	1870	87	4.7	1.036	.093	9.0

Table 9: Absorptiometric measurements on the midshaft of the humerus in male and female children by year.

Prior to the adolescent growth spurt there appears to be a similar rate of growth (about 8% annually) for the radius, ulna and humerus in both boys and girls. From ages 13 to 16 boys grow at about 13% annually, and from 17 to 20 years the growth is about 4% annually. Females have an earlier growth spurt; from ages 11 to 14 they grow at about 11% annually, but only at 1 to 2% annually thereafter til age 20. The changes of bone width are of lesser magnitude and there is a less well-defined growth spurt, at least in this cross-sectional data. Boys and girls increase width by about 4% annually until adolescence; from adolescence to adulthood boys increase width at about 2% annually and girls at about 1% annually.

The pattern of mineral-width ratio changes was somewhat similar to the above. This ratio changed by about 4% annually prior to adolescence in both sexes; this growth rate doubled during peak adolescent growth. Post-adolescent changes amounted to about 2 to 3% annually in males and 1 to 2% in females.

The coefficients of variation for each age-sex group amounted to about 10 to 15% for bone mineral, 8 to 12% for bone width, and about 10% for the mineral-width ratio. In general the use of the mineral-width ratio decreased the variation indicating that the variation in bone mineral at each age was a reflection of bone size differences. This reduced variation, however, does not make this ratio a more sensitive indicator than the bone mineral itself. Bone mineral content during this period of growth doubles in females and almost triples in males. In contrast the mineral-width ratio changes are only half as large. As a consequence the signal (age change) to noise (variation) ratio is greater for the mineral content than for the mineral-width ratio.

DISCUSSION AND CONCLUSIONS

Adults

A decrease of the amount of bone with age has been demonstrated using both direct and indirect methods for many populations (Barzel, 1970). The extent and magnitude of the bone loss, the age at which loss begins, and the nature of sex differences have not been defined with exactitude. Indirect methods, such as radiographic photodensitometry or measurement of compact bone area, are inaccurate indicators of the amount of bone and are subject to large systematic, as well as random, errors. Hence the great majority of results on age trends of bone loss, which have been obtained with these methods are in question. For example Dequeker (1972) examined populations in the Netherlands, Nigeria and Belgium and found that women lost 5.7% and men 3.1% per decade of their compact bone between the ages of 40 and 80 years. The same rate of loss was found in iliac crest biopsies. Garn et al. (1967) showed that in U.S. white and negro and in Central American populations the rate of loss was similar and amounted to about 3% per decade for males and 8% per decade for females. However, this referred to changes of compact bone thickness, rather than area. Changes in the latter, which are more directly related to the amount of bone, were about 2.8% per decade in males and 6.3% per decade in females (Garn, 1970, p. 64). The present results showed a decrease over the 4 decades from 40 to 80 years which was relatively constant for different sites and different bones amounting to about 8.6% per

decade in females and 3.2% per decade in males. However, our data showed that the onset of bone loss was different in males and females, and that there were two phases to the rate of bone loss in females. Females lost bone rapidly (about 9.5% per decade between the ages of 45 and 75) and more slowly (4.4% per decade) thereafter. Males did not lose bone until after the fifties, with a loss between 55 and 85 years amounting to about 4.7% per decade.

The plateau of bone mineral loss in the very old females may represent two somewhat distinct phenomena. First, there may be a selection process in which women with bone mineral values lower than those seen in the elderly groups either die, or are not included in the sample because of fractures. Interestingly the level of this plateau in bone loss was about equal to the discriminant value between fracture and non-fracture groups in women (Smith and Cameron, 1973). Secondly, there may actually be two distinct phases to bone loss, with a more rapid loss in the post-menopausal decades, and a slower loss, analagous to that evident in elderly males, in subsequent decades. Such a two-component analysis indicated that females lose bone by about 10 to 15% per decade due to a rapid process between 45 and 70 years, and at about 4% per decade after age 50 by a slower process.

Comparable data on the patterns of aging bone loss are not available. Johnston and Goldsmith (1971) surveyed large samples of white, negro and oriental populations in California using photon absorptiometry on the distal radius. However, the sample sizes above age 60 were very small. Their data on white males and females up to age 80 does support the present findings. The data of Johnston _et al._ (1968) and Smith _et al._ (1972) are even more limited, and do not allow conclusions.

Children

A number of investigators have attempted to examine skeletal growth, but in general the methods used have limited precision, accuracy and sensitivity (Mazess and Cameron, 1971, 1972). Bone lengths give only linear growth, and bone widths give only an approximation of appositional changes. Garn (1970) summarized extensive findings on compact bone thickness and area; he also found that appositional growth ended at about age 15 in females and at 20 years in males. The rate of pre-adolescent bone growth seems to be somewhat over estimated by compact bone measures, and the extent of sexual dimorphism appeared inaccurate, especially toward the end of growth. Compact bone area, despite its numerous shortcomings, does indicate about the same magnitude of bone increase during growth from 6 to 18 years as does photon absorptiometry, that is, about 260% in males and 215% in females. The magnitude of changes in actual skeletal weight is somewhat larger than this, about 400% in males and 330% in females (Trotter and Peterson, 1970). The difference is due to the linear element of skeletal growth which can be measured by height or bone length changes, and which is about half the magnitude of the appositional bone growth.

ACKNOWLEDGEMENTS

REFERENCES

Barzell, U.S. (ed) 1970. Osteoporosis. Grune and Stratton, New York.

Dequeker, J. 1972. Bone Loss in Normal and Pathological Conditions. Leuven University Press, Belgium.

Garn, S.M. 1970. The Earlier Gain and the Later Loss of Cortical Bone. C.C. Thomas, Springfield.

Garn, S.M., C.G. Rohmann and B. Wagner 1967. Bone loss as a general phenomenon in man. Fed. Proc. 25: 1729-1736.

Johnston, C.C., D.M. Smith, P.L. Yu and W.P. Deiss, Jr. 1968. In vivo measurement of bone mass in the radius. Metabolism 17: 1140-1153.

Johnston, J.O. and N.F. Goldsmith 1971. The Osteoporosis Prevalence Survey conducted at the Multiphasic Clinic of Kaiser Foundation Hospital. Final Report on USPHS Contract PH 86-68-181.

Mazess, R.B. and J.R. Cameron 1971. Skeletal growth in school children: maturation and bone mass. Am. J. Phys. Anthrop. 35: 399-408.

Mazess, R.B. and J.R. Cameron 1972. Growth of bone in school children: comparison of radiographic morphometry and photon absorptiometry. Growth 36: 77-92.

McCammon, R.W. 1970. Human Growth and Development. C.C. Thomas, Springfield.

Smith, D.M., C.C. Johnston and P.L. Yu 1972. In vivo measurement of bone mass. J.A.M.A. 219: 325-329.

Smith, E. and J.R. Cameron (submitted for publication). Interpretation of fracture index charts.

Trotter, M. and R.R. Peterson 1970. Weight of the skeleton during post-natal development. Am. J. Phys. Anthrop. 33: 313-324.

****

DISCUSSION

B.L. Riggs: If age related bone loss in females includes a subgroup who are losing bone faster than others (i.e. who will become osteoporotics), then the population variance should increase with age. Does it?

R.B. Mazess: The coefficient of variation increases above age 50 in both males and females, but this is due in part to declining bone mineral. There is actually only a slight increase of absolute variance in elderly females and a somewhat larger increase in elderly males. The data do not support the notion of a female population consisting of two subgroups, one of which loses bone and the other which does not.

A.M. Parfitt: (Comment) A recent controlled prospective study from Scotland has confirmed the several uncontrolled prospective studies that estrogen replacement from the time of the menopause prevents part of the bone loss. This agrees with your finding of two components of involutional bone loss in women and the data together suggest that one component is common to both sexes, and the second component in women is due to estrogen lack.

PREDICTION OF FEMORAL NECK AND SPINE BONE MINERAL
CONTENT FROM THE BMC OF THE RADIUS OR ULNA AND
THE RELATIONSHIP BETWEEN BONE STRENGTH AND BMC

Charles R. Wilson

Department of Radiology (Medical Physics), University
of Wisconsin Hospitals, Madison, Wisconsin

ABSTRACT

The bone mineral content (BMC) is extensively used
to provide information about the status of entire skeleton.
Changes in BMC are employed to evaluate the effect of
various drugs, both beneficial and detrimental, disease
states, weightlessness, exercise, renal dialysis and others
on the skeleton. This report discusses more specific
clinical and functional information that may be derived
from the BMC of a limited region of the skeleton. In
particular there is a fairly high degree of correlation
between the BMC of the radius or ulna and that of the
femoral neck, r about 0.85 and a somewhat lower rela-
tionship between the BMC of the radius or ulna and the
thoracic vertebrae, r about 0.65. Also the BMC is highly
related to the strength of bone at that scan site.

Key Words: Absorptiometry - Bone Mineral Content - Bone
Strength - Femoral Neck - Osteoporosis - Spine.

INTRODUCTION

The physiologic information provided by the measurement of the bone
mineral content (BMC) of the arm has been under extensive investigation
during the past ten years (Whedon and Cameron, 1968; Cameron 1970). Studies of
the BMC in relation to exercise, weightlessness, diagnosis and treatment of
osteoporosis, renal disease, arthritis, and other factors have been performed.
The interpretation of these studies is based on the generally accepted hypothesis
that the BMC of a single site provides information concerning the status of the
entire skeleton (Mazess, 1968; Horsman et al., 1970; Chestnut et al., 1973;
Cohn et al., in press). This report focuses on more specific clinical and
functional information that may be derived from the BMC of a limited region
of the skeleton. In particular the report examines: A) the relationship of
the BMC of the radius or ulna to the BMC of the femoral neck or spine, and
B) the relationship between the BMC at a particular site and the strength
of bone tissue at that site. With regard to the first (A), the BMC of scan
sites on the radius or ulna are highly interrelated and to a lesser degree to
the BMC at sites on other bones (Mazess, 1968). Since the strength of the

femoral neck or spine are highly related to the amount of bone present (Vose et al., 1961; Bartley et al., 1966) if the BMC of the radius or ulna can provide a quantitative estimate of the BMC of the femoral neck or spine it would therefore provide an estimate of the strength of these areas and possibly the risk of spontaneous fracture. With regard to the second (B), compact bone is a porous material with vascular channels and resorption spaces running throughout the bone. There is a negative correlation between the mechanical strength and the porosity of bone (Evan, 1958; Currey 1959). For a given size specimen of bone the maximum load is closely related to the actual area occupied by bone - the strength decreases as the number or the area of the pores in the specimen increases. Since the BMC is independent of the distribution of bone in the scan path the BMC is directly proportional to the area occupied by the bone and therefore should provide a better estimate of the strength than the total area of the specimen. These two hypotheses were investigated. The results of the investigations of the feasibility of quantitatively estimating the BMC of the femoral neck and spine from the BMC at a site on the radius or ulna have been published elsewhere (Wilson, submitted for publication) and only a summary of this study will be presented here.

METHODS

Relationship Between the BMC of the Radius and Ulna and that of the Femoral Neck and Spine

The BMC at sites on the radius, ulna, femoral neck and the thoracic vertebrae of twenty-four skeletons were measured using the photon absorptiometric technique (Cameron and Sorenson, 1963). The bones scanned were obtained from cadavers used in a gross anatomy course through the courtesy of the University of Wisconsin Department of Anatomy. The skeletons, 7 females and 17 males, ranged in age from 35 to 89 years. No data were available on medical history, race, length of bed confinement prior to death or cause of death.

Before scanning most of the soft tissue was removed from the bones. They were scanned in a uniform thickness of water and BMC was expressed in grams of bone mineral per centimeter. Dissection of soft tissue from the bones does not affect the accuracy of the measurement of BMC (Cameron et al., 1968). The radii and ulnae were scanned at sites corresponding to 25, 33, 50 and 75% of the total length measured from the distal end. The sites were called distal (D), distal third (DT), midshaft (M), and proximal (P), respectively. The coefficent of variation for a set of four or five scans was typically 1 to 2%. The BMC of the femoral neck was measured at the narrowest portion of the neck. To reduce the effect of anatomical variation on the BMC several sets of four or five scans were made with the femoral neck repositioned between each set. The coefficient of variation in the BMC of the four or five scans in a set was about 1% and the coefficient of variation in the mean BMC of the femoral neck was about 5%. The BMC of the individual thoracic vertebrae was obtained by scanning each vertebrae in the coronal plane through the maximum width. Correlation coefficients among the BMC's of the various sites and linear least square regression equations were calculated to evaluate the accuracy of estimating the mass of bone mineral in the femoral neck and spine from the BMC of the radius or ulna, and age.

Relationship Between BMC and Bone Strength

The compressive tests of compact bone specimens were performed on a Universal Testing Machine, Model TM6, MB Electronics Company, at the University of Wisconsin Department of Engineering Mechanics. The bone specimens used in this test were machined hollow cylinders from the left femoral midshaft from each of the 24 skeletons. Test results for only 17 specimens were obtained as some specimens were either destroyed during machining or the load versus elongation curve was not valid. The axis of the cylinder was parallel to the long axis of the bone. The specimens were about 1.5 cm long with an outside diameter of about 2.5 cm and a wall thickness of between 0.12 to 0.45 cm. The specimens were progressively loaded in compression until failure. A constant rate of deformation, 0.002 inches per second – essentially static – was used to avoid variations due to the viscoelastic response of bone to mechanical loads (McElhaney, 1966; Burstein and Frankel, 1968). Prior to the compressive tests the machined cylinders were scanned in water to determine their BMC and their physical dimensions were measured. The cross-sectional area of the specimen was calculated from its dimensions.

RESULTS

Relationship Between the BMC of the Radius and Ulna and that of the Femoral Neck and Spine

There was a high degree of correlation among the BMC's of sites on the same bone, $r \geq 0.95$, and among sites on different long bones, $r \geq 0.85$. This indicates systematic interrelationships between sites and minimizes the relative value of multiple variable regression formulae involving the BMC at two or more sites on the radius or ulna to predict the BMC of either the femoral neck or spine. The correlation coefficients between the sites usually measured clinically, i.e. the D and DT sites on the radius and the femoral neck were 0.84 and 0.86, respectively. While these were the highest they are representative of the coefficients between the other sites on the radius and ulna, and the femoral neck. For the most part the differences between the magnitudes of the coefficients among sites on the radius and ulna, and the femoral neck and spine were only slightly significant. The accuracy in estimating the femoral neck BMC from the BMC of either site was about the same. The percent standard error of estimate was about 16% in both cases. There was no statistically significant increase in predictability for the multiple variable regression equation using the BMC of the radius and age.

The associations between the BMC of the radius or the ulna and the BMC of the thoracic vertebrae were somewhat lower than those with the BMC of the femoral neck; r was typically about 0.60 to 0.7. There was no statistically significant difference in estimating the vertebral BMC from sites on either the radius or ulna. The vertebral BMC could be estimated from the BMC of a site on the radius and age with a percent standard error of estimate of about 17%.

Relationship Between BMC and Bone Strength

Compact bone is a porous material with vascular channels and resorption spaces running throughout the bone. As expected, for a given size bone specimen there is a negative correlation between the area of number of pores in the specimen and the strength of the bone in the specimen (Chestnut et al., 1973; Vose et al., 1961). Models in which bone is taken to be a "porous block" have been devised which describe the relationship between the micro-structure of bone and its mechanical properties (McElhaney et al., 1970; Stech, 1966). The basic assumption in these models is that the strength of the bone between the pore or voids is constant and that any differences in load bearing capacity among different bone specimens are due to differences in the amount of the specimen occupied by voids. The maximum load that a bone can bear is proportional to the actual area of its cross-section occupied by bone tissue. Figure 1 illustrates the porous bone model. In this model it is assumed: 1) the cylindrical voids are predominantly oriented parallel to the long axis of the bone; 2) they are randomly distributed along the long axis, so that the area voids at any level is approximately constant, i.e. on the average as many voids start as stop in a thin slab, ΔZ, through the bone. Then, for a compressive load applied in the z direction the maximum load, L_m, is

$$L_m = S_o \cdot A_B \tag{1}$$

where S_o is the ultimate strength of the bone tissue and A_B is the area occupied by bone, $A_B = A_T - A_V$.
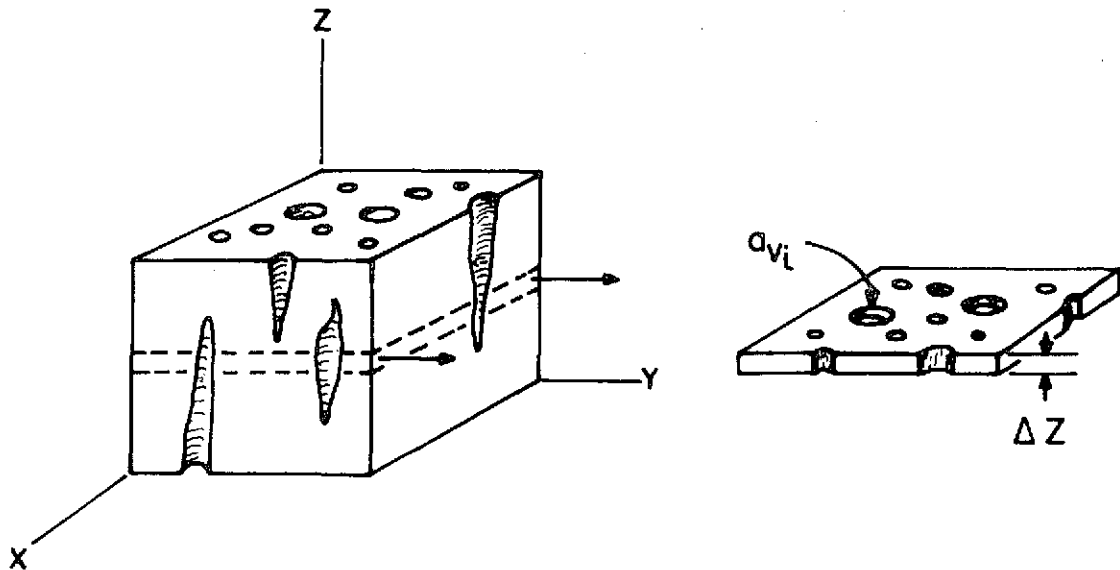
Figure 1: Porous bone model.

The BMC provides a direct measure of the load bearing area, A_B, of the bone. To illustrate this relationship consider the slab of bone of thickness ΔZ, Figure 1. The mass of bone in the slab, M_B, is

$$M_B = \rho_o \, A_B \cdot \Delta Z \qquad\qquad (2)$$

where ρ_o is the density of void-free bone. The composition of bone is relatively constant (Woodward, 1962; Strandh and Norlen, 1965) and so the mass of bone mineral in the slab is

$$BM = C \cdot M_B \qquad\qquad (3)$$

where C is the ratio of the mass of bone mineral per unit mass of bone. C equals 0.59 ± 0.03 g/g (Gong et al., 1964). Substituting equation 3 into equation 2

$$BM = C \cdot \rho_o \, A_B \cdot \Delta Z. \qquad\qquad (4)$$

Since BMC is defined as the mass of bone mineral per unit length, $BMC = BM/\Delta Z$, the BMC is

$$BMC = (C \cdot \rho_o) \cdot A_B. \qquad\qquad (5)$$

BMC therefore provides a direct measure of A_B, the load bearing area of bone and thus should give a better estimate of the maximum load borne by a bone specimen than the specimen's total cross-sectional area. This was experimentally investigated.

Table 1 contains the average value of the mechanical properties determined in this test. Although the ages of the skeletons ranged from 35 to 89 years the standard deviations of the various properties were quite small, $\%\sigma \simeq 10\%$. There was a slightly significant decrease in these values with age. The rates of decrease of the properties listed were less than 0.5% per year, $p \le 0.1$.

	Average	SD	Number of Observations
Maximum Compressive Stress (N/cm^2)	15,400	$\pm 1,600$	17
Strain at Failure (cm/cm)	0.0161	± 0.0031	16
Modulus of Elasticity (N/cm^2)	1.25×10^6	$\pm 0.14 \times 10^6$	17
Energy Absorbed to Failure $(N \cdot cm/cm^2)$	157	± 55	17

Table 1: Average values of the compressive properties of bone from the femoral midshaft.

Figure 2 is a plot of the maximum compressive load versus the total cross-sectional area, A_T, and the BMC of the test specimens. The open circles represent the maximum load versus A_T and the dots are the maximum load versus BMC. Linear regression equations were calculated between the maximum load and the independent variables, A_T and BMC. For the choice of scales on the abscissa, both regression lines were essentially the same and they are shown as a single solid line in the figure. The two pairs of dashed lines represent the standard error of estimate, SEE, in the maximum load from the regression line. The inner pair is for the regression equation between the maximum load and the BMC and the outer pair is for the regression equation between the maximum load and the cross-sectional area. The BMC is a more accurate estimator of the maximum load than the area as can be seen from a comparison of the SEE of the load from the independent variables. The SEE of the load from the BMC is about half that from the cross-sectional area: $SEE_{L_m, BMC} = \pm 1,600$ Newtons (∿5.5%) and $SEE_{L_m, A_T} = \pm 3,300$ Newtons (∿11%). The correlation coefficients were $r_{L_m, BMC} = 0.986$ and $r_{L_m, A_T} = 0.965$.
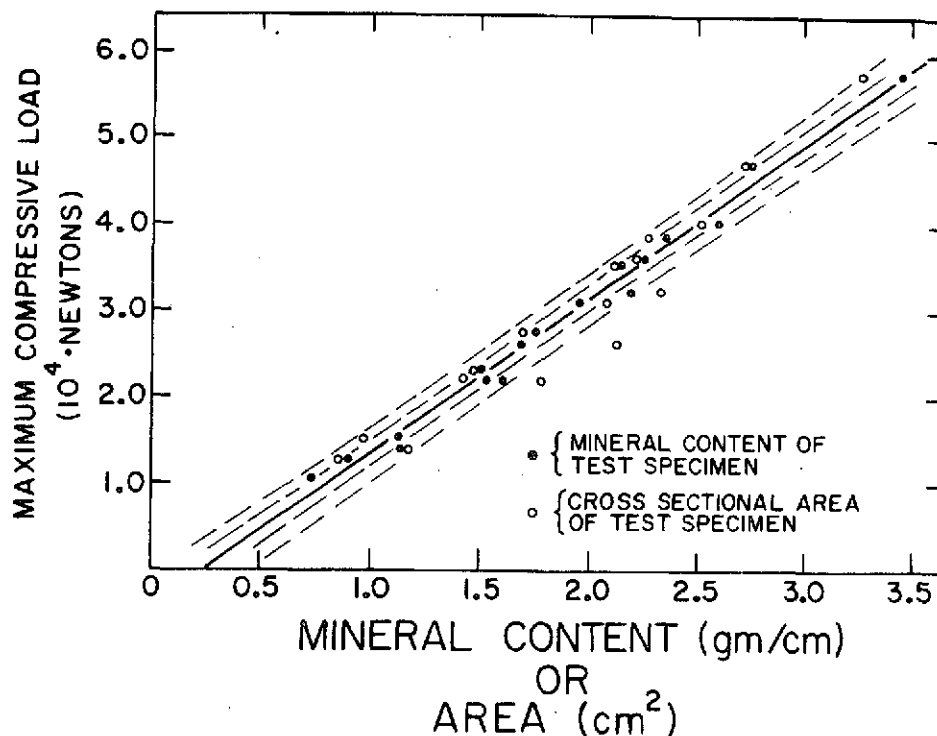
Figure 2: Maximum compressive load of machined bone specimens from the mid-diaphysis of femur versus BMC and total cross-sectional area.

DISCUSSION AND CONCLUSIONS

The BMC of the radius or ulna can provide an estimate (% SEE of 16-20%) of the BMC of the femoral neck or spine. Any site on the radius or ulna is statistically about as accurate as any other site for making these estimates,

but the relationships are not sufficient to accurately predict the BMC of the femoral neck or spine of a given individual. However, the relationships are sufficient to assign an individual to one of several broad classes of BMC of the femoral neck or spine on the basis of the BMC of the radius or ulna. Such classification should be useful in assessing an individual's risk of incurring a spontaneous hip fracture. For example, Smith (1971) in a comparison of the BMC of the radius in osteoporotic and normal women found that approximately 80% of the osteoporotic women had a BMC of the radius less than 0.68 g/cm and approximately 80% of the normals were over this value. In the skeletons measured in this study six of the skeletons showed evidence of femoral neck abnormality. The majority of these, five to one, were in skeletons in which the radius BMC was less than 0.68 g/cm.

The BMC of a bone specimen is a better estimator of the maximum load than the area of the specimen since the BMC is more closely related to the actual load bearing area of a specimen than is its total area. Extension clinically of this finding to the assessment of the strength of bone from the BMC in vivo would be very difficult. However, functionally the close relation between BMC and maximum load makes the BMC potentially very useful in providing a better normalization for the mechanical properties of bone than specimen area. Usually in mechanical test of bone a specimen is machined to a known cross-sectional area, loaded in tension or compression to failure and the strength, the maximum load per unit area, is computed. Any differences in porosity among the specimens produce variability in the measured strength. Evans (1958) demonstrated histologically that this variability could be reduced by measuring the area actually occupied by bone in the cross-section. This technique is not easily utilized and so the true source of variation cannot readily be obtained. A considerable effort has been devoted to investigating the differences in bone strength associated with age, sex, specimen size, which bone and the location in the bone from which the specimen was taken and there is still considerable uncertainty and ambiguity among the published findings of various investigators. These parameters are treated as the source of variation in the strength while the actual variate is more likely the porosity of the bone. Using the BMC as the normalization for computing the maximum load per unit BMC rather than maximum load per unit area provides for the first time an easy method for reducing the variability in the measurements related to bone porosity and should provide a better base for assessing the effects of various biological parameters on the strength of bone.

The BMC while providing information on the entire skeleton in addition provides information concerning the BMC of particular areas such as the hip or spine and information on the strength of the bone at the scan site.

ACKNOWLEDGEMENTS

REFERENCES

Bartley, M.H., J.S. Arnold, R.K. Haslam and W.S. Lee 1966. The relationship of bone strength and bone quantity in health, disease and aging. J. Geron. 21: 517-521.

Burstein, A.H. and V.H. Frankel 1968. The viscoelastic properties of some biological materials. Ann. N. Y. Acad. Sci. 146: 158-165.

Cameron, J.R. (ed) 1970. Proc. Bone Measurement Conference. U.S. Atomic Energy Comm. Conf. 700515. U.S. Dept. of Commerce (CFSTI), Springfield, Va.

Cameron, J.R. and J.A. Sorenson 1963. Measurement of bone mineral in vivo: an improved method. Science 142: 230-232.

Cameron, J.R., R.B. Mazess and J.A. Sorenson 1968. Precision and accuracy of bone mineral determination by direct photon absorptiometry. Invest. Radiol. 3: 141-150.

Chestnut, C.B., E. Manski, D. Baylink and W.B. Nelp 1973. Correlation of total body calcium (bone mass) and regional bone mass. Clin. Res. 21: 200 (abstract).

Cohn, S.H., K.J. Ellis, I. Zanzi, J.M. Letteri and J. Aloia 1974. Correlation of radial bone mineral content with total-body calcium in various metabolic disorder. In: R.B. Mazess (ed) Proc. Intern. Conf. on Bone Mineral Measurement. U.S. Govt. Printing Office, Washington, D.C.

Currey, J.D. 1959. Differences in the tensile strength of bone of different histological types. J. Anat. 93: 87-95.

Evan, F.G. 1958. Relations between the microscopic structure and tensile strength of human bone. Acta Anat. (Basel) 35: 285-301.

Gong, J.K., J.S. Arnold and S.H. Cohn 1964. Composition of trabecular and cortical bone. Anat. Rec. 149: 325-332.

Horsman, A., L. Buluso, H.B. Bently and B.E.C. Nordin 1970. Internal relationship between skeletal parameters in twenty-three male skeletons. In: J.R. Cameron (ed) Proc. Bone Measurement Conference. U.S. Atomic Energy Comm. Conf. 700515. U.S. Dept. of Commerce (CFSTI), Springfield, Va.

Mazess, R.B. 1968. Estimation of bone and skeletal weight by the direct photon absorptiometric method. Amer. J. of Phys. Anth. 29: 133.

McElhaney, J.H. 1966. Dynamic response of bone and muscle tissue. J. Appl. Physiol. 21: 1231-1236.

McElhaney, J.H., J.L. Fogle, W. Melvin, R.R. Haynes, V.L. Roberts and N.M. Alem 1970. Mechanical properties of cranial bone. J. Biomech. 3: 495-511.

Smith, E.L. 1971. <u>Bone, Changes with Age and Physical Activity</u>. Doctoral Thesis. University of Wisconsin, Madison, Wisconsin.

Stech, E.L. 1966. A descriptive model of lamellar bone anisotropy. ASME Paper #66 HUF-3.

Strandh, J. and H. Norlen 1965. Distribution per unit volume bone tissue of calcium, phosphorus and nitrogen from individuals of varying ages as compared with distribution per unit weight. <u>Acta Orthop. Scan.</u> 35: 257-263.

Vose, G.B., B.J. Stover and P.B. Mack 1961. Quantitative bone strength measurements in senile osteoporosis. <u>J. Geron.</u> 16: 120-124.

Whedon, G.D. and J.R. Cameron (eds) 1968. <u>Progress in Methods of Bone Mineral Measurement</u>. U.S. Dept. of HEW. U.S. Government Printing Office, Washington, D.C.

Wilson, C.R. (Submitted to <u>J. Bone Jt. Surg.</u>). Estimation of the bone mineral content of the femoral neck and spine from the bone mineral content of the radius or ulna.

Woodward, H.Q. 1962. The elementary composition of human cortical bone. <u>Health Phys.</u> 8: 513-517.

BONE STANDARDS FOR THE INTERCOMPARISON AND CALIBRATION
OF PHOTON ABSORPTIOMETRIC BONE MINERAL MEASURING SYSTEMS

Robert M. Witt

Department of Radiology (Medical Physics),
University of Wisconsin Hospitals, Madison,
Wisconsin

ABSTRACT

In order for different laboratories to compare and
collate their values for bone mineral content (BMC)
results there must be uniform calibration and standardi-
zation of their measuring systems.

Bone standards have been constructed to provide
for the intercomparison and calibration of photon
absorptiometric bone measuring systems. The standards
are composed of polymethyl methacrylate blocks with
three annular cavities which are filled with a saturated
solution of dipotassium hydrogen phosphate, KHP. The
saturated KHP solution has linear attenuation properties
similar to those of compact bone. The dimensions of the
inner and outer diameters of the annular cavities are
similar to the dimensions of the midshafts of radii
and metacarpals. The bone mineral content, BMC, of these
standards was calibrated by ash bone sections in units
of g/cm of bone ash.

Six of these standards, all identical, were scanned
in six different laboratories with bone mineral measuring
systems with digital output of the transmission counts.
The coefficient of variation of the BMC for each chamber
for all laboratories was the same as the coefficient of
variation of the same chamber measured by a single labora-
tory. For comparison our clinical laboratory has
measured one of these standards over a 33 month period
with an analog bone mineral measuring system. The
coefficients of variation for the BMC's were 2.3% for
the small chamber, 1.5% for the medium chamber, and 1.2%
for the large chamber.

The bone standards can be used to linearly calibrate
absorptiometric bone measuring systems in terms of the
ashed bone sections. A calibration equation for a
system can be determined from a linear regression analysis
of the assigned calibration values and the output units

of the system for the three chambers of the standard.
This linear calibration has been shown to be valid for
various radionuclide photon sources useful in the
absorptiometric method. Because of spectrum hardening
with increasing bone mineral mass, the linear calibration
for ^{125}I photon sources only would be valid for bones
ranging in size from metacarpals to radii.

Key Words: Absorptiometry – Bone Mineral Content –
Calibration.

INTRODUCTION

In order to intercompare and collate bone mineral content (BMC)
measurements from different laboratories there is a need for a common method
of intercomparison and standardization. To provide for intercomparison and
calibration of different bone mineral measuring systems bone reference
standards have been constructed. The standards are composed of polymethyl
methacrylate blocks with annular cavities filled with a saturated solution
of dipotassium hydrogen phosphate, KHP.

METHODS

Standard Material

The KHP solution was first used by Meema as a bone equivalent material
in a calibration step wedge (Meema et al., 1964). The saturated KHP solution
potentially is an excellent bone equivalent material since it has x-ray
attenuation properties very similar to those of compact bone over an energy
range from 15 keV to 100 keV (Figure 1). This energy range includes most
photon sources used in bone mineral measuring systems.

Dipotassium hydrogen phosphate is a readily available phosphate salt and
is very soluble in water at room temperature. The solubility limit is 167 g
of KHP per 100 g of water at 20°C (Handbook of Chemistry & Physics, 1964).
The saturated solution has a physical density of 1.71 g/cm³ and is close to
the reported densities of hydrated compact bone which range from 1.85 g/cm³
to 2.00 g/cm³ (Gong et al., 1964a,b; Mueller et al., 1966; Lindahl, 1967;
Blanton, 1968). Since the solution's physical density is nearly the same as
compact bone, the linear attenuation properties of the KHP solution are also
close to those of compact bone. The mass attenuation coefficients were
measured for compact bovine bone slabs and the KHP solution with ^{125}I and
^{241}Am photon sources, and were tabulated with values extrapolated from Spiers
attenuation data for bone tissue (1946) (Table 1). The attenuation coefficients
for the solution compared to bovine bone were 3.4% low at 27.4 keV and 1.9%
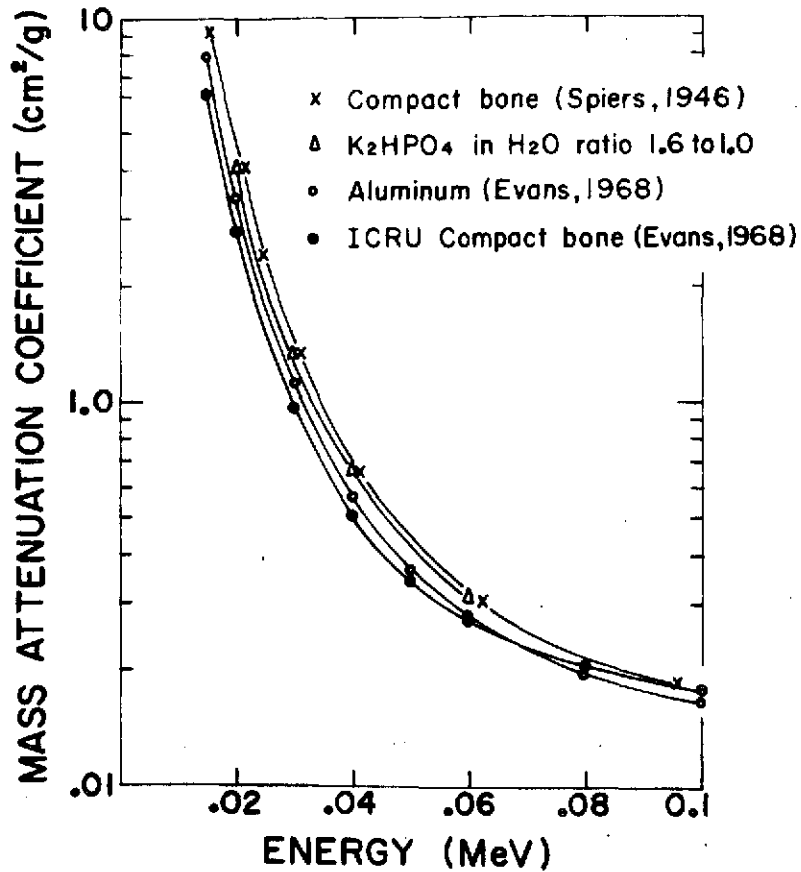low at 59.7 keV.

x Compact bone (Spiers,1946)

Δ K₂HPO₄ in H₂O ratio 1.6 to 1.0

○ Aluminum (Evans,1968)

● ICRU Compact bone (Evans,1968)

Figure 1: Logrithm of the mass attenuation versus energy for various materials. X - compact bone calculated by Spiers (1946), Δ - K_2HPO_4 in water mixed in a ratio of 1.6 to 1.0, ○-aluminum and ● - compact bone with ICRU composition calculated and tabulated in Evans (1968).

Energy MeV	Bovine (femur)	Compact Bone (femur) Spiers (1946)	K_2HPO_4 (1.6 to 1.0)
.0274	1.75	1.89	1.69
.0597	0.319	0.34	0.313

Table 1: Mass attenuation coefficients, cm^2/g.

Reference Standard   Construction

The reference standards were machined from polymethyl methacrylate sheet stock. Because the linear attenuation properties of the solution are similar to those for compact bone, the dimensions of the annular cavities could be made similar to those of diaphyseal bone. The most recent phantom design has three annular cavities with inner and outer diameters which have dimensions of a typical adult female metacarpal, and of a typical adult female and male radius, Figure 2.
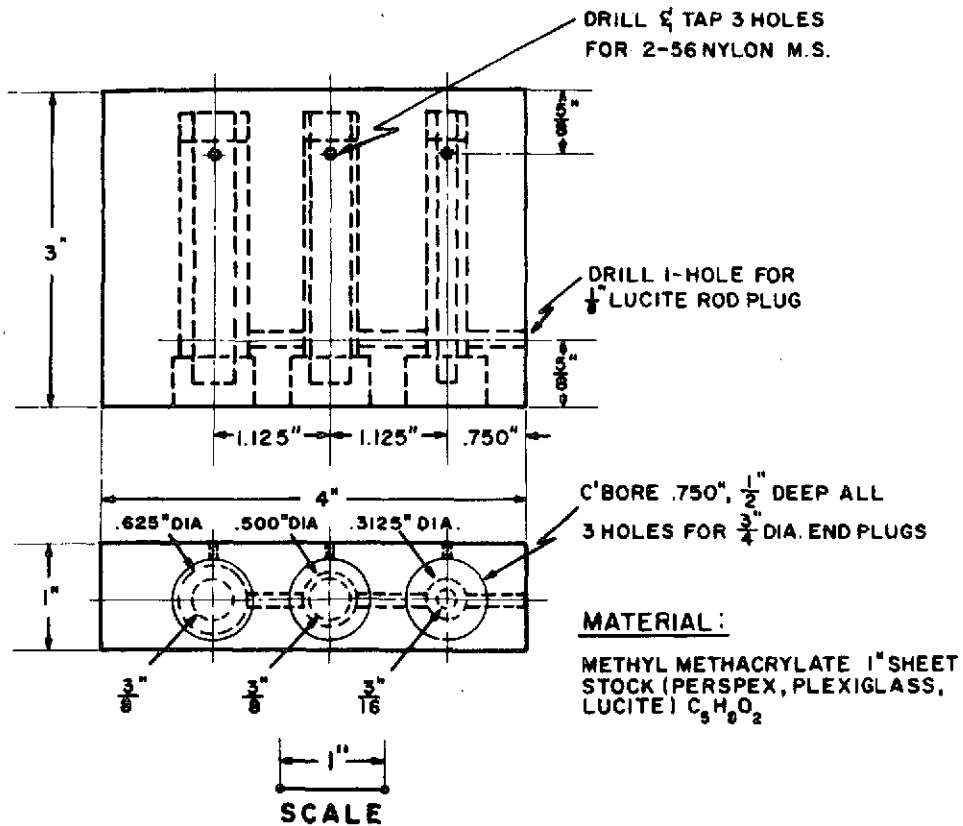
Figure 2:   The improved methylmethacrylate (Plexiglass or equivalent), K_2HPO_4 bone standard with three chambers whose dimensions approximate the midshaft dimensions of the adult male and female radius and the adult female metacarpal.

The reference standards can be machined reproducibly. Nine standards of an similar design were machined as a group, filled with the KHP solution, and scanned with an analogue bone mineral measuring system (Mazess et al., 1972). The per cent coefficient of variation for the BMC measurements for the three chambers for the nine standards as a group was approximately equal to the per cent coefficient variation for the three chambers of each standard. For all measurements, the per cent coefficient of variation was less than the scanning system's long-term reproducibility of 2 per cent coefficient of variation.

The solution filled phantoms are rugged and leak proof so that they can be shipped through the mail. The saturated solution remains stable in the phantom chambers at room temperature, but it can crystallize if subjected to low temperatures.

Although the KHP solution filled cavities in the plastic blocks do not have the same contrast as compact bone in soft tissue, it is possible to calibrate the reference standards relative to the BMC of ashed bone sections. For calibration, the BMC of a transmission scan measurement is defined to be the average ash mass contained in a 1 cm long transverse section of diaphyseal bone. Each chamber of the reference standards was calibrated from the results of three linear bone ash calibration studies where a tin filtered ^{125}I was the photon source. The arithmetic mean of the three BMC values was taken as the best estimate of the calibration value for each chamber (Witt et al., 1970).

RESULTS

Intercomparison Study

Six identical bone phantoms were distributed to six different laboratories for measurement. Each laboratory possessed a bone mineral scanning system with digital output of the transmission scan counts. Each laboratory scanned all chambers of a phantom and analyzed the scan data with a digital computer. All laboratories used their own algorithms for determining the bone-tissue edge and for computing the integral for bone mineral content. All scans of the standard for this intercomparison study were made with a tin filtered ^{125}I photon source.

To compare the results from the different laboratories all scan values were expressed as a common arbitrary quantity "Integral Bone Mineral Content" (IBMC). IBMC has been defined as the product of the integral of the natural logarithm of the ratio of I_0^* and I_i, and the distance the mechanical scanner travels between each datum point in millimeters, ΔX, Table 2. I_0^* is the transmission count rate when the photon beam is attenuated by a constant thickness of soft tissue and I_i is the transmission count rate when the photon beam is attenuated by both soft tissue and bone.

The overall mean IBMC's for each chamber for all laboratories were computed and are given in Table 2. The per cent coefficients of variation were 2.5% for the small chamber, 1.4% for the medium chamber, and 1.9% for the large chamber. The coefficients of variation of the measurements for the three chambers between the seven laboratories were the same as the coefficients of variation for the three chambers measured by a single laboratory. For comparison our clinical laboratory has measured an identical standard over a 33 month period with an analog bone mineral measuring system (Mazess et al., 1972). The coefficients of variation of the BMC's were 2.3% for the small chamber, 1.5% for the medium chamber, and 1.2% for the large chamber. Most differences in the mean IBMC between laboratories were small (< 2%) and are not statistically significant. Differences in the tin filtration of ^{125}I photon sources, the algorithms for the data analysis, scanning speeds, and source-detector collimination which were present between the measuring systems

could introduce systematic differences in the scan results which are greater than 2% (Judy, 1970). The good agreement among these intercomparison results indicates that different laboratories are measuring the same quantity of BMC.

Chamber Laboratory	Small	Medium	Large
Indiana	7.6	12.8	27.2
Philadelphia	7.93	13.14	28.38
U.S.P.H.S.H.	7.91	13.10	28.05
Rochester	7.47	12.78	28.51
New York	7.82	13.02	27.81
Wisconsin	7.92	13.24	28.69
Average	7.77	13.01	28.11
SD	$\pm$ .194	$\pm$ .187	$\pm$ .546
Per cent Coef. of Var.	2.5	1.4	1.9

Table 2: Comparison of Integral Bone Mineral Content based on measurements of the University of Wisconsin 3 chamber K_2HPO_4 bone reference standard. The Integral Bone Mineral Content = $\Delta X \cdot \int_X \log [I_0^*/I(x)] \, dx$; where ΔX = distance traveled between data point.

Calibration

The calibrated reference standards can permit other laboratories to linearly calibrate their absorptiometric bone mineral measuring systems in terms of the ashed bone sections. A calibration equation for a bone measuring system can be determined from a linear regression analysis of the assigned calibration values and the output units of the system for the three chambers of the standard.

To verfy this calibration procedure, Judy (1972) scanned the reference standard with three different radionuclide photon sources: [125]I with a photon energy of about 28 keV; [153]Gd with two photon energies of about 44 keV and 100 keV; and [241]Am with a photon energy of 60 keV. A straight-line calibration equation was obtained for each of the four photon energies. The slopes of the regression equations were plotted as a function of the photon energy, Figure 3. The slope of the calibration equation should be the same as the quantity, R, where,

$$R = \rho_{Bone}/(\mu_{Bone} - \mu_{Soft \; Tissue}).$$

The quantity R was calculated from tabulated values for the mass attenuation coefficients for water and hydroxyapatite, and plotted for photon energies from 10 keV to 100 keV.
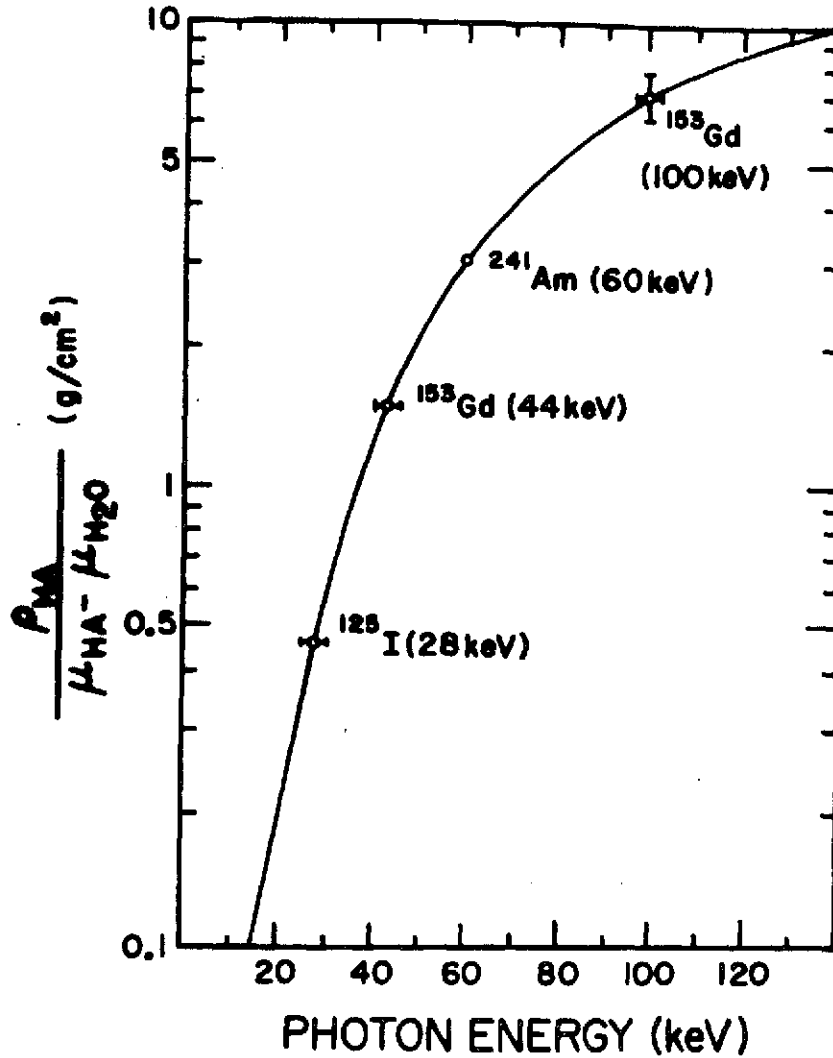
Figure 3: Comparison of the measured and theoretical values of the density of bone mineral divided by the difference of the linear attenuation coefficients of bone mineral and soft tissue, R.

Within the experimental errors in determining the regression slopes and in assigning a single energy to each of the photons, there is good agreement between the slopes which are based on the assigned calibration values for each chamber and the calculated quantity R over this range of photon energies.

It should be noted that for a linear calibration of scanning systems for measuring BMC whether by a bone reference standard or by bone ash studies, an intercept will be present. The value of the intercept will vary if the spatial resolution of the scanning system is determined by the distance traveled per data interval. It will remain constant if the spatial resolution of the system is determined by the size of the photon beam. Usually the latter is true, (Judy, 1970).

For systems with ^{125}I sources, Sandrik and Judy (1973) have shown that the quantity of BMC determined by the absorptiometric method is a nonlinear function of the amount of BMC. This nonlinearity implies that the calibration equations for the original bone ashing studies and those obtained from the reference standard should also have been nonlinear. However, if one limits the linear calibrations to bones ranging in size from the adult metacarpal to the adult radius, the calibration equations will give values of BMC within $\pm$ 1% of those predicted by the nonlinear equations. Since the bones scanned in the ashing studies and the bones simulated in the reference standard lie within this range, the linear calibrations are valid to the error made in originally assigning the BMC values to the chambers of the standard.

DISCUSSION AND CONCLUSIONS

A saturated solution of dipotassium hydrogen phosphate in water can serve as a bone equivalent material for human compact bone. The solution has been shown to have a physical density and mass attenuation properties similar to those for compact bone. The saturated solutions can be made reproducibly and easily from a readily available phosphate salt. The bone phantoms were machined from commercially available acrylic plastic sheets and were designed to contain the KHP solution in three annular cavities whose dimensions were similar to those of diaphyseal bone of the lower limb and hand. Groups of phantoms can be made reproducibly, and therefore, can serve as intercomparison standards to compare the output results from different digital systems which determine bone mineral content in vivo by the absorptiometric scanning technique. Moreover, when the three KHP solution filled chambers are calibrated to bone ash studies, the phantoms can serve as common secondary calibration standards, and can thus be used to calibrate the output units of both digital and analog bone mineral scanning systems in units of gram per centimeter of bone ash.

REFERENCES

Blanton, P.L. and N.L. Biggs 1968. Density of fresh and embalmed human compact and cancellous bone. Amer. J. Phys. Anthro. 29: 39-44.

Evans, R.B. 1968. X-ray and γ-ray Interactions. In: F.H. Attix and W.C. Roesch (eds) Radiation Dosimetry, Volume 1, 2nd edition. Academic Press, New York, pp. 93-155.

Gong, J.K., J.S. Arnold and S.H. Cohn 1964a. The density of organic and volatile and non-volatile inorganic components of bone. Anat. Rec. 149: 319-324.

Gong, J.K., J.S. Arnold and S.H. Cohn 1964b. Composition of trabecular and cortical bone. Anat. Rec. 149: 325-332.

Handbook of Chemistry & Physics, 45th edition, The Chemical Rubber Co., Cleveland, Ohio 1964.

Judy P.F. 1970. The theoretical accuracy and precision in the photon attenuation measurement of bone mineral. In: J.R. Cameron (ed) Proc. Bone Measurement Conference U.S. Atomic Energy Comm. Conf. 700515. U.S. Dept. of Commerce (CFSTI), Springfield, Va.

Judy, P.F. and J.R. Cameron 1972. Bedrest subject measurements at USPHS. USAEC Report COO-1422-121.

Lindahl, O. and Åke G.H. Lindgren 1967. Cortical bone in man. 1. Variation of the amount and density with age and sex. Acta Orthop. Scand. 38: 133-140.

Mazess, R.B., J.R. Cameron and H. Miller 1972. Direct readout of bone mineral content using radionuclide absorptiometry. Int. J. Appl. Rad. Isotopes 23: 471-479.

Meema, H.E., C.K. Harris and R.E. Pourrett 1964. A method for determination of bone-salt content of cortical bone. Radiology 82: 986-997.

Mueller, K.H., A. Trias and R.D. Ray 1966. Bone density and composition. J. Bone Jt. Surg. 48(A): 140-148.

Sandrik, J.M. and P.F. Judy 1973. Effects of the polyenergetic character of the spectrum of ^{125}I on the measurement of bone mineral content. Invest. Radiol. 8: 143-149.

Spiers, F.W. 1946. Effective atomic number and energy absorption in tissues. Brit. J. Radiol. 19: 52-63.

Witt, R.M., R.B. Mazess and J.R. Cameron 1970. Standardization of bone mineral measurements. In: J.R. Cameron (ed) Proc. Bone Measurement Conference. U.S. Atomic Energy Comm. Conf. 700515. U.S. Dept of Commerce (CFSTI), Springfield, Va.

ANALYSIS OF ^{153}Gd AND OF ^{125}I - ^{241}Am SOURCES

James Hanson

Department of Radiology (Medical Physics),
University of Wisconsin Hospitals, Madison,
Wisconsin

ABSTRACT

The precision of the dual photon bone mineral technique
was modeled mathematically as an expression based on counting
statistics. For a given amount of bone and soft tissue there
is an optimal photon energy pair. When the initial intensities
of the photon beams are equal, the optimal lower photon energy
increases with increasing mass of bone and soft tissue for a
given higher photon energy. Dual sources of interest are
^{125}I/^{241}Am (28 and 60 keV) and ^{153}Gd (43 and 100 keV). The
bone mineral measured in thin anatomical locations (i.e. hand
and forearm) with ^{125}I/^{241}Am is more precise than with ^{153}Gd.
For thick locations (i.e. upper arm and calf) ^{153}Gd is more
precise than ^{125}I/^{241}Am.

Key Words: Absorptiometry - Bone Mineral Content -
Optimization - Precision.

INTRODUCTION

The precision, or reproducibility, of the dichromatic attenuation
technique (DAT) has been investigated by Judy (1970), Wooten (1971) and Watt
(1973). The precision of a measurement is related to counting statistics,
photon energies and the amount of tissue being measured. The purpose of this
paper is to predict the optimal conditions for a given measurement. The basic
model (Judy, 1970) has been used to express the expected precision of a point
DAT measurement of bone mineral in various amounts of bone and soft tissue for
different pairs of photon energies. For a constant ratio of initial counts
there is an optimal value of the lower photon energy. This optimal value
depends on the amount of bone and soft tissue present; as the amount of bone
and soft tissue increases the optimal lower photon energy also increases. For
maximum precision the choice of a suitable dual photon energy source will
depend on the anatomical site being measured.

Figure 1 shows the mass attenuation coefficients for bone and soft tissue
for photon energies of 10 to 100 keV. To precisely determine the amount of
bone mineral the difference in attenuation between bone and soft tissue should
be maximized. This occurs below approximately 40 keV. As the photon energy
decreases, the difference in attenuation between bone and soft tissue increases,

MASS ATTENUATION COEFFICIENTS(cm²/g)

100

10

BONE

1

SOFT
TISSUE

0.1

0   20   40   60   80   100
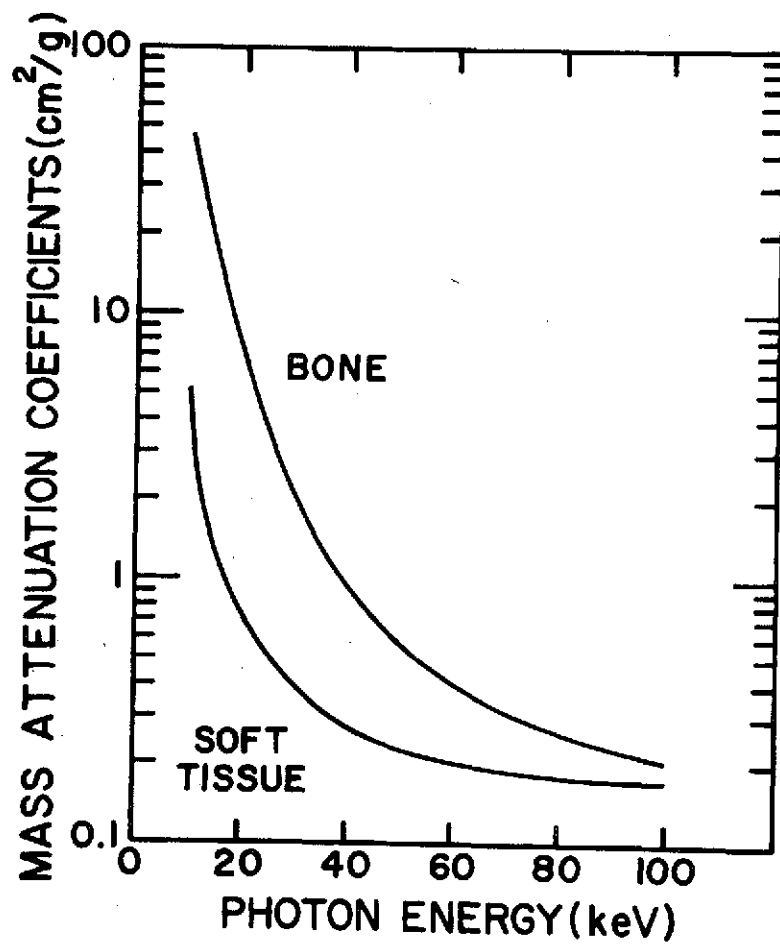
PHOTON ENERGY(keV)

Figure 1: Mass attenuation coefficients for bone and soft tissue
from 10 to 100 keV.

but the value of the attenuation coefficients are increasing, which reduces the photon transmission. The lower photon energy, E_1, will have an optimal value. The optimal value of E_1 is reached when any gain in precision due to an increased difference in attenuation will be counteracted by an increased error because of the reduction in transmission. For given E_1, the precision is fairly independent of the higher photon energy, E_2, for values of E_2 greater than 50 keV.

METHODS

The exponential attenuation equations for a DAT system are

$$I_1 = I_{0,1} \exp(-\mu_{BM,1} m_{BM} - \mu_{ST,1} m_{ST})$$

$$I_2 = I_{0,2} \exp(-\mu_{BM,2} m_{BM} - \mu_{ST,2} m_{ST})$$

where the subscripts 1 and 2 denote the lower and higher energies respectively. The total counts are $I_{0,1}$ and $I_{0,2}$; I_1 and I_2 are the transmitted counts; m_{BM} and m_{ST} are the bone mineral and soft tissue masses in g/cm^2 and μ_{BM} and μ_{ST} are the respective attenuation coefficients (cm^2/g) at energies E_1 and E_2 as denoted by subscripts 1 and 2.

The mass of bone mineral, m_{BM}, can be expressed in terms of the attenuation coefficients and the natural logarithm of the ratio of initial to transmitted counts

$$m_{BM} = \frac{\ln\left(\frac{I_{0,1}}{I_1}\right) \mu_{ST,2} - \ln\left(\frac{I_{0,2}}{I_2}\right) \mu_{ST,1}}{\mu_{BM,1} \mu_{ST,2} - \mu_{BM,2} \mu_{ST,1}} \tag{1}$$

The assumption that the compositions of bone mineral and soft tissue are invariant makes the attenuation coefficients in equation 1 constant. With constant values of attenuation coefficients the precision of equation 1 only depends on counting statistics.

For the general case of $x = F(u,v)$ the variance of x is given by Bevington (1969)

$$\sigma_x^2 = \left(\frac{\partial x}{\partial u}\right)^2 \sigma_u^2 + \left(\frac{\partial x}{\partial v}\right)^2 \sigma_v^2 \tag{2}$$

where u and v are uncorrelated variables.

The expected precision for determining the bone mineral mass from equation 1 is from the propagation of errors expression given by

$$\sigma_{m_{BM}}^2 = \left(\frac{\partial m_{BM}}{\partial T_1}\right)^2 \sigma_{T_1}^2 + \left(\frac{\partial m_{BM}}{\partial T_2}\right)^2 \sigma_{T_2}^2 \tag{3}$$

This is the expected variance of bone mineral as a function of counting statistics where T_1 and T_2 are $\ln(I_{0,1}/I_1)$ and $\ln(I_{0,2}/I_2)$ respectively. The variances of T_1 and T_2 are determined by Poisson statistics and are given by

$$\sigma_{T_K}^2 = \left(\frac{\partial T_K}{\partial I_{0,K}}\right)^2 \sigma_{I_{0,K}}^2 + \left(\frac{\partial T_K}{\partial I_K}\right)^2 \sigma_{I_K}^2 \qquad (4)$$

where the subscript K denotes the general case.

Equation 4 reduces to

$$\sigma_{T_K}^2 = \frac{1}{I_{0,K}} + \frac{1}{I_K}$$

Since $\sigma_I^2 = I$. Solving equation 3 in terms of initial intensities, attenuation coefficients, and mass of bone mineral and soft tissue allows the prediction of the expected precision for a given amount of bone mineral and soft tissue for any pair of photon energies.

The expected coefficient of variation of bone mineral, CV_{BM}, of a point measurement is

$$CV_{BM} = \frac{\sqrt{\sigma_{m_{BM}}}}{m_{BM}}$$

RESULTS

In order to demonstrate the dependency of the precision of a point measurement of bone mineral on the choice of photon energies, the coefficient of variation of bone mineral was calculated for a two component system consisting of 1.0 g/cm^2 of bone mineral and 5.0 g/cm^2 of soft tissue; both initial counts were 2.5×10^5.

The coefficient of variation of m_{BM} is shown in Figure 2 with E_2 along the abcissa and E_1 plotted as a family of curves. For the case of 1.0 g/cm^2 of bone mineral, 5.0 g/cm^2 of soft tissue and constant ratio of initial counts the optimal lower photon energy is 30 keV. The CV_{BM} remains fairly independent of the higher photon energy for values of E_2 greater than 50 keV.

For larger amounts of bone mineral and soft itssue in the beam the optimal value of E_1 increases. A higher E_1 is needed to compensate for reduction of transmission because of a greater amount of tissue in the beam. The CV_{BM}, as a function of E_1 for a given E_2 of 60 or 100 keV, is shown in Figure 3. For the case of 1.0 g/cm^2 of bone mineral and 5.0 g/cm^2 of soft tissue (Figure 3A) the optimal value of E_1 is 30 keV. For the case of 2.0 g/cm^2 of bone mineral and 10 g/cm^2 of soft tissue (Figure 3B), the optimal value of E_1 is 37 keV for an E_2 of 60 keV, and 40 keV for an E_2 of 100 keV.
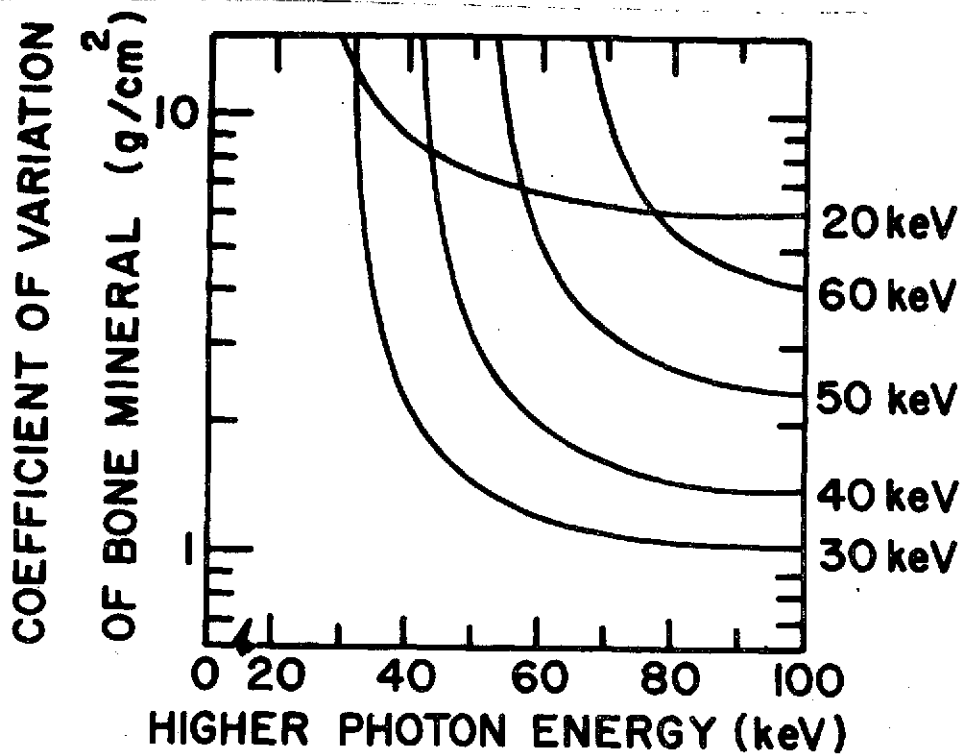
Figure 2: Coefficient of variation as a function of photon energies. Initial counts are 2.5 x 10^5; the bone mineral and soft tissue masses are 1.0 g/cm^2 and 5.0 g/cm^2 respectively.
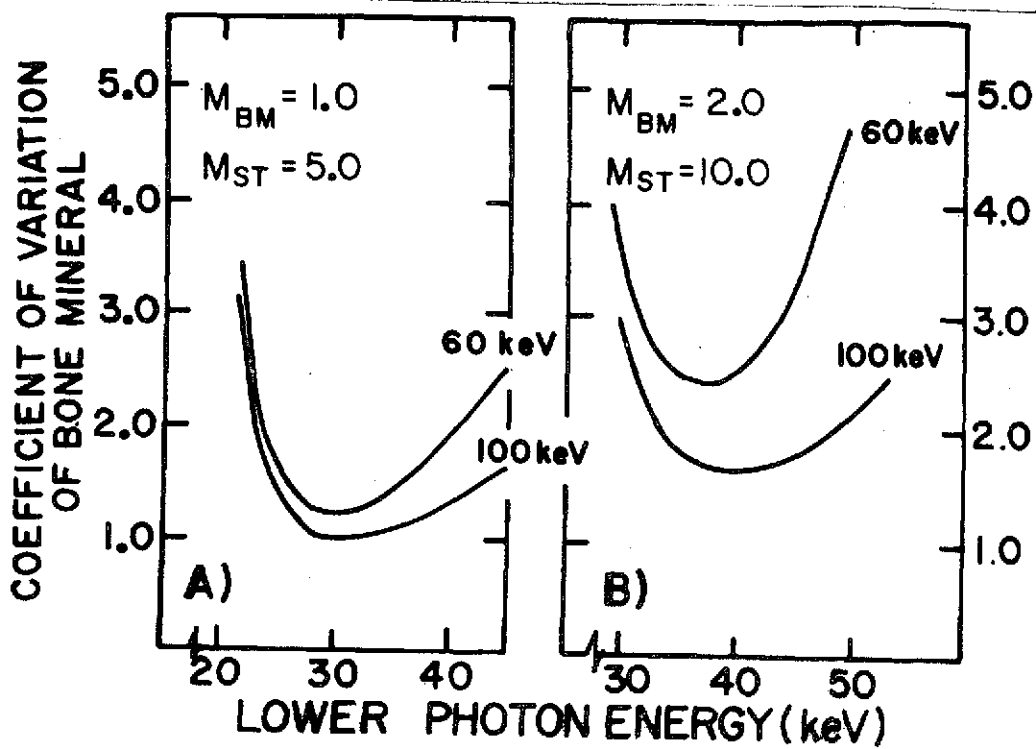

Figure 3: Coefficient of variation for two tissue thicknesses (A and B) as a function of lower photon energy for two given higher energies.

Figure 4 shows the coefficient of variation of bone mineral plotted against increasing bone mineral for two dual energy photon sources of interest. The ratio of bone mineral mass to soft tissue mass is 1/5 and the initial counts are 2.5×10^5. For thin sections everything to the left of the point of intersection in Figure 4 (i.e. forearms, fingers), the dual source of $^{125}I/^{241}Am$, with E_1 and E_2 of 28 and 60 keV respectively, is more precise than the dual source of ^{153}Gd, with E_1 and E_2 of 43 and 100 keV. For thick sections everything to the right of the intersection (i.e. upperarms, calves), ^{153}Gd is more precise than $^{125}I/^{241}Am$.
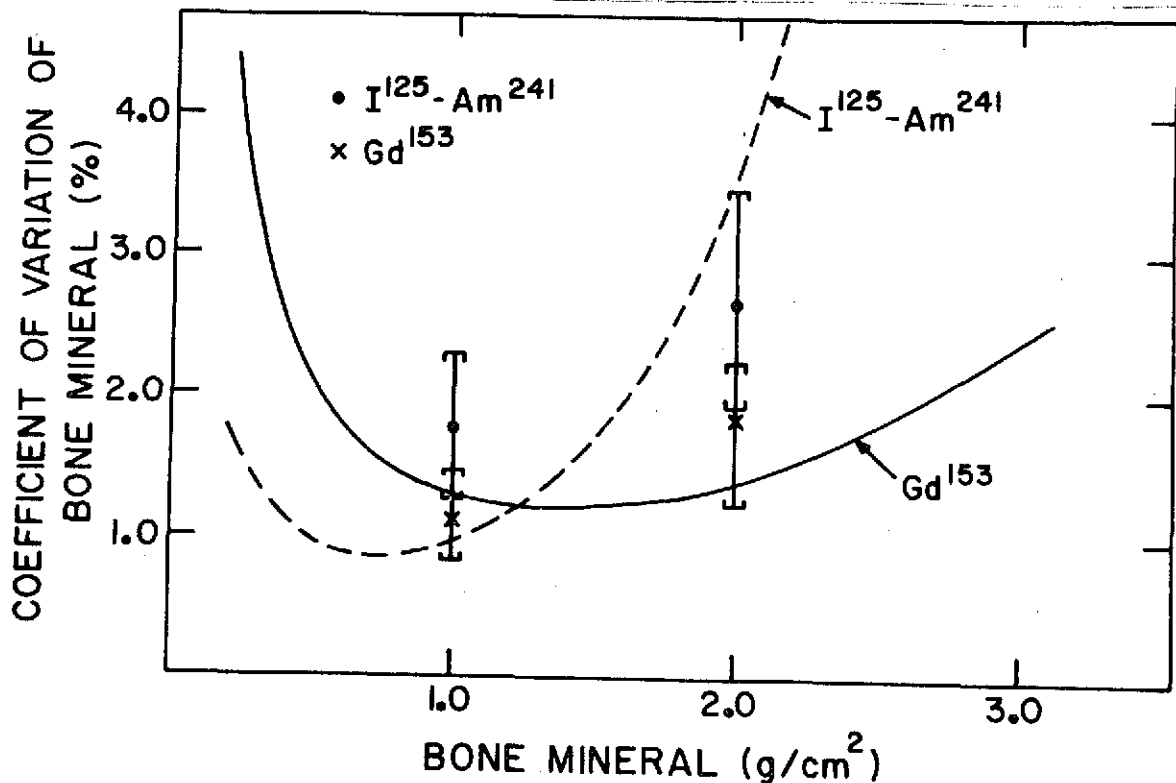
Figure 4: Coefficient of variation of bone mineral plotted against increasing bone mineral for the dual sources of $^{125}I/^{241}Am$ and ^{153}Gd.

A preliminary experimental verification of this model consisted of 25 DAT point measurements of 2 bone mineral and lucite phantoms. The experimental values of the coefficient of variation are shown with 90% confidence limits. These results are not conclusive, as over 100 such measurements are needed.

DISCUSSION AND CONCLUSIONS

The precision of bone mineral measurements made at different anatomical sites can be optimized by selecting the proper dual source in accordance with tissue thickness. As the amount of bone and soft tissue increases the optimal lower energy also increases. A photon energy that is too high won't give maximum contrast between the bone and soft tissue, whereas a photon energy that is too low won't have maximum transmission. However these suboptimal counting

conditions can be remedied by using sources of higher activity or by otherwise increasing the counts collected. It also must be recognized that the achievement of optimum conditions with regard to counting statistics is not the only or even the chief factor in establishment of a measuring system. Errors of accuracy, which are associated with scattering, beam hardening, source geometry and uncertainties in absorption coefficients are also critical. In addition questions of cost, efficiency and availability contribute to the selection of sources and of measurement conditions. It is only through careful consideration of practicality, precision and accuracy that useful biomedical decisions may be made to the technique and applications of absorptiometry.

REFERENCES

Bevington, P.R. 1969. Data Reduction and Error Analysis for the Physical Sciences. McGraw Hill Book Company, New York.

Judy, P.F. 1971. A Dichromatic Attenuation Technique for the In Vivo Determination of Bone Mineral Content. Ph.D. Thesis, University of Wisconsin, Madison, Wisconsin.

Watt, D.E. 1973. Personal communication.

Wing, K. 1973. Personal communication.

Wooten, W.W. 1971. Bone Densitometry: The Two Photon Technique and Fat Content of the Bone. M.S. Thesis, University of California, Los Angeles, California.

****

DISCUSSION

M. Greenfield: (Comment) Results appear to be in aggrement with those of W. Wooten, M.S. thesis, UCLA, circa 1971.

DIRECT READOUT OF BONE MINERAL CONTENT WITH DICHROMATIC ABSORPTIOMETRY

W.C. Kan, C.R. Wilson, R.M. Witt and R.B. Mazess

Department of Radiology (Medical Physics)', University of Wisconsin
Hospitals, Madison, Wisconsin

ABSTRACT

An analog device has been constructed which provides immediate
readout of bone mineral content and bone width from absorptiometric
scans with two photon beams with different energies such as ^{153}Gd
(43 keV and 100 keV) or ^{125}I/^{241}Am (28 keV and 60 keV). The
system and preliminary results are presented in this paper.

Key Words: Absorptiometry – Bone Mineral Content – Dichromatic
Absorptiometry – Direct Readout.

INTRODUCTION

An analog system has been constructed to calculate the bone mineral mass and
bone width from the transmission of two photon beams with different energies
such as ^{153}Gd (43 keV and 100 keV) or ^{125}I and ^{241}Am (28 keV and 60 keV). The
major advantage of using a dichromatic attenuation technique to measure bone
mineral content (BMC) over the technique of using a monoenergetic photon beam
is that it does not require the bone to be covered with a constant thickness of
soft tissue.

The transmission of two monoenergetic photon beams through a bone and soft
tissue system can be expressed as:

$$I(A) = I_o(A) \exp\left(-\mu_{BM(A)} M_{BM} - \mu_{ST(A)} M_{ST}\right) \tag{1}$$

$$I(B) = I_o(B) \exp\left(-\mu_{BM(B)} M_{BM} - \mu_{ST(B)} M_{ST}\right) \tag{2}$$

$I_o(A)$ = the unattenuated intensity at energy A

$I_o(B)$ = the unattenuated intensity at energy B

$I(A)$ = the attenuated intensity at energy A

$I(B)$ = the attenuated intensity at energy B

$\mu_{BM(A)}$ = mass attenuation coefficient of bone mineral at energy A (cm^2/gm)

$\mu_{ST(A)}$ = mass attenuation coefficient of soft tissue at energy A (cm^2/gm)

$\mu_{BM(B)}$ = mass attenuation coefficient of bone mineral at energy B (cm^2/gm)

$\mu_{ST(B)}$ = mass attenuation coefficient of soft tissue at energy B (cm^2/gm)

M_{BM} = mass per unit area of bone mineral (gm/cm^2)

M_{ST} = mass per unit area of soft tissue (gm/cm^2)

These equations can be solved, with point bone mineral mass, M_{BM}, and point soft tissue mass, M_{ST}, expressed as

$$M_{BM} = K_S [R \log I(B) - \log I(A)] - [R \log I_o(B) - \log I_o(A)] \qquad (3)$$

$$M_{ST} = K_B [-R' \log I(B) + \log I(A)] - [-R' \log I_o(B) + \log I_o(A)] \qquad (4)$$

where

$$K_S = \frac{\ln(10) \ \mu_{ST(B)}}{\mu_{BM(A)}\mu_{ST(B)} - \mu_{BM(B)}\mu_{ST(A)}} \qquad\qquad R = \frac{\mu_{ST(A)}}{\mu_{ST(B)}}$$

$$K_B = \frac{\ln(10) \ \mu_{BM(B)}}{\mu_{BM(A)}\mu_{ST(B)} - \mu_{BM(B)}\mu_{ST(A)}} \qquad\qquad R' = \frac{\mu_{BM(A)}}{\mu_{BM(B)}}$$

METHODS

As in the earlier single photon direct readout unit (Mazess, 1972) the integration of M_{BM} with respect to distance across the bone yields the direct readout of bone mineral content per unit length of bone (g/cm); simultaneously, integration of a fixed current source indicates the bone width.

The dichromatic analog system functions similarly to the single photon system and uses the output of a basic nuclear counting system (Figure 1a) a NaI(TL) scintillation crystal, photomultiplier tube, amplifiers, two single channel analyzers, two scalers with buffers, timer and the control system. This permits collection of digital data from the pulse height analyzer channels. The digital data collection system has been previously described (Judy, 1971). In the former data collection system the contents of the scaler buffers are recorded on magnetic tape. The tape is subsequently processed by a computer which calculates the bone mineral content and the bone width.
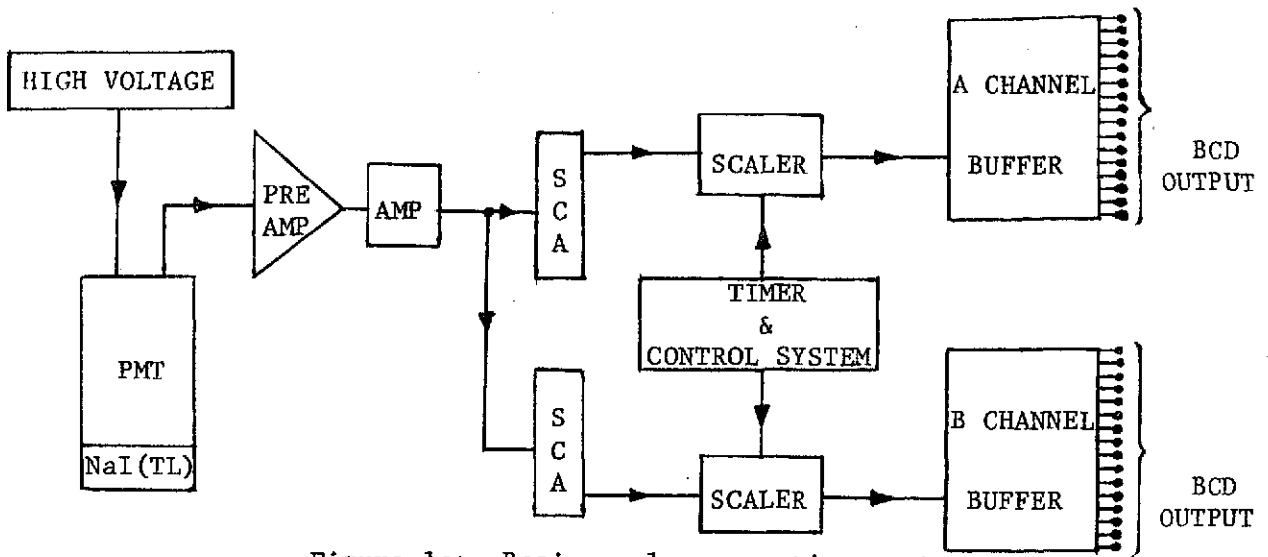
Figure 1a: Basic nuclear counting system.

In the new analog system (Figure 1b), the digital contents of the scaler buffers are converted to analog voltage signals. These signals are then processed in an analog fashion to compute M_{BM} at each point during the scan according to equation (3). The analog system described here is a bread-board model. An engineering portable model has been constructed.
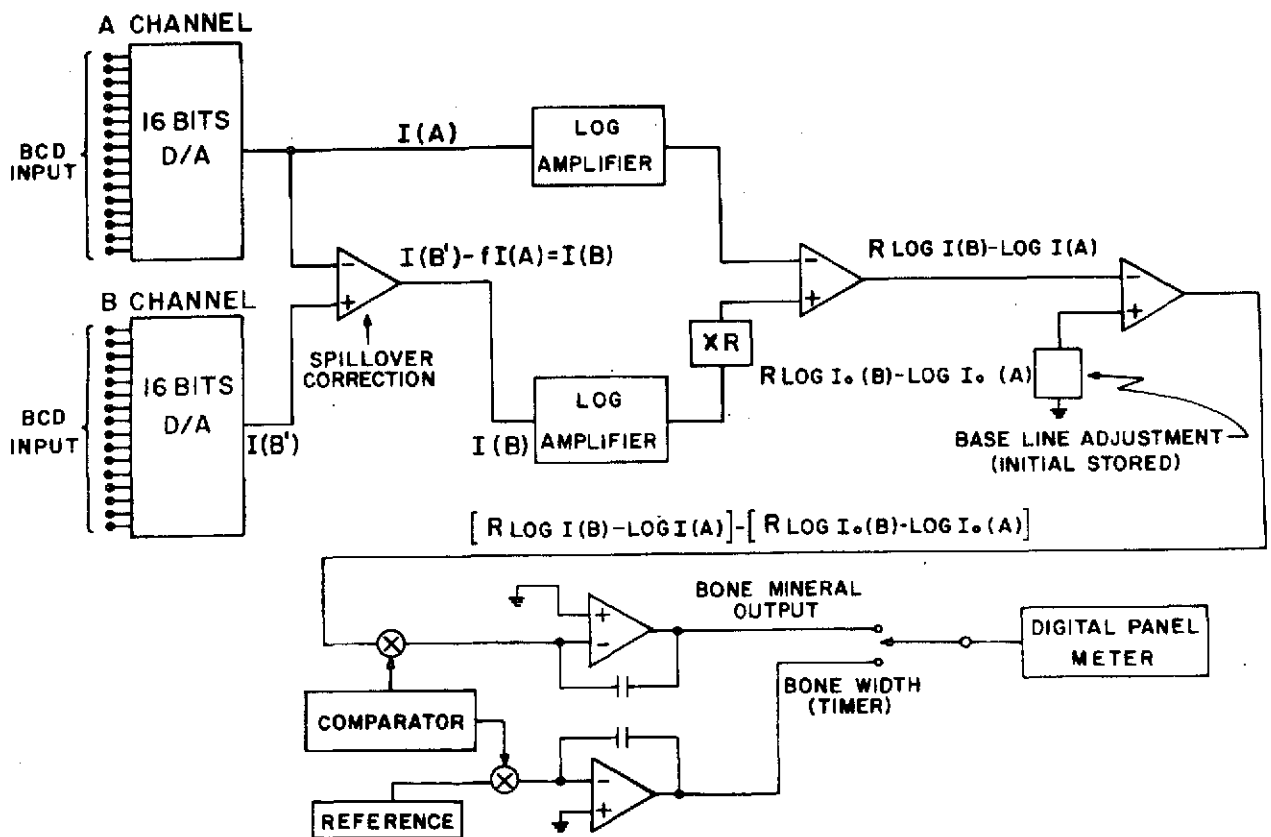

Figure 1b: Dichromatic analog system.

Some of the counts in the lower energy channel are due to Compton inter-
actions of the higher energy photon in the scintillator and the surrounding
materials. A correction factor must be subtracted from the lower channel vol-
tage to correct for this "spill-over". This fraction depends upon the photon
energy, the window setting, the crystal size, and the source-detector geometry.
An estimate of this correction factor can be found by attenuating the beam
until nearly all the counts in the lower channel are due to the "spill-over"
from the upper energy photons. For the ^{153}Gd source, the correction factor, f,
was found to be approximately 3% of the upper energy channel counts. The
corrected voltage for channel B becomes $I(B') - f \cdot I(A)$, Figure 1b.

After the spill-over correction, the two logarithmic amplifiers take the
logarithm of the analog signals from both channels. Channel B is multiplied
by the coefficient R, in BMC equations, and subtracted from channel A by a
low drift linear differential amplifier. The resulting analog signal is equal
to $[R \log I(B) - \log I(A)]$.

Prior to entering the bone, $M_{BM} = 0$ and $\mu \log I(B) - \log I(A) = \mu \log I_o^*(B) -$
$\log I_o^*(A)$. The value of $\mu \log I_o^*(B) - \log I_o^*(A)$ is set and stored as a constant
D.C. voltage. This value is determined at the beginning of each scan by
activating an automatic averaging circuit over a fixed interval of time. This
establishes a baseline reference, and is shown in Figure 1b as the "Baseline
Adjustment".

As the beam moves from the soft tissue region into the bone the quantity,
$[R \log (B) - \log I(A)] - [R \log I_o(B) - \log I_o(A)]$ is no longer equal to zero.
The comparator stage (Figure 1b), which consists of a differential amplifier
and a relay, automatically detects the edge of the bone. When the above quantity
deviates from zero by a preset value, the comparator activates the relay. The
closing of the relay contacts begins the integration of the output (M_{BM}) from
the differential amplifier. When the beam leaves the other edge of the bone,
the comparator causes the relay to open and terminates the integration. The
opening and closing of the relay also starts the integration of a constant
current source which gives a measure of the bone width.

After integration across the bone is completed, the voltages of the two
integrators can be displayed in the digital panel meter as a direct readout of
BMC and bone width. A simple resistive divider network provides the multipli-
cation factor K as indicated earlier in the bone mass, M_{BM}, equation (3).

RESULTS

Preliminary tests of the analog system were performed by scanning an upper
arm standard. The arm standard is composed of an aluminum tube (outside
diameter 2.24 cm, wall thickness 0.23 cm) embedded in a methyl methacrylate
block with round edges and flat sides over the aluminum tube. The approximate
dimensions are $5.6 \times 7.05 \times 8$ (cm)^3. This simulates the human bone (Figure 2).
The scans were made with a 22 mCi ^{153}Gd source at a scan speed of 1.2 mm/sec
and with detector collimation 6.4 mm in diameter. The point bone mineral
expression $[R \log I(B) - \log I(A)] - [R \log I_o^*(B) - \log I_o^*(A)]$ from the output
of the differential amplifier were plotted by an x-y plotter, Figure 2. The

step nature of the plot is related to the scaler buffers which receive the
contents of the scaler at the end of each timer interval and maintain the same
contents during next timer interval. The average value for six consecutive
scans of the arm standard was 6.27 (arbitrary units) with standard deviation
of 0.09, coefficient of variation 1.45%. Similar precision test was performed
by scanning the upper arm of a normal subject. The average value for eleven
consecutive scans was 2.26 with standard deviation of 0.04, coefficient of
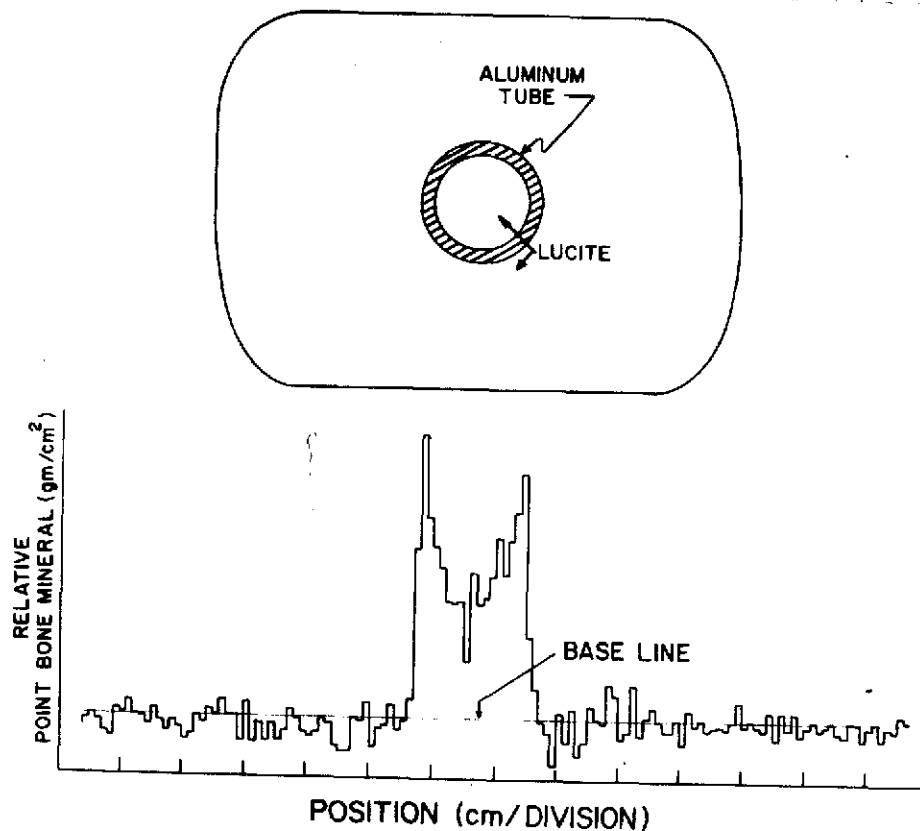variation 1.81%.

Figure 2: Point bone mineral mass versus
           scan position across arm standard.

As previously stated one advantage of dichromatic attenuation technique
is that it does not require the bone to be covered with a constant thickness
of soft tissue. When no bone is present, M_{BM} is simply zero and independent
of the amount of soft tissue cover. To show this independence, a 5 cm thick
methyl methacrylate block was scanned in air and the point values for bone
mineral mass were recorded with the x-y recorder along the scan path (Figure 3).
The baseline level differs little when scanning from air into the methyl
methacrylate and then back into air. However, the fluctuations of point bone
mineral values were larger when the beam is traveling through the plastic
block than the air because of the increased variation due to the decrease
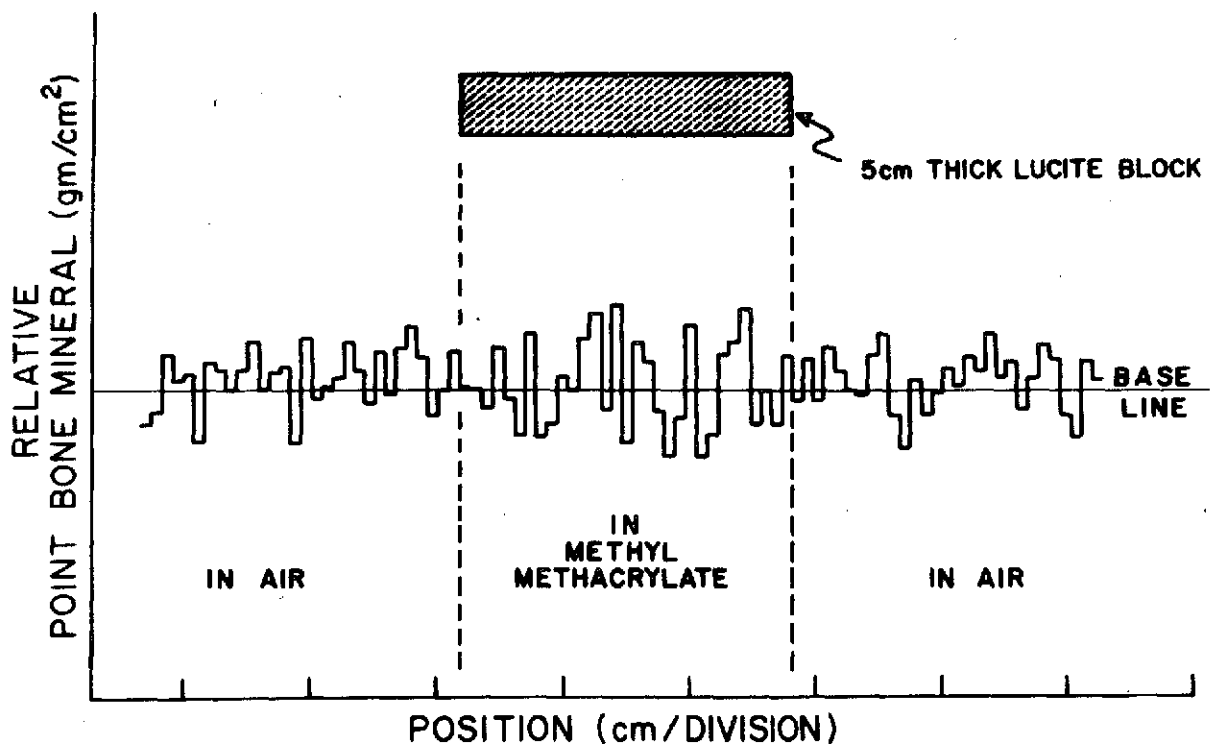in counting statistics.

Figure 3: Point bone mineral mass versus scan position
across 5 cm block of methyl methacrylate.

DISCUSSION AND CONCLUSIONS

The preliminary results indicate that the dual photon analog system is comparable to our previous digital system in precision and accuracy. There are numerous advantages for using the dichromatic analog system which are analogous to those of single photon direct readout analog systems (Mazess et al., 1972).

The dichromatic direct readout analog system eliminates the need for expensive digital output devices such as incremental magnetic tape recorders and interfaces; furthermore, it eliminates the need of computer or calculator for analysis of results. This greatly reduces the equipment as well as operation cost.

Since the dichromatic analog system is small in size, including the basic nuclear counting system, the total system can be readily miniaturized. Such a portable system has been completed earlier this year. The mobility provides a convenient mean in "field" measurement.

The immediate data readout is a third advantage. Often, either due to system error or other error such as patient movement during a scan, the immediate display of the results is extremely useful for correction and remeasurement. The immediate readout reduces data loss and prevents delay in analysis of data.

Although both single photon and dual photon direct readout analog systems can be used in bone mineral measurement of limbs, the unique capability of dichromatic attenuation technique enables us to do scanning of the lumbar vertebrae with ^{153}Gd. This methodological development is now being carried out in our laboratory. The dichromatic analog system should be easily applied to the vertebral scans.

These advantages suggest that the dichromatic direct readout analog system will prove useful in biomedical investigation of bone mineral content.

REFERENCES

Judy, P.F., M.G. Ort, K. Kianian and R.B. Mazess 1971. Developments in the dichromatic attenuation technique for the determination of bone mineral content in vivo. USAEC Progress Report COO-1422-97.

Mazess, R.B., J.R. Cameron and H. Miller 1972. Direct readout of bone mineral content using radionuclide absorptiometry. Int. J. Appl. Rad. Isot. 23: 471-479.

BONE GROWTH AND PHYSICAL ACTIVITY IN YOUNG MALES

Ronald C. Watson

Faculty of Physical Education, University of Western
Ontario, London, Ontario, Canada

ABSTRACT

Photon absorptiometry (^{125}I) was utilized to probe the
relationship between bone mineral content and the physical
activity of amateur baseball players ranging in age from
8 to 19 years (n = 203). The study focused principally
upon the dominant non-dominant differences in mineral
content within age groups and the changes in this variable
over age. Two small groups of non-competitive individuals
(n = 10), and baseball players over 19 years (n = 9) were
also measured. Upper and lower arm limb girths as well
as grip strength were measured to validate physical stress
dominance.

The most consistent finding throughout the investiga-
tion was that the dominant humerus was significantly
(p < 0.001) more mineralized for all age groups and the
degree of dominance increased significantly (p < 0.001)
with age. This characteristic held when the influence of
bone size was accounted for by testing the mineral/width
ratio. The patterns for mineral dominance of the radius
and ulna were inconsistent. Inspection of the data for the
three groups gave the impression that bone mineral differ-
ences between arms increased from the non-competitive group
to the main baseball sample to the older baseball group.
However, analysis of the relationship between mineral
dominance and the stress factors revealed insignificant
relationships. While humeral mineral dominance was real,
its relationship to physical stress remained in doubt.

Key words: Absorptiometry - Athletes - Bone Mineral Content -
Exercise - Growth and Development.

INTRODUCTION

Wolff's law (Bassett, 1965) predicts that "the form of the bone being
given, the bone elements place or displace themselves in the direction of the
functional pressure and increase or decrease their mass to reflect the
amount of functional pressure." Accordingly, exercise stress should lead

to increases (or decreases) in bone mass in man. Verification of this expectation is noticeably lacking. Bennett (1947), and Tullos and King (1972) have reported consistent humeral cortical hemihypertrophy in professional and amateur baseball players but the technical problems associated with the standard radiographic technique employed, and the lack of precise quantification undermine their findings. Similarly, the reports of Mashkara (1969) and Prives (1960), that physical labor and sports participation are related to skeletal growth, can be subjected to the same criticisms.

Nilsson (1971) found an apparent relationship between the type of physical activity and bone mineral content. Femoral mineral content determined by photon absorptiometry, increased in different athletic groups from a low in inactive controls to a high in international class weight-lifters. However, comparison of different groups does not answer the question of migration versus modification. Larger individuals may gravitate to events for which size and strength are important requisites rather than the events modifying the individual. In order to overcome the aforementioned difficulties, a photon absorptiometric technique was utilized to study the bilateral relationships for bone mineral content in the upper extremities of age-group baseball players.

METHODS

Two hundred and three volunteer, amateur baseball players, ranging in age from 8-19 years, were measured on the following variables: mineral, width, mineral-width, maximum limb girth, limb length and grip strength. The mineral and width measurements were taken at distal third of the forearm and mid-humerus. The principles and procedures of bone mineral and width assessment are outlined in Cameron (1963). Two small groups of non-competitive subjects (n = 10) and baseball players over 19 years of age (n = 9) were also measured for observational comparison with the main sample.

RESULTS

It is evident from Table 1 that the bilateral differences between the age-group means for the radius, ulna, and humerus do not show the same significance pattern. The most striking feature is the very consistent pattern of significance for humeral mineral, width, and mineral-width differences. The radius and ulna lack this inter- and intra- variable consistency. The differences between the bilateral means for forearm limb girth and grip strength are significant for all age groups (Table 2). Upper arm girth differences are significant for only the 16-17 and 18-19 age groups.

Figure 1 is presented to illustrate the pattern of change characteristic of humeral mineral, width, and mineral-width. Note that the bilateral difference increased over age groups. This was also true for forearm and upper arm girths as well as hand grip strength (Table 2). The degree of association between limb girth and mineral content was fairly high (relative to previous studies) for all of the associations (Table 3). However, when the influence of body weight was partialled out the relationships were very low. The standard error of estimate (SEE) associated with predicting bone mineral content from the various girths was about 18%. The sample was divided

Age	n	Mineral (g/cm)			Width (cm)			Mineral/Width		
		R	U	H	R	U	H	R	U	H
8-9	30	ns	ns	0.01	ns	ns	0.01	ns	ns	ns
10-11	38	0.01	0.01	0.01	0.01	ns	0.01	ns	0.01	0.01
12-13	38	ns	ns	0.01	ns	ns	0.01	ns	ns	0.01
14-15	35	0.01	0.01	0.01	ns	ns	0.01	ns	ns	0.01
16-17	32	0.01	0.01	0.01	0.01	ns	0.01	ns	ns	0.01
18-19	30	0.01	ns	0.01	0.01	ns	0.01	ns	ns	0.01

R = radius, U = ulna, H = humerus

Table 1: Newman-Keuls comparison of the bilateral differences in mineral, width, and mineral/width of the upper extremities in age-group baseball players.

Age	n	Forearm Girth (mm)		Upper Arm Girth (mm)		Grip Strength (kg)	
		$\bar{X}_d$	p	$\bar{X}_d$	p	$\bar{X}_d$	p
8-9	30	2.50	0.01	1.83	ns	1.82	0.01
10-11	38	4.92	0.01	3.76	ns	2.51	0.01
12-13	38	3.66	0.01	4.11	ns	2.92	0.01
14-15	35	7.51	0.01	5.40	ns	3.32	0.01
16-17	32	8.71	0.01	8.72	0.01	5.39	0.01
18-19	30	9.50	0.01	10.07	0.01	6.15	0.01

$\bar{X}_d$ = difference between means of each arm

Table 2: Newman-Keuls comparison of the bilateral differences in limb girth and grip strength in the upper extremities of age-group baseball players.
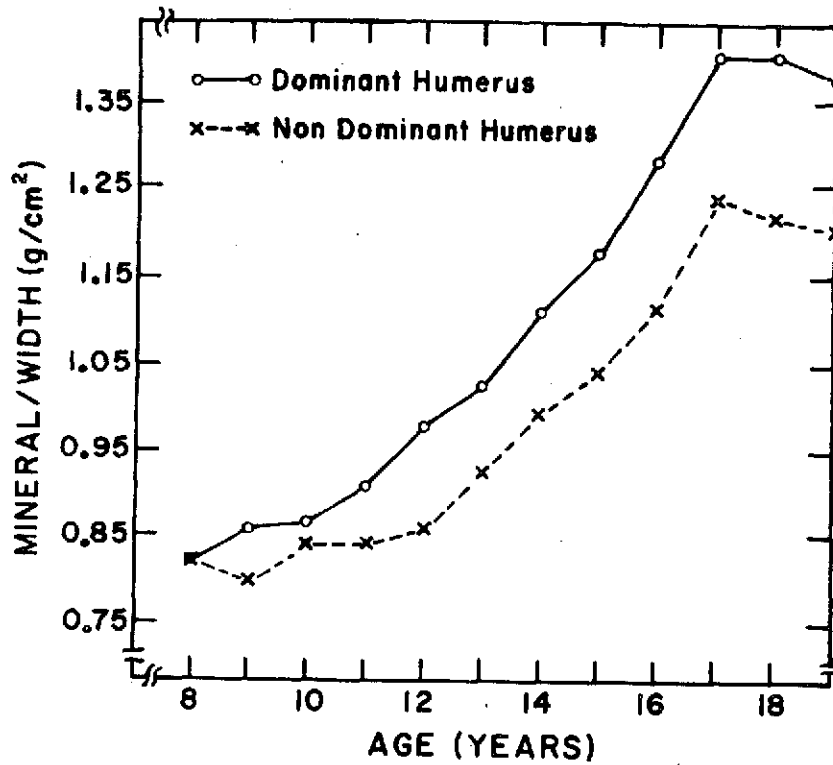
Figure 1: Bilateral changes in the mineral/width ratio of the humerus in age-group baseball players.

		r	Slope	Intercept	SEE
Mineral (DH)	Girth (DU)	0.832	0.012	-1.055	0.45
	Girth (DF)	0.738	0.014	-1.131	0.55
Mineral (NDH)	Girth (NDU)	0.810	0.012	-0.853	0.37
	Girth (NDF)	0.953	0.005	0.492	0.20

D = dominant, ND = non-dominant, H = humerus, U = upper arm, F = forearm

Table 3: Association between bone mineral content and limb girth in the upper extremities of age-group baseball players.

into three groups on the basis of per cent girth dominance. The 25th and 75th percentiles were used as the boundaries for the groups. An analysis of covariance (weight covariate) revealed that the three groups were not significantly different from one another. Newman-Keuls analysis showed no significant differences in forearm or upper arm length for most of the age groups.

DISCUSSION AND CONCLUSIONS

The consistently significant superiority of the dominant humerus on all the bone variables, while the corresponding forearm bones failed to demonstrate any consistent pattern of dominance, may have a number of explanations. This is not an unrealistic observation considering the stress brought to bear upon the arm segments in the act of throwing. It can be argued that the greater mass of the muscles whose origins and insertions are on the humerus, relative to the mass of those on the forearm bones, would make it possible for greater forces to be exerted upon the humerus in the act of throwing (Doyle, 1970). The forearm flexors and extensors, which insert on the proximal parts of the radius and ulna, are used principally to stabilize the elbow.

The failure of the forearm bones to demonstrate mineral dominance could be due to what Latimer (1965) referred to as "compensatory differences." The percentages of the baseball sample that showed greater mineral in the non-dominant radius (31.2%) and ulna (34.2%) were much larger than for the non-dominant humerus (3.0%). These percentages are considerably lower, particularly for the humerus, than the right-left bone weight asymmetry reported by Lowrance (1957).

The mineral-width ratio was used to control for differences in skeletal size. This is both a common and necessary procedure since bone mineral correlates significantly with height, weight, and bone width (Mazess, 1966). The bone widths in the present study were significantly larger on the dominant side. The correlations between humeral mineral and limb girth were higher than the value of $r = 0.65$ previously reported by Mazess (1966). While the baseball players demonstrated a stronger mineral-girth relationship, the interesting observation is that the average correlation ($r = 0.78$) is considerably lower on the dominant side compared to the non-dominant side ($r = 0.88$). Body weight accounted for almost all of the associations between mineral and girth. The fact that the baseball group had an average mineral dominance of 20% and only a 2% girth dominance, made it desirable to explore the extent of mineral dominance relative to girth dominance. The analysis of covariance (weight covariate) did not reveal significant differences among degrees of dominance. When weight was accounted for the low mineralized group was no different from the high mineralized group.

Comparisons made of the main sample with the non-competitive group and the older group of baseball players do not definitely indicate relationships in view of the small numbers and the preponderance of the younger ages in the non-competitive group. However, the non-competitive group had virtually no humeral mineral dominance and the older baseball players were more mineralized than were the younger baseball players. The impression created was that humeral mineral dominance is an exercise stress related phenomenon.

The difficulties experienced in trying to establish this relationship most likely stemmed from the criteria of stress employed. Limb girth dominance and grip strength dominance may not have been sufficiently sensitive to study the relationship. The high variability of these variables (coefficient of variations from 62 - 75%) certainly has to be considered as a principal limiting factor. The whole area of bone-muscle relationships is sufficiently devoid of strong associations to contribute to the limitations of the exercise stress factors. However, much of the difficulty surrounding the insignificant relationship between the exercise stress factors and mineral dominance may be as much a product of the high variability of mineral dominance (absolute 71%, relative 55%), as with the muscle-bone relationship.

REFERENCES

Bassett, C. and L. Andrew 1965. Electrical effects in bone. Scientific American 213: 18-25.

Bennett, G.E. 1947. Shoulder and elbow lesions distinctive of baseball players. Annals of Surgery 126: 107-110.

Cameron, J.R. and J. Sorenson 1963. Measurement of bone mineral in vivo: an improved method. Science 142: 230-232.

Doyle, F., J. Brown and C. LaChance 1970. Relation between bone mass and muscle weight. The Lancet 1: 391-393.

Griffiths, H.J., C.J. D'Orsi and E. Zimmerman 1972. Use of ^{125}I photon scanning in the evaluation of bone density in a group of patients with spinal cord injury. Invest. Radiol. 7: 107-111.

Latimer, H.B. and E.W. Lowrance 1965. Bilateral asymmetry in weight and in length of human bones. Anatomical Record 152: 217-224.

Lowrance, E.W. and H.B. Latimer 1957. Weights and linear measurements of 105 human skeletons from Asia. Am. J. of Anat. 101: 445-459.

Mashkara, K.I. 1969. Effect of physical labor on the structure of the bones of the upper extremities. Arkhiv Anatomii, Gistologii, i Embryologii 56: 7-15.

Mazess, R.B. and J.R. Cameron 1966. Skeletal growth in school children: maturation and bone mass. Am. J. of Phys. Anthrop. 35: 399-407.

Nilsson, B.E.R. and N.E. Westlin 1971. Bone density in athletes. Clin. Orthopaedics 77: 179-182.

Pande, B.S. and I. Singh 1971. One sided dominance in the upper limbs of human fetuses as evidenced by asymmetry in muscle and bone weight. J. of Anat. 109: 457-459.

Prives, M.G. 1960. Influence of labor and sport upon skeleton structure in man. Anatomical Record 136: 261.

Tullos, H.S. and J.W. King 1972. Lesions of the pitching arm in adolescents. J. Am. Med. Assoc. 220: 264-271.

****

DISCUSSION

A.M. Parfitt: What was the difference in width of the humerus between dominant and non-dominant sides? What was the contribution of size to the differences in mineral?

R. Watson: The dominant humerus was slightly wider, but the significant finding was the much greater mineral content.

THE EFFECTS OF PHYSICAL ACTIVITY ON BONE IN THE AGED

Everett L. Smith

Department of Preventive Medicine, University of Wisconsin, Madison, Wisconsin

ABSTRACT

Physical activity has been used as a preventive and rehabilitative therapy for osteoporosis. Few studies have accumulated data to support the concept that physical activity will prevent bone loss or increase bone accretion in an aged population. The purpose of this investigation was to study physical activity in slowing bone mineral loss and increasing bone accretion in the aged. Thirty-nine subjects were involved and included both sexes with an age range of 55 to 94 years. The subjects were studied for eight months with 21 in a control, 12 in a physical activity group, and 6 in a physical therapy group.

The physical activity group demonstrated a significant, ($p < .05$) bone mineral increase of 2.6 % during the 8 month study while the control group demonstrated no bone mineral change. The bone mineral value of the physical therapy group increased 7.8 % ($p < .05$). The bone mineral change from the first to the last measurement (T_4-T_1) between the control group and physical activity group was not significant of the .05 level. The bone mineral change (T_4-T_1) between the control group and the physical therapy group was significant ($p < .05$).

Key Words: Absorptiometry - Aging - Bone Mineral Content - Exercise - Physical Therapy.

INTRODUCTION

Age, genetics and environmental stresses affect the dynamic equilibrium of bone accretion and bone loss in man. Bone mineral in man decreases by about 15 % (Garn et al., 1967) in males and 24 % (Garn et al., 1967) in females between the ages of thirty and seventy. Bone has two main external physical stresses acting upon it: gravity and muscle contraction. Physical activity, which increases both gravitational and muscular stress in bone, has been suggested as a preventive and rehabilitative therapy for bone loss in the aged. However, few studies have been done to support this position.

Saville and Smith (1966) demonstrated that increased weight-bearing in bipedal rats caused an increase in bone mineral mass in the femora of rats. Chamay and Tschantz (1972), working with dogs, removed sections of each radius, thus causing increased weight-bearing of the ulna. The ulna

increased in bone mineral both at the periosteal surface and the endosteal surface. Smith and Felts (1968) and Saville and Whyte (1969) exercising mice and rats respectively on a motor driven treadmill demonstrated increases in bone mineral and bone strength in exercised groups compared to their control groups. Watson (1973) observed significantly increased bone mineral in the dominant humerus over the nondominant in 203 amateur male baseball players. He found that this lateral difference increased significantly with years of participation in boys 8 to 19 years of age. Nilsson and Westlin (1971) used the photon absorption technique to measure the femora bone mineral of 64 top athletes compared to 39 controls. The athletes demonstrated a significantly greater bone mineral than the controls. The athletes also showed bone hypertrophy in relationship to their specific sport activity. Weight lifters demonstrated greater bone mineral mass than throwers; throwers greater than runners, runners greater than soccer players and soccer players greater than swimmers. The control group consisted of an exercise group and a non-exercise group. The control exercise group was involved in regular physical activity and demonstrated a highly significant greater bone mineral than the non-exercise group.

Nilsson concluded that even moderate physical activity increased bone mass but could not conclude that physical activity would increase bone mineral or slow bone mineral loss in patients suffering from osteoporosis.

Therefore, the purpose of this investigation was to test the hypothesis that physical activity effectively slows the process of bone loss and may cause bone accretion in the aged.

METHODS

In vivo bone mineral mass measurements were obtained by using the Cameron-Sorenson technique of measuring the absorption of an ^{125}I monoenergetic (28 keV) beam in bone and soft tissue (Cameron and Sorenson, 1963; Sorenson and Cameron, 1967). The bone mineral and width of the radius were measured at a point one-third the distance from the olecranon to the head of the ulna. This point on the radius (called the standard site) is anatomically uniform and demonstrates minimal bone mineral and width variation on either side of the scanning site.

Subjects of both sexes age 55 to 94 years (n = 39) were involved in the study. The subjects were selected on the basis of cooperation, patient history, and their physicians approval. The subjects were placed into three groups on availability; 21 subjects in a control group, 12 subjects in a physical activity group, and 6 subjects in a physical therapy group. The standard radius site was measured over an eight month period -- on the first month (T_1), the fifth month (T_2) and the eighth month (T_3). The control group had no formal physical activity program during the study. The physical activity group participated in an exercise program for 8 months 3 times a week for 30 minutes. The average energy expenditure during the exercise sessions was 2 to 3 times the subjects' resting metabolic rate. The physical therapy subjects received supervised physical therapy which averaged 2 to 3 times their resting metabolic rate. These subjects were clinically similar and all lived in the Manor House of Madison Nursing Home.

RESULTS

The mean age of the three groups was 80.2 years for the control group, 74.8 years for the physical activity group, and 82.3 years for the physical therapy group. The bone mineral, bone width and bone mineral divided by bone width of the three groups were compared (Table 1).

The mean bone mineral changes are presented in Table 2. The bone mineral values showed a 0.4 per cent increase for the control group, a 2.6 per cent increase for the physical activity group, and a 7.8 per cent increase for the physical therapy group. A one tailed paired t-test demonstrated no significant change for the control group and a significant change at the .05 level for the physical activity and physical therapy groups.

The changes of bone mineral divided by bone width are also presented in Table 2. The bone mineral divided by bone width values demonstrated a -0.5 per cent decrease for the control group, a 1.7 per cent increase for the physical activity group and a 7.8 per cent increase for the physical therapy group. A one tailed paired t-test demonstrated no significant change for the control and physical activity groups, but a significant change at the .05 level was observed in the physical therapy group. There was no significant change in bone width in these groups.

The analysis of variance single classification for the change in bone mineral, bone width, and bone mineral divided by bone width is presented in Table 3. A significant change was obtained in bone mineral, and bone mineral divided by bone width. In order to examine group differences Duncan's (1957) multiple range post test was performed.

The study groups were arranged from the greatest to the least bone mineral change between T_1 and T_3 (Table 4). Between group differences were obtained by subtracting the mean value of the groups, $\bar{X}_i - \bar{X}_j$ where $\bar{X}_i$ is the mean of one group and $\bar{X}_j$ is the mean of a second group.

Duncan's multiple range test sequence for the significance of bone mineral at the standard site of the radius between groups were obtained from the formula $a_{ij} (\bar{X}_i - \bar{X}_j)$ where a_{ij} is the adjustment factor for the unequal numbers in the groups being compared.

The adjusted differences were compared to the significant range factor R'p* level of significant differences between the groups (Table 5). Duncan's multiple range test for bone mineral divided by bone width ranked treatment means were used for comparison of the physical therapy group to the control group. This comparison resulted in a ranked treatment mean difference of 0.046 g/cm^2 which was significant at the .05 level (Table 6). The comparison of the physical therapy group to the physical activity group resulted in a ranked treatment mean difference of 0.03 g/cm^2 which was not significant at the .05 level (Table 6). The comparison of the physical activity group to the control group resulted in a ranked treatment mean difference of 0.014 g/cm^2 which was not significant at the .05 level (Table 6).

MEASUREMENT	CONTROL		PHYSICAL ACTIVITY		PHYSICAL THERAPY	
	$\bar{X}$	S.D.	$\bar{X}$	S.D.	$\bar{X}$	S.D.
Age	80.2 years	9.8	74.8 years	10.0	82.3 years	4.6
Bone Mineral						
1st Month	0.80g/cm	0.22	0.86g/cm	0.36	0.80g/cm	0.27
5th Month	0.80g/cm	0.23	0.87g/cm	0.35	0.84g/cm	0.25
8th Month	0.80g/cm	0.24	0.88g/cm	0.38	0.86g/cm	0.25
Bone Width						
1st Month	1.31cm	0.17	1.34cm	0.21	1.44cm	0.14
5th Month	1.31cm	0.18	1.35cm	0.20	1.45cm	0.20
8th Month	1.30cm	0.16	1.34cm	0.21	1.45cm	0.17
Bone Mineral/Width						
1st Month	$0.61g/cm^2$	0.15	$0.63g/cm^2$	0.22	$0.55g/cm^2$	0.16
5th Month	$0.60g/cm^2$	0.14	$0.64g/cm^2$	0.21	$0.58g/cm^2$	0.15
8th Month	$0.61g/cm^2$	0.16	$0.65g/cm^2$	0.22	$0.60g/cm^2$	0.14

Table 1: Age, bone mineral content, bone width and bone mineral/bone width at the standard site of the radius for the control, physical activity and physical therapy groups during the eight month study.

GROUP	$\bar{d}$	%	S.D.	t-test	Sig.
Bone Mineral					
Control	.003g/cm	+0.4%	0.032	0.427	none
Physical Activity	.022g/cm	+2.6%	0.042	1.830	.05
Physical Therapy	.062g/cm	+7.8%	0.067	2.311	.05
Bone Width					
Control	0.006cm	0.4%	0.033	.86	none
Physical Activity	0.005cm	0.5%	0.040	.42	none
Physical Therapy	-0.015cm	-1.04%	0.038	.94	none
Bone Mineral/Width					
Control	$-0.003g/cm^2$	-0.5%	0.014	-1.00	none
Physical Activity	$0.011g/cm^2$	1.6%	0.028	1.38	none
Physical Therapy	$0.043g/cm^2$	7.8%	0.045	2.39	0.05

Table 2: Bone mineral, bone width and bone mineral/bone width change at the standard site of the radius in the control, physical activity and physical therapy groups during the eight month study T_1 to T_3.

Measurements	Source of Variation	df[*]	Sum of Squares	Mean Square	F Ratio	Sig.
Bone Mineral	Between Groups	2	0.0164	0.0082		
					4.7	.05
	Within Groups	36	0.0625	0.0017		
Width	Between Groups	2	0.0021	0.0011		
					0.8	none
	Within Groups	36	0.0474	0.0013		
Bone Mineral Width	Between Groups	2	0.0099	0.0049		
					8.2	.01
	Within Groups	36	0.0242	0.0006		

[*] Degrees of freedom

Table 3: Analysis of variance single classification for the bone mineral, bone width, and bone mineral divided by bone width changes at the mid-shaft of the radius during the eight month study T_1 to T_3.

Differences Between Groups ($\bar{X}_i - \bar{X}_j$)

Groups	$\bar{d}$	P.A. = 0.022 g/cm	C = 0.0003 g/cm
Physical Therapy	0.062 g/cm	0.040 g/cm	0.059 g/cm
Physical Activity	0.022 g/cm		0.019 g/cm
Control	0.003 g/cm	0.019 g/cm	

Table 4: Duncan's multiple range test ranked treatment means for bone mineral change at the mid-shaft of the radius between T_1 and T_3.

Groups $\bar{X}$	$\bar{X}_i - \bar{X}_j$	Adjustment Factor a_{ij}	Comparison Between Groups $a_{ij}(\bar{X}_i - \bar{X}_j)$	R'p	Sig.
P.T.-C.	0.059g/cm	3.06	0.184	0.124	.05
P.T.-P.A.	0.040g/cm	2.83	0.113	0.118	none
P.A.-C.	0.019g/cm	3.91	0.070	0.118	none

Table 5: Duncan's multiple range test sequence for bone mineral change at the mid-shaft of the radius between T_1 and T_3.

Groups $\bar{X}$	$\bar{X}_i - \bar{X}_j$	Adjustment Factor a_{ij}	Comparison Between Groups $a_{ij}(\bar{X}_i - \bar{X}_j)$	R'p	Sig.
P.T.-C.	0.046 g/cm^2	3.06	0.140	0.124	.05
P.T.-P.A.	0.032 g/cm^2	2.83	0.090	0.118	none
P.A.-C.	0.014 g/cm^2	3.91	0.054	0.118	none

Table 6: Duncan's multiple range test sequence for the bone mineral divided by bone width change at the mid-shaft of the radius between T_1 and T_3.

DISCUSSION

The hypothesis that physical activity effectively slows the process of bone loss and causes bone accretion in the aged was supported by the results of this study.

Physical activity slowed the normal process of bone loss. This was evidenced by a significant ($p < .05$) bone mineral increase of 2.6 per cent for the physical activity group (Table 2); however the bone mineral change during the eight month study of the physical activity group compared to the control group was not significant (Table 5). The physical therapy group demonstrated a significant ($p < .05$) bone mineral increase of 7.8 per cent between T_1 and T_3 (Table 2). The bone mineral divided by bone width change in the control group and the physical activity group was not significantly different between T_1 and T_3 (Table 2). The increased bone mineral divided by bone width value of 1.7 per cent for the physical activity between T_1 and T_3 demonstrates a positive trend even though not significant at the .05 level. The increased bone mineral divided by the bone width values of 7.8 per cent for the physical therapy group between T_1 and T_3 was significant ($p < .05$) (Table 2).

The greater mineralization of the physical therapy group in relation to the physical activity group may be due to the lower bone mineral present in the physical therapy group at the beginning of the study (0.80 g/cm versus 0.86 g/cm). The physical therapy group included some subjects who had been at bed rest for a number of weeks and were being rehabilitated. The lower starting bone mineral in conjunction with increased weight-bearing, muscular contraction, and a high degree of motivation should be considered in the significant bone mineral increase of the physical therapy group.

This study indicates that the bone mineral content of the elderly does increase with physical activity. The animal studies by Smith and Felts (1968), Saville and Whyte (1969), and Johnson (1927), all indicate that bone adapts to increased stress placed upon it by increased mineral content. Similar increased bone mineral was observed by Nilsson and Westlin (1971) in physically active national ranked athletes and an exercise group compared to a non-active control group. Vogel (1969) found remineralization upon activity of subjects on long-term bed rest who had lost as much as 40% of the bone mineral of the calcaneus.

The cause of the bone mineral increase in the physically active subjects in the study was not isolated. But present research and that reviewed would indicate the following contributory factors:
(1) an increased stress on the bone as a result of increased weight-bearing;
(2) an increased stress applied to the bone by increased muscular contraction
(3) an increase in growth hormone as a result of physical activity; or
(4) an increased blood flow to the bone as a result of cardiovascular stimuli during physical activity.

Regardless of the specific cause of the bone mineral increase of the subjects in this study, it appears that physical activity diminishes bone loss

with age and that physical therapy increases bone mineral content over that of non-active controls.

CONCLUSIONS

The hypothesis that physical activity effectively slows the progress of bone loss and causes bone accretion in the aged was supported by the results of this study. Physical activity slowed the normal process of bone loss, as seen by bone mineral increases of the physical activity group (2.6%) and the physical therapy group (7.8%). When compared to the control group, the physical activity group, while demonstrating a positive increase, was not significant for the 8 month period of the study; the physical therapy group when compared to the control group was significant.

REFERENCES

Cameron, J.R. and J.A. Sorenson 1963. Measurement of bone mineral in vivo; an improved method. Science 142: 230-232.

Chamay, A. and P. Tschantz 1972. Mechanical influences in bone remodeling. Experimental research on Wolff's law. J. Biomech. 5: 173-180.

Duncan, D.B. 1957. Multiple range tests for correlated and heteroscedastic means. Biometrics 13: 164-176.

Garn, S.W., C.G. Rohmann and B. Wagner 1967. Bone loss as a general phenomenon in man. Fed. Proc. 26: 1729-1736.

Johnson, R.W. 1927. A physiological study of the blood supply of the diaphysis. J. Bone Jt. Surg. 9: 153.

Nilsson, B.E.R. and Nils E. Westlin 1971. Bone density in athletes. Clin. Orthop. 77: 179-182.

Saville, P.D. and R.E. Smith 1966. Bone density; breaking force and leg muscle mass as functions of weight in bipedal rats. Amer. J. Phys. Anthro. 25: 35-40.

Saville, P.D. and M.P. Whyte 1969. Muscle and bone hypertrophy positive effect of running exercise in the rat. Clin. Orthop. 65: 81-88.

Smith, E.L., Jr. and W.J.L. Felts 1968. The effects of physical activity on bone. Bone Mineral and Body Composition Progress Report, University of Wisconsin, Department of Radiology, COO-1422-33.

Sorenson, J.A. and J.R. Cameron 1967. A reliable in vivo measurement of bone mineral content. J. Bone Jt. Surg. 49(A): 481-497.

Vogel, J.M. 1969. Changes in bone mineral content of the os calcis induced by prolonged bed rest. Fed. Proc. 28: 374.

Watson, R.C. 1973. <u>Bone Growth and Physical Activity in Young Males</u>. Ph.D. Thesis, University of Wisconsin, Madison, Wisconsin.

****

DISCUSSION

<u>G.D. Whedon</u>: Since many of us have for years been looking for something that would put bone back into osteoporotic patients or into older people, would you give us some detail on the regimens, particularly the physical therapy regimen. To paraphrase, how hard did you work these poor old folks?

<u>E.L. Smith</u>: I worked those old folks as long and as hard as they could and would tolerate. The exercise program was 3 days per week for 30 minutes. You first have to realize that the individuals that are confined to an institution, such as a nursing home, have a maximum work capacity of 2 to 3 Mets, while a community group will be 3 to 5 Mets. By Met I mean a metabolic equivalent, or that energy required to rest in bed. Therefore, their maximum -- and I have to stress their maximum -- energy expenditure is about 3 times what it takes to rest in bed. Therefore, the physical activities that they participate in have a very low energy cost for you and me but are very strenuous for the elderly.

The physical activities that the elderly subjects participated in were classified into 4 areas of consideration: 1) endurance, 2) range of motion, 3) muscle tone and strength, 4) balance and reflex. An example of the exercises that they participated in is the hand close. Hold your arm parallel to the floor, do not support it with anything, and close your hand and make a fist and open it up; close and make a fist and open it up. Now, if you do this at a rate of 2 per second for 30 seconds you'll find a tremondous tightening of the forearm muscles with the arm becoming very heavy for you to support.

From that little demonstration, you can see the amount of stress that's placed on the individual musculature. Now, for the elderly, this amount of activity far exceeds what they normally do thereby producing additional stress on the bone structure. This activity involvement should aid in maintenance and rehabilitation.

The exercises which the elderly group participated in ranged from 1.5 Mets (1.5 times the energy required to rest in bed) to about 3.5 Mets. The importance of physical activity for the elderly is to develop endurance in these individuals. Frequently, the most work an elderly person does in a nursing home is walking from their room down to the dining room for meals. Thus, a physical activity program for 30 minutes with activities that are geared from 1.5 Mets to 3.5 Mets is quite an additional stress. In order to meet their needs you must design your program with what I call sequential exercises in which an individual will begin an exercise at 1.5 Met and then move to an exercise at 3.5 Met without stopping, thereby increasing the individual's heart rate and blood pressure. The elderly work at each level of activity for a short duration -- when I say a short duration -- I mean anywhere from 30 seconds to a minute and a half. After an activity of 3.5 Mets we reduce the

level of activity to 1.5 Mets again, so that their blood pressure and heart rates will decrease. You repeat this sequence of high and low stress activities with the objective being to start them out with a series of activity they can sustain for 2 or 3 minutes without rest. In the course of working with a group for 4 to 6 months, you seek to develop a sustained continual activity for 10-15 minutes with few or no rest periods.

A.M. Parfitt: Why were these people in the nursing home? What effect did their diseases have on the results?

E.L. Smith: I excluded people with heart failure, venous disease and other diseases likely to affect bone.

A.M. Parfitt: What was the period of time between the onset of disease, with entry into the home, and start of your program?

E.L. Smith: I did not examine this in detail.

CORTICOSTEROID THERAPY ACCELERATED OSTEOPOROSIS
IN RHEUMATOID ARTHRITIS

Mark N. Mueller, Richard B. Mazess and John R. Cameron

Department of Medicine, University of Wisconsin
Hospitals, Madison, Wisconsin

ABSTRACT

Bone mineral content (BMC) at two sites of the radius was assessed in 236 Caucasian women with rheumatoid arthritis (RA), using monoenergetic absorptiometric scanning. To evaluate the effects of disease on bone separately from superimposed effects of corticosteroid therapy, examination at distal (D) and mid-shaft (M) sites of the radius were made on 127 rheumatoid women with no exposure to steroids (non CS) and 109 who had been treated with corticosteroids (CS). Individuals were matched for age, duration and severity of disease.

BMC, % change from normal

Severity	Stage@	N	RA, non CS D %	RA, non CS M %	N	RA, CS D %	RA, CS M %
Mild	I/II	47					
Definite	II/III	33	+1.3	-1.3	20	-12.5†	-8†
Classic	II	15	-6.3	-5.0	19	-17.5†	-18†
Classic	III	32	-13.8†	-15.0†	56	-30.0†	-25†
Classic	IV				14	-40.0†	-41.3†

†p is less than .05; @ function impairment (Steinbrocker); N = number of patients.

Decline in BMC was clearly related to duration of RA, and was significant after 3 years in the CS group, but only after 15 years in the non CS group. Loss of BMC was similar at both sites of measurement, and was equally severe in premenopausal and postmenopausal patients.

The data suggest that corticosteroid therapy has early and marked detrimental effects on the skeleton of women with RA which are superimposed on the disease effects. The premenopausal group were not spared such bone mineral loss.

Similar observations of bone mineral were made in a population of 77 male and female patients with a diagnosis of

asthma. Preliminary analysis indicates that:

(1) Asthma untreated with corticosteroids has no discernible detrimental effect on bone mineral content.

(2) Superimposition of corticosteroid therapy on the disease asthma is associated with no discernible effect on bone mineral content.

Thus, asthma patients treated with corticosteroids, even for prolonged periods with equivalent daily dosages, appear to be at less risk than patients with rheumatoid arthritis in terms of their bone mineral content.

Key Words: Absorptiometry – Asthma – Bone Mineral Content – Corticosteroid Therapy – Osteoporosis – Rheumatoid Arthritis.

****

DISCUSSION

H.W. Wahner: How do you explain the difference between bone loss in rheumatoid arthritis group with steroid and the absence of bone loss in the asthma group with steroid? Is it part of rheumatoid arthritis or is it due to the fact that asthma patients take steroids only intermittently?

M.N. Mueller: I believe the difference in bone loss in the two groups exposed to corticosteroids may be related to the difference in physical activity exhibited by patients with rheumatoid arthritis compared to asthmatics. Undoubtedly other as yet undefined factors also play a role. I do not believe the difference in bone mineral can be attributed to intermittancy of dose of steroids in the asthmatic group, since many of the asthmatics that we studied were on proportionately higher doses of steroid for periods of 3 years or more on a regular basis.

A.M. Parfitt: Have you studied any patients prospectively from the time of diagnosis or from the time of initiation of corticosteroid therapy?

M.N. Mueller: Yes, but it is difficult to generalize the results. However it is clear that some patients begin to lose bone very quickly after the start of therapy.

H.K. Genant: (Comment) I would like to comment on your findings of the absence of osteoporosis early in rheumatoid arthritis and the absence of localized osteoporosis.

We have studied over 200 RA patients with fine-detail radiographic technique and have observed mild to marked intracortical striation in the shafts of metacarpals and phalanges adjacent to involved joints while neighboring bones with uninvolved joints may show normal, uniformly compact cortex. Such findings may occur early in the course of RA before gross articular erosions are demonstrated. The involved joints, however, invariably

show periosticular soft tissue swelling, which raises the possibility of hyperemia as a cause of this localized osteoporotic appearance.

PROGRESS IN DUAL PHOTON ABSORPTIOMETRY OF BONE

R.B. Mazess, C.R. Wilson, J. Hanson, W. Kan, M. Madsen, N. Pelc and R. Witt

Department of Radiology (Medical Physics), University of Wisconsin Hospital,
Madison, Wisconsin 53706 U.S.A.

ABSTRACT

Dual photon absorptiometry has not been as extensively
investigated and utilized as has single photon absorptiometry
for measurement of bone mineral content. For several appli-
cations dual photon absorptiometry is not only useful but
essential. We have investigated the errors of precision and
accuracy associated with both single and dual photon methods.
A relative error function has been calculated for different
radionuclides and their combinations to illustrate the vari-
ation to be expected at different bone and soft tissue thick-
nesses as a result of counting statistics. This permits
choice of optimum sources for a particular application.
However, factors other than counting statistics, such as cost,
availability, range of desired applications, and desire for
accuracy, are more important in the choice of which method
and which source to use.

The errors associated with the fat content of soft tissue,
and the distribution of fat, have been assessed. In some
cases the dual photon approach eliminates or minimizes the
inaccuracies found with the single photon method. We have
also developed an instrument providing direct digital readout
of bone mineral content using the dual photon approach; this
may decrease some of the technical problems involved in clin-
ical application of the dual photon method. Finally the dual
photon method has been used for scanning of spinal bone mineral
with a 153-Gd source. These measurements have fairly high
precision and accuracy (1 to 3% error) and can be used to look
at the problem of localized spinal demineralization in osteo-
porosis. The method is also being developed for scanning of the
femoral neck and total body mineral.

Keywords: Absorptiometry - Bone Mineral Content - Dual Photon
Method - Effects of Fat - Optimization - Spine Scanning

INTRODUCTION

Single photon absorptiometry (SAT) for the determination of bone mineral content has had widespread acceptance (Cameron, 1970; Mazess, 1974). Use of absorptiometry at two discrete energies (DAT) has been far less widely investigated and utilized. Part of this gap in investigation has been due to the success of the single photon approach, which has inhibited efforts of measuring the same quantity, bone mineral content, using an apparently more complex method. The lack of suitable radionuclide sources with two discrete emissions at appropriate energies and the added equipment and operational requirements have also restricted interest, especially since the only apparent advantage is the elimination of the need for a constant tissue cover. However, one cannot apply the single photon method to areas of clinical interest, like the femoral neck, or the spine, or to measurement of total body mineral, and for these applications the dual photon approach is mandatory. We have attempted to examine the dual photon approach both to allow measurements not previously possible, as well as to provide an alternative to the single photon method on the limbs.

The fundamental bases for dual photon absorptiometry are well-known. Some of the first work on bone was done in Sweden by Jacobsen (1964). Judy (1970, 1971) has closely examined the theoretical grounds, and investigated the errors of precision and accuracy associated with both the dual photon and single photon approaches. Our laboratory has continued to examine these problems and to develop new instrumentation and methods. In this report we deal with some of our work, particularly with optimization with regard to counting statistics, the errors due to fat, dual photon direct digital readout, and spinal scanning.

COUNTING STATISTICS AND OPTIMAL SOURCES

Both Watt (1974) at Dundee and our laboratory have concentrated on the errors of precision introduced by counting statistics in order to optimize source selection for different combinations of soft tissue mass and bone mineral content. In order to make evaluations we calculate a relative error function (REF) which gives the actual variation when multiplied by the square root of the initial count rate, and thus provides a comparative index independent of the count rates. Figure 1 shows the REF is nearly always lower for the SAT than DAT; at least for this particular combination where the soft tissue is five times the mass of the bone. The SAT approach with ^{125}I has the lowest error for bones below the size of those of the forearm; for larger bones the SAT with ^{241}Am is optimal. Using the DAT it is evident that ^{109}Cd is optimal for finger bones; $^{125}I/^{241}Am$ and ^{133}Xe are optimal for radius and ulna; while ^{153}Gd is optimal for larger bones.

In considering optimization and precision one should remember that suboptimal counting statistics can readily be remedied by increasing the counts collected. The achievement of optimum conditions with regard to counting statistics is not the only, or even the major factor, in choice between the single and dual photon approaches or in the choice of the radionuclide. Errors of accuracy are also critical and there are the additional questions of cost, efficiency, availability, range of sites to be measured which dictate which approach and which source will be used.
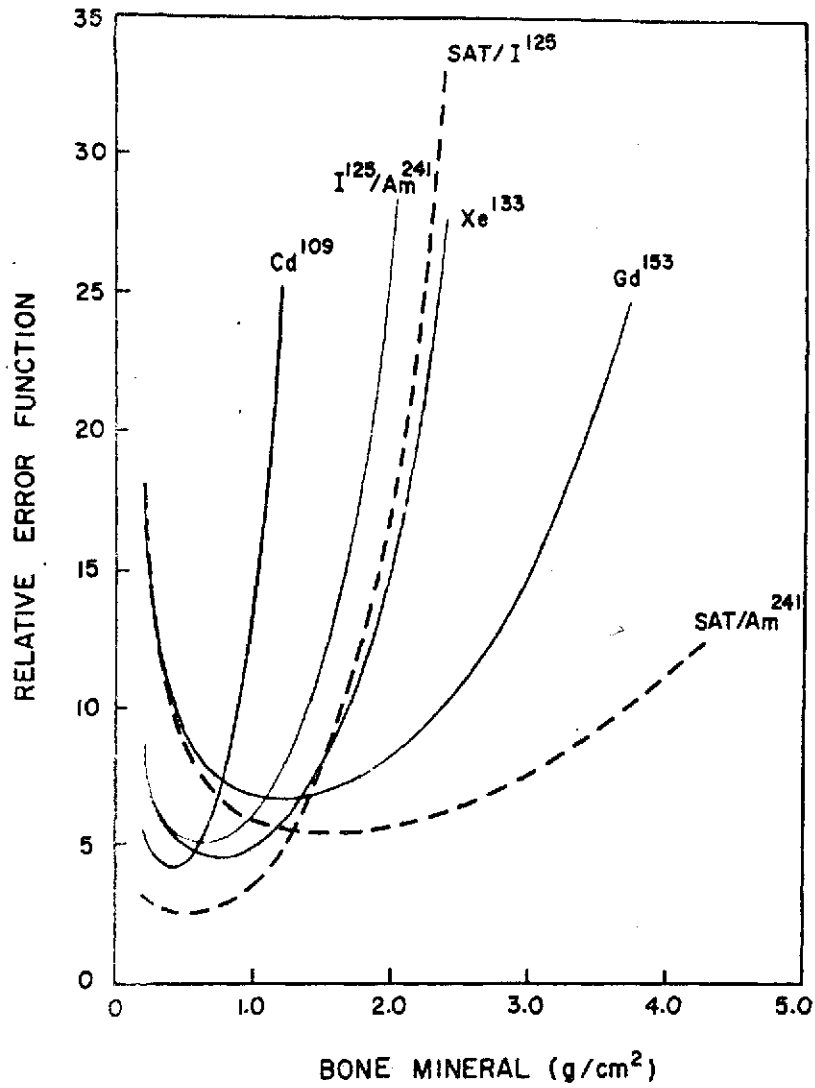
Figure 1. The relative error function for four
dual photon sources (solid lines) and two single
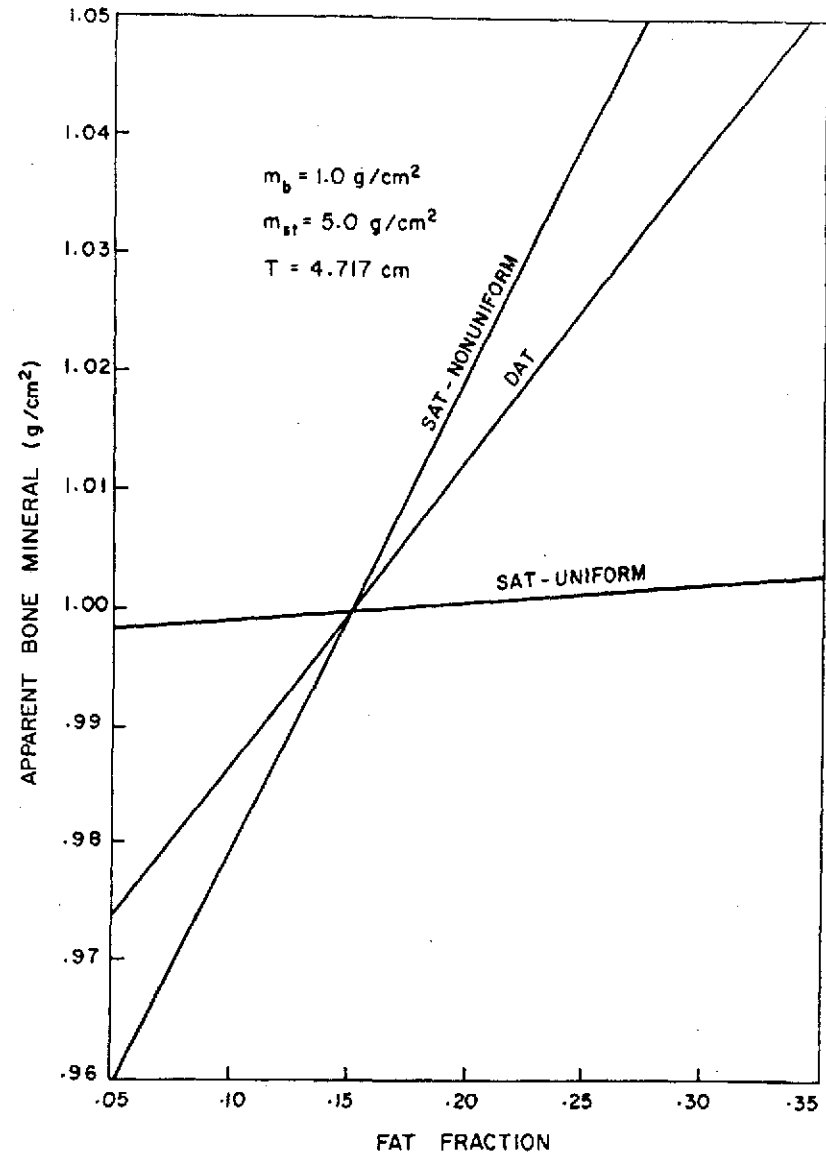photon sources (dashed lines).

Figure 2. The deviation from the actual mineral
content caused by fat for the SAT with 125-I
and the DAT with 125-I/241-Am.

EFFECT OF SOFT TISSUE DISTRIBUTION OVER THE BONE

The single photon approach to bone mineral measurement assumes that there is a constant thickness of soft tissue over the bone of uniform composition. The effect of varying amounts of fat, in a uniform layer, across the bone is quite small (Sorenson and Mazess, 1970; Wooten, 1973) but a non-uniform fat distribution can produce serious errors (Zeitz, 1973). Non-uniformities of fat distribution appear due to subcutaneous fat and to fat deposits adjacent to the bone. [If there is a record of the scan one may visually select an approximately appropriate I_o^* location or have a computer algorithm to do the same. With SAT direct readout devices, however, errors due to fat distribution cannot be readily corrected, and large discrepancies may occur particularly on obese individuals.] With the DAT there is an analagous problem, for at least when using the ^{153}Gd source one must assume a fat fraction in order to calculate bone mineral content. If the actual fraction deviates from the assumed an error will result. On the other hand when using the $^{125}I/^{241}Am$ dual photon source one may make an actual determination of the fat fraction adjacent to the bone. If there is a uniform fat distribution across the bone then no error is introduced by the fat. These relationships are shown in Figure 2. The apparent bone mineral content is seen to increase slightly for a uniform increase in the fat fraction with the single photon method using ^{125}I; very large deviations in the apparent bone mineral are seen if the fat fraction varies from the 15% level at which the SAT system is calibrated. The deviations for the DAT using $^{125}I/^{241}Am$ are somewhat smaller.

DIRECT READOUT OF BONE MINERAL CONTENT

Several years ago we developed an analog system for direct digital readout of bone mineral content using the single photon approach (Mazess et al, 1972). This type of instrument has proved to be quite useful because of low equipment and operational costs, ease of operation, portability, and the immediate availability of results without manual, calculator, or computer manipulation. These advantages have led us to develop a similar system using the dual photon approach (Kan et al, 1974). The dichromatic analog system operates similarly to the single photon model, but data is collected from two channels (Figure 3). A correction is made for spill-over into the lower energy channel, and logarithmic amplifiers are used. The precision and accuracy of this new instrument was comparable to that obtained with digital data treatment, or with the single photon approach. The results are independent of tissue cover.
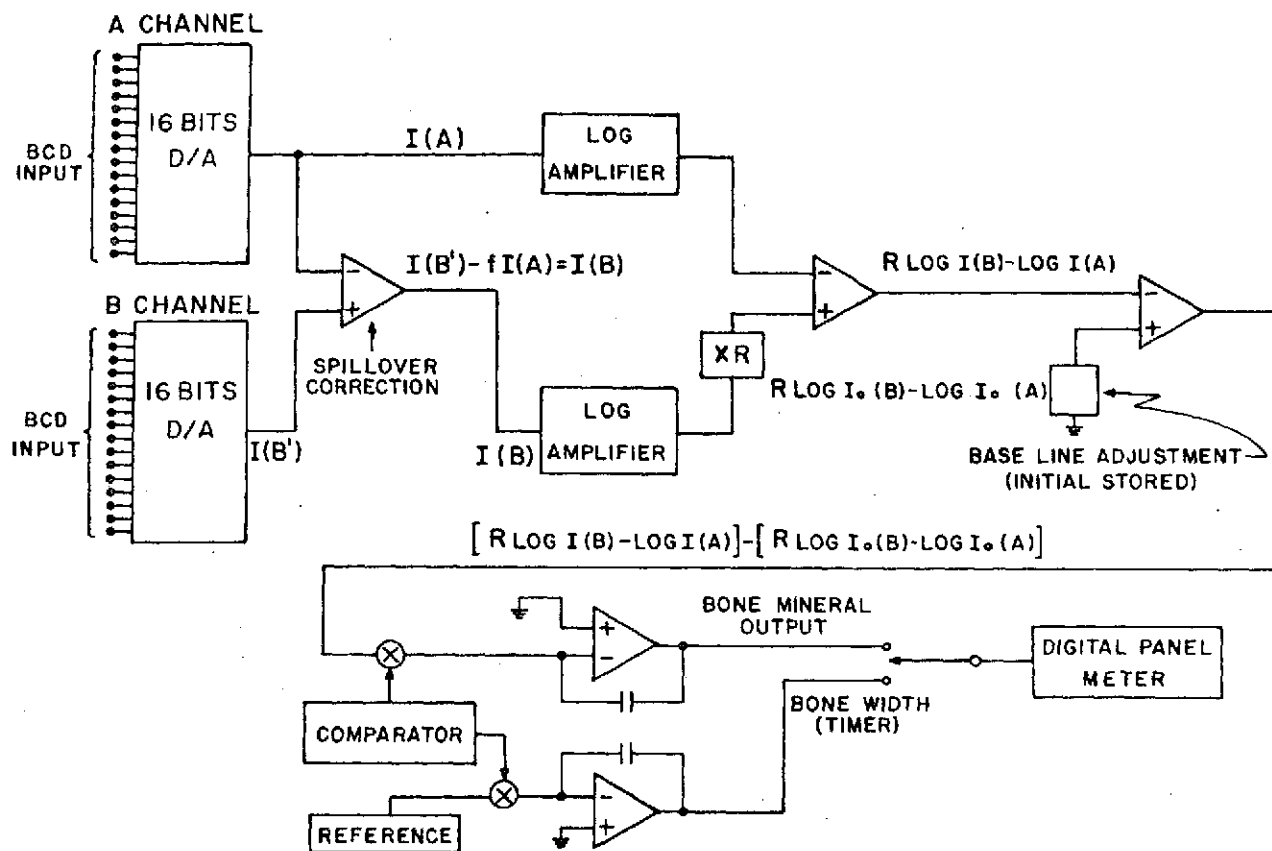
A CHANNEL

BCD INPUT — 16 BITS D/A — I(A) — LOG AMPLIFIER

B CHANNEL

BCD INPUT — 16 BITS D/A — I(B')

SPILLOVER CORRECTION

$I(B') - f\,I(A) = I(B)$

$I(B)$ LOG AMPLIFIER

X R

R LOG I(B)-LOG I(A)

R LOG I_o(B)-LOG I_o(A)

BASE LINE ADJUSTMENT (INITIAL STORED)

$$\left[\,R \text{ LOG } I(B) - \text{LOG } I(A)\,\right] - \left[\,R \text{ LOG } I_o(B) - \text{LOG } I_o(A)\,\right]$$

BONE MINERAL OUTPUT

COMPARATOR

REFERENCE

BONE WIDTH (TIMER)

DIGITAL PANEL METER

Figure 3. Outline of the analog calculator section of the dual photon direct readout system. The inputs are two channels of four decade scalers.

SCANNING OF THE SPINE, FEMORAL NECK, AND TOTAL SKELETON

In biomedical studies of the skeleton a measurement on the shaft of a limb bone, such as the common radius shaft measurement, is frequently considered inadequate for evaluating clinical problems although it has been demonstrated that in normal subjects a radius shaft measurement is not only correlated highly (r = 0.95) with the weight of the long bones and of the total skeleton (Mazess, 1971; Horsmann, 1970; Wilson, 1974; Cohn et al, 1974; Chestnut et al, 1973) but is moderately correlated with the mineral content of the vertebrae and the femoral neck (Wilson, 1974). However, for examination of patients a more precise, accurate, and direct measurement is often desirable, for example to assess spinal mineral in a patient with compression fractures or total body mineral in a renal patient. The single photon approach cannot be used for these determinations, and it is mandatory to use the dual photon approach. We have pursued the latter using [153]Gd as a source; this radionuclide has emissions at about 44 and 100 keV (see Figure 4).
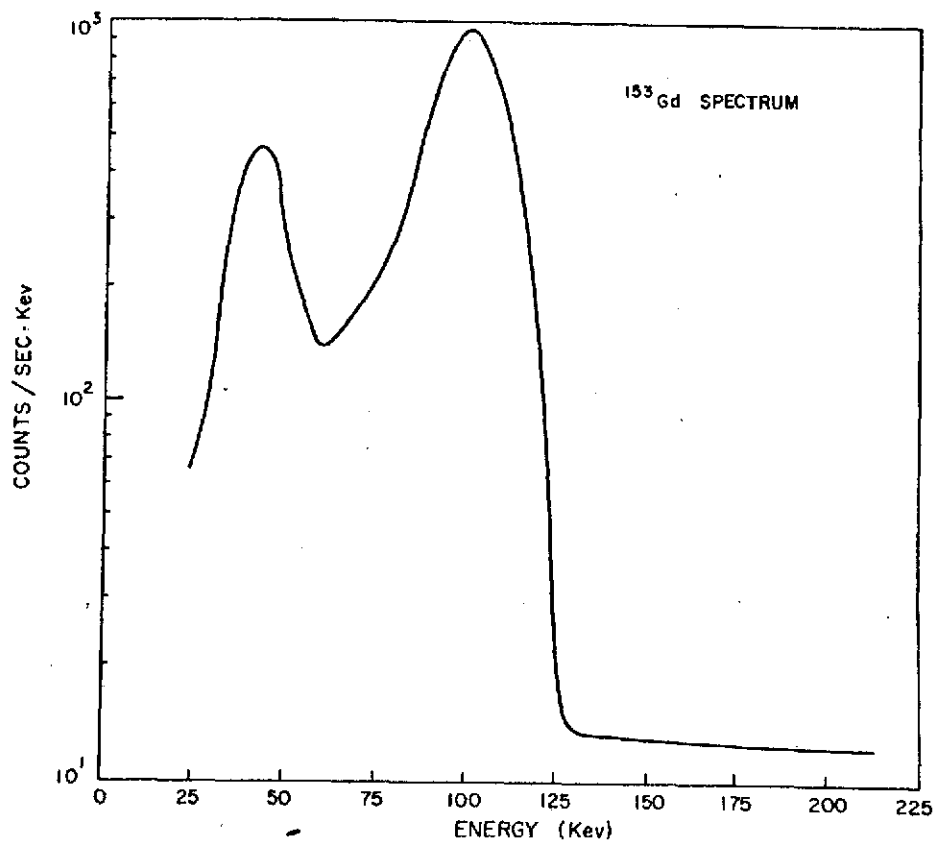
Figure 4. The spectrum of 153-Gd with peaks at 44 and
100 keV using NaI(tl) detector.

We initially began our scanning with a manually driven yoke, which was
imprecise, but we now have an Ohio-Nuclear Whole Body Scanner (Figure 5). The
pelvic phantom shown on the scanner was used to determine the dose received in
a typical spinal determination with 10 passes over the patient. The dosimetry
was done with thermoluminesence of lithium flouride crystals (TLD-100). The
dose to the skin, ovaries, and testicles for such a determination was 2.0, 0.09,
and 0.03 mrad respectively.
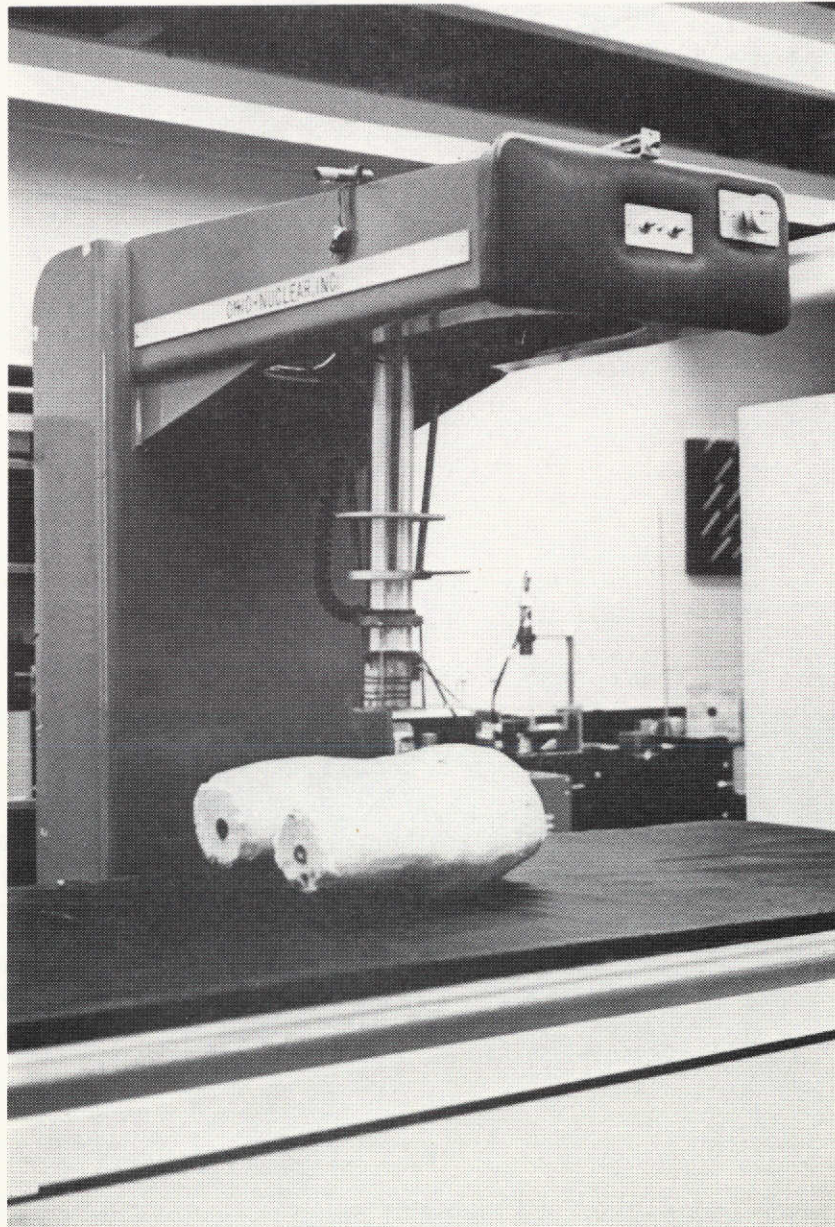
Figure 5. Ohio-Nuclear whole body scanner. Shown is the scanning yoke with modified scintillation-detector and a pelvic phantom.

In order to have exponential attenuation at both 44 and 100 keV it is necessary to make a correction for the Compton contribution from the 100 keV photons which are seen ("spill-over") in the lower energy channel. This correction was determined experimentally by filtering out the 44 keV peak with Cu and Al attenuators. After such correction the 44 keV peak shows exponential absorption (Figure 6).
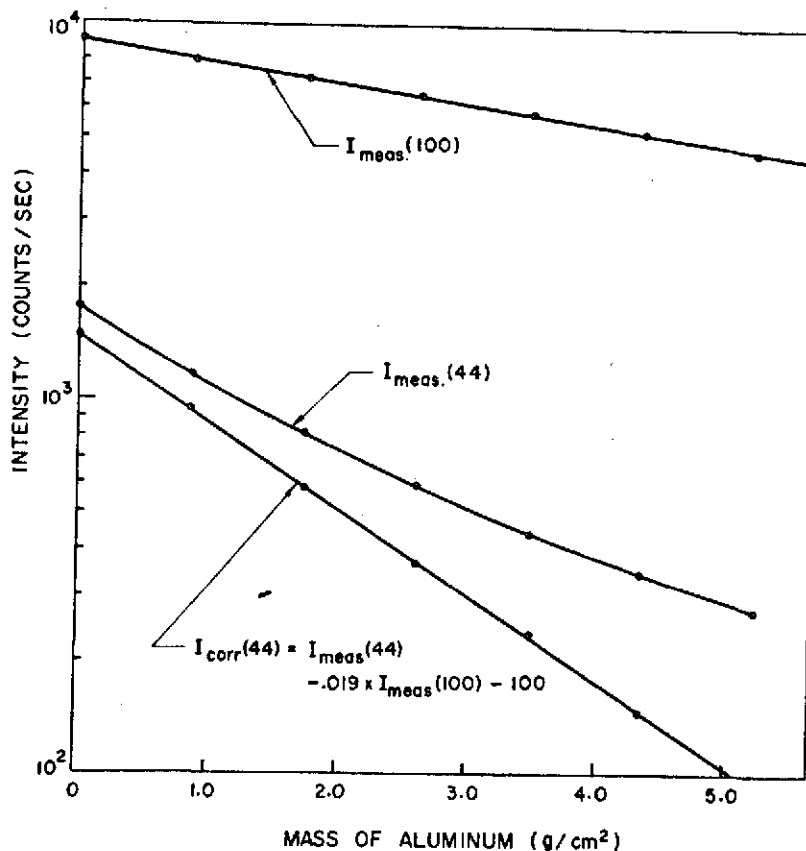
Figure 6. The attenuation of the 44 and 100 keV beams from ^{153}Gd by aluminum. Correction is necessary to achieve exponential attenuation at 44 keV.

The accuracy of determinations was assessed by measuring the mineral content of bottles filled with dipotassium hydrogen phosphate immersed in 15, 20 and 25 cm of water. The accuracy of measurement on these vertebral phantoms was very high (1 to 2%) (see Figure 7). Normal subjects have been measured on several occasions over a one month period with a precision of from 1 to 3%. We measure these subjects lying on their backs, the scan is started at the top of the iliac crest, and six passes are made at 1.25 cm intervals, so that a 7.5 cm section of the lumbar spine is measured. The bone mineral content along the spine tends to be relatively uniform (3% variation) in normal subjects; our preliminary results suggest that not only may there be demineralization in osteoporosis but that particular areas of the spine may show exaggerated osteopenia (Figure 8). We are currently investigating spine scans on normals and osteoporotics, and are further refining the system to do both the femoral neck and total body mineral.
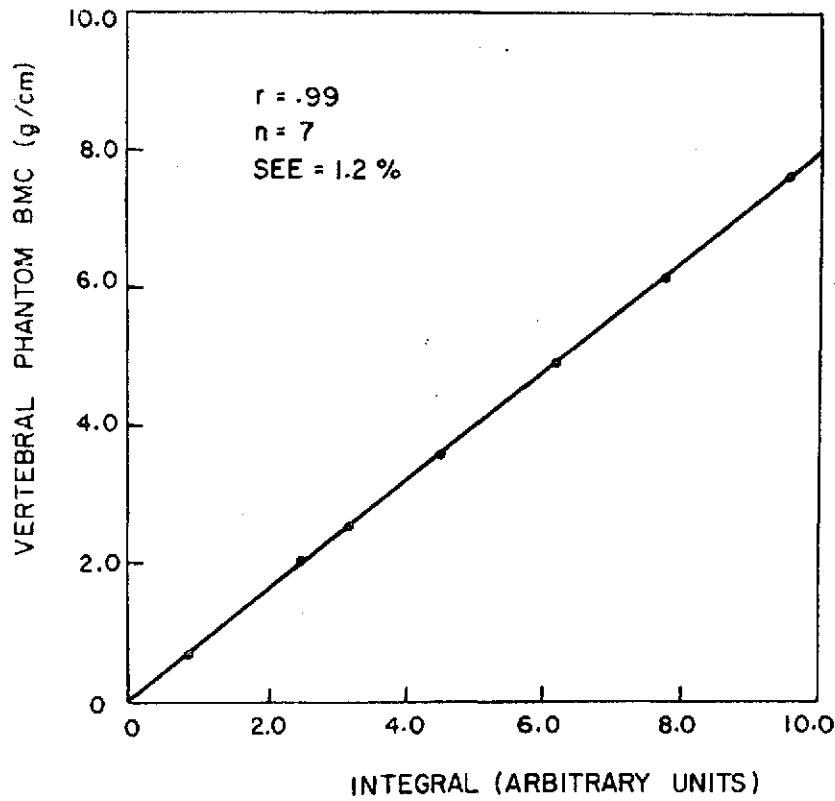
Figure 7. The accuracy of bone mineral determinations on dipotassium hydrogen phosphate standards immersed in a 20-cm water bath using ^{153}Gd.
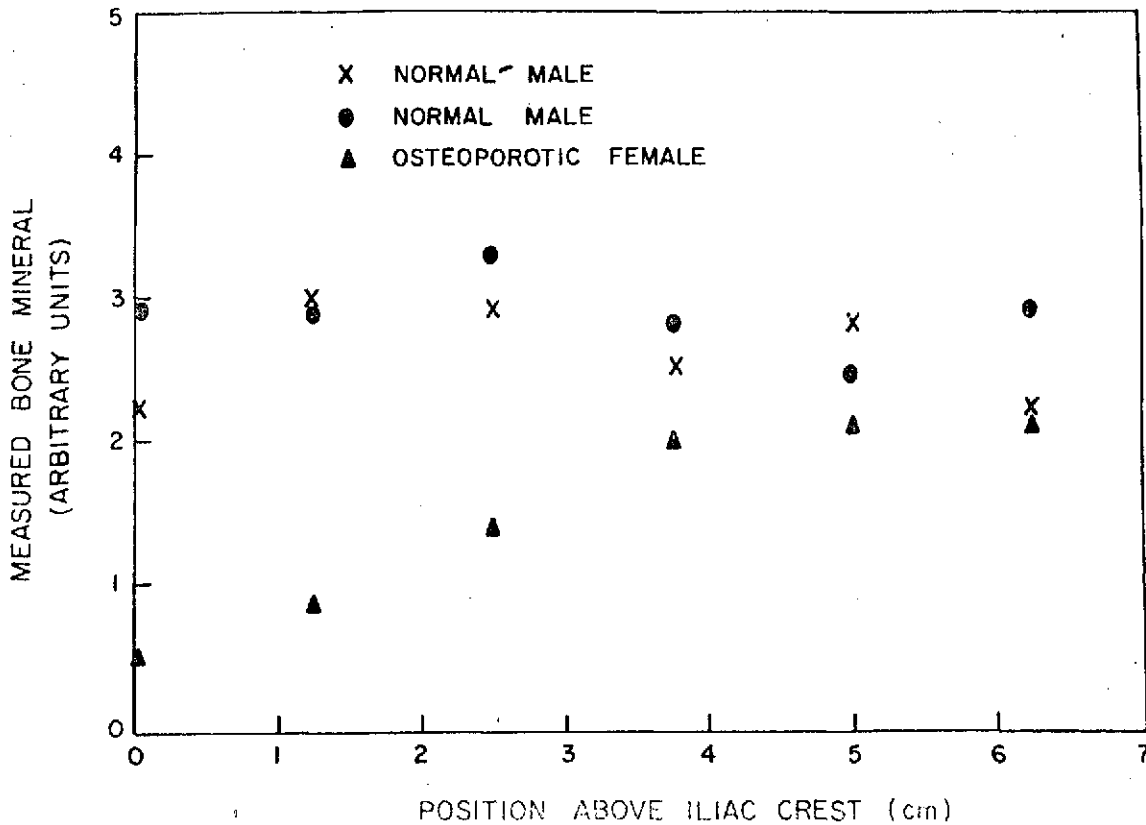
Figure 8. The distribution of measured bone mineral content (adjusted for bone width) in two normal males and in an osteoporotic female. The osteoporotic female appears particularly demineralized in the vertebral area immediately above the iliac crest.

DISCUSSION AND CONCLUSIONS

Dual photon absorptiometry is not an entirely novel technique but rather one which has not had a thorough and systematic evaluation. Lack of suitable sources, complexities of instrumentation, and uncertainties of the biomedical applications have produced this hiatus in our knowledge. Our efforts have been toward achieving some progress by (1) defining the errors of precision and accuracy, in order to achieve optimal technical conditions, (2) examination of new and interesting sources such as ^{153}Gd, (3) development of new instrumentation for direct digital readout of bone mineral, and (4) application of the dual photon approach to anatomical areas, such as the spine and femoral neck, where the single photon approach is inapplicable.

Some of the above developments in dual photon absorptiometry may be combined. For example direct digital readout could be used for spine scans with ^{153}Gd. This suggests that with only minor modification, and with minimal operational and equipment costs, many existing whole body scanners in nuclear medicine laboratories could be converted to measure spinal bone mineral content. Secondly a combined ^{125}I/^{241}Am source could be used to do measurement of both fat and lean components of the soft tissue, and the bone mineral content, in limb scans. We are now doing this routinely in our laboratory. This of course resolves some of the difficulties with uneven fat distribution over the bone, but perhaps more importantly it provides an indication of the muscle mass at the scan site. Such a measurement may be quite useful as a morphological reference against which one can assess normality of bone mineral content.

It is quite clear that in terms of ease and simplicity the single photon approach to measurement of bone mineral content has marked advantages over the dual photon approach. On the other hand the dual photon approach appears to have certain advantages and for certain applications, which in fact may be the critical applications for assessing skeletal disease, the dual photon approach is obligatory. Consequently it behooves us to examine the defects and the potential of that approach with care.

ACKNOWLEDGEMENTS

REFERENCES

Cameron, J.R. (Ed) Proceedings of Bone Measurement Conference, U.S. Atomic Energy Comm. Conf. 700515 (1970).

Chestnut, C.W., Manske, E., Baylink, D., and Nelp W.B, Correlation of total body calcium (bone mass) and regional bone mass, Clin. Res. 21: 200 (1973).

Cohn, S.H., Ellis, K.J., Zanzi, I., Letteri, J.M., and Aloia J., Correlation of radial bone mineral content with total-body calcium in various metabolic disorders, In: Proc. Intern. Conf. on Bone Mineral Measurement [Mazess, R.B. (Ed)], U.S. Govt. Printing Office, Washington, D.C. (in press).

Horsmann, A., Bulusu, L., Bentley, H.B., and Nordin, B.E.C., Internal relationships between skeletal parameters in twenty-three male skeletons, In: Proc. Bone Measurement Conference [Cameron, J.R. (Ed)], U.S. Atomic Energy Comm. Conf. 700515 (1970).

Jacobson, B., X-ray spectrophotometry in vivo, Amer. J. Roentgenol. 91: 202-210 (1964).

Judy, P.F., A Dichromatic Attenuation Technique for the In Vivo Determination of Bone Mineral Content, Ph.D. Thesis in Radiological Sciences, University of Wisconsin, Madison, Wisconsin (1971).

Kan, W.C., Wilson, C.R., Witt, R.M. and Mazess, R.B., Direct readout of bone mineral content with dichromatic absorptiometry. In: Proc. Intern. Conf. on Bone Mineral Measurement [Mazess, R.B. (Ed)], U.S. Govt. Printing Office, Washington, D.C. (in press).

Mazess, R.B., Estimation of bone and skeletal weights by direct photon absorptiometry, Invest. Radiol. 6: 52-60 (1971).

Mazess, R.B. (Ed) Proceedings International Conference on Bone Mineral Measurement, U.S. Govt. Printing Office, Washington, D.C. (in press).

Mazess, R.B., Cameron, J.R., and Sorenson, J.A., Determining body composition by radiation absorption spectrometry, Nature 228: 771-772 (1970).

Judy, P.F., Theoretical accuracy and precision in the photon attenuation measurement of bone, In: Proceedings of Bone Measurement Conference [Cameron, J.R. (Ed)], U.S. Atomic Energy Comm. Conf. 700515 (1970).

Sorenson, J.A., and Mazess, R.B., Effects of fat on bone mineral measurements, In: Proceedings of Bone Measurement Conference [Cameron, J.R. (Ed)], U.S. Atomic Energy Comm. Conf. 700515 (1970).

Watt, D.E., Optimum photon energies for the measurement of bone mineral and fat fractions, Brit. J. Radiol. (in press).

Wilson, C.R., Estimation of the bone mineral content of the femoral neck and spine from the bone mineral content of the radius and ulna, J. Bone Jt. Surg. (in press).

Wooten, W.W., Judy, P.F., and Greenfield, M.A., Analysis of the effects of adipose tissue on the absorptiometric measurement of bone mineral mass, Invest. Radiol. 8: 84-87 (1973).

Zeitz, L., Effect of subcutaneous fat on bone mineral content measurement with the "single-energy" photon absorptiometry technique, Acta Radiologica 11: 401-410 (1972).

PHYSICAL ASPECTS OF ^{125}I BONE ABSORPTIOMETRY

Philip F. Judy

Department of Radiology, Harvard Medical School,
Peter Bent Brigham Hospital, Boston, Massachusetts

ABSTRACT

The magnitude of the errors in the absorptiometric measurement of bone mineral mass has been estimated from a detailed physical description of the measurement and an analysis of the validity of the assumptions made in the derivation of the formula used to calculate the bone mineral mass. The derivation assumes exponential attenuation and a division of the human body into two components, each having a unique mass attenuation coefficient and density.

The accuracy of bone mineral absorptiometry using the radionuclide, ^{125}I, as the photon source was found to be determined by hardening the photon beam and variation in the distribution of adipose tissue in the body. The hardening error was estimated to be +2% when the system was calibrated over the biological range of bone mineral mass. The variations of adipose tissue thickness inside the bone and subcutaneously have been shown to depend critically on the method of determining the baseline. The errors caused by the detection of scattered radiation and the finite size of the photon beam have been shown to be less than 1% for a system calibrated by an ash study.

The instrumental reproducibility of the ^{125}I measurement of bone mineral mass has been limited by the number of photons detected. The activity of ^{125}I, the detector geometry, and the scan rate in the clinical instruments have been such that the precision of measurement of bone mineral mass of the radius is 1% -2%.

Key Words: Absorptiometry - Bone Mineral - Error Analysis.

INTRODUCTION

The physical processes that determine the absorption of photons, the scattering of photons, and the energy spectrum of x and gamma-ray beams have been described and can be used to predict the instrumental accuracy and precision of bone absorptiometry. The instrumental accuracy and precision

have been defined for this discussion as the accuracy and precision neglecting biological variation (e.g. patient movement and temporal changes in body composition). The instrumental accuracy and precision of bone absorptiometry using ^{125}I as the photon source have been evaluated empirically (Cameron et al., 1968). Excised bones were measured under water to stimulate the soft tissue surrounding the limb and the mass of ashed sections were compared with the absorptiometric measurement. Accuracies of 2 to 4% and precisions of 1 to 2% were reported for such ash studies. This paper will concentrate on the physical aspects of this particular technique that determine magnitude of these errors, because bone absorptiometry using ^{125}I has become the standard method for determination of appendicular bone mass in vivo.

The physical processes or parameters that have been shown to be significant in determining accuracy are hardening, photon beam size, x-ray scattering and spatial variation of soft tissue composition. They are significant in the sense that processes can be described and their contribution to the accuracy can be stated. In general, these errors are small with respect to the precision in vivo and the biological variability. The precision of the absorptiometric measurement has been estimated by propagation of the variance of Poisson probability distribution through the absorptiometric formula and has been shown to be a valid estimate of the instrumental precision (Judy, 1970).

Previous reports have used beam profiles to describe the spatial resolution aspects of bone absorptiometry (Judy, 1970). For the 3.2 mm detector aperture used in commercial systems, the measurements of bone mineral mass of radius was estimated to be not more than 0.05 g/cm less than the actual value, if the system was calibrated by an ash study. This error would be less than 1% for typical radii.

The ^{125}I source emits photons of energies of 27.2 keV to 35 keV. A measured spectrum from a ^{125}I source, that is filtered with tin, is shown in Figure 1. Using this spectrum and the mass attenuation coefficients for soft tissue and bone mineral, a theoretical analysis has predicted the transmission of this beam and an unfiltered beam (Sandrik and Judy, 1973). The theoretical analysis was verified by measurements. The error caused by hardening for a soft tissue cover of 7 cm was less than 2% from 0.5 to 1.8 g/cm of bone mineral mass, again, for a system calibrated by an ash study.

The soft tissues that surround bone are composed of proteins, lipids and water. The mass attenuation coefficients of protein and lipid are less than that of water as illustrated in Figure 2 (Hubbell, 1969). The lipid content of adipose tissue is large compared to that of other soft tissues. The consequence of this on the measurement of bone mineral mass has been analyzed mathematically (Wooten et al., 1973) and experimentally (Zeitz, 1972). The mathematical analysis suggested error caused by adipose tissue inside the bone should be less than 2%. Experimentally errors of 30% have been claimed and are consistent with distribution of adipose tissue in the phantom used to simulate the subcutaneous adipose distribution. The consequence of these results in estimating the error caused by subcutaneous adipose tissue in non-obese patients depends primarily on the distribution of the adipose tissue and the method of determining the baseline.

The detector apertures size and source collimation has been shown to be such that as much as 10% of the photons detected have been scattered (Judy, 1971). This paper will describe an investigation of this.
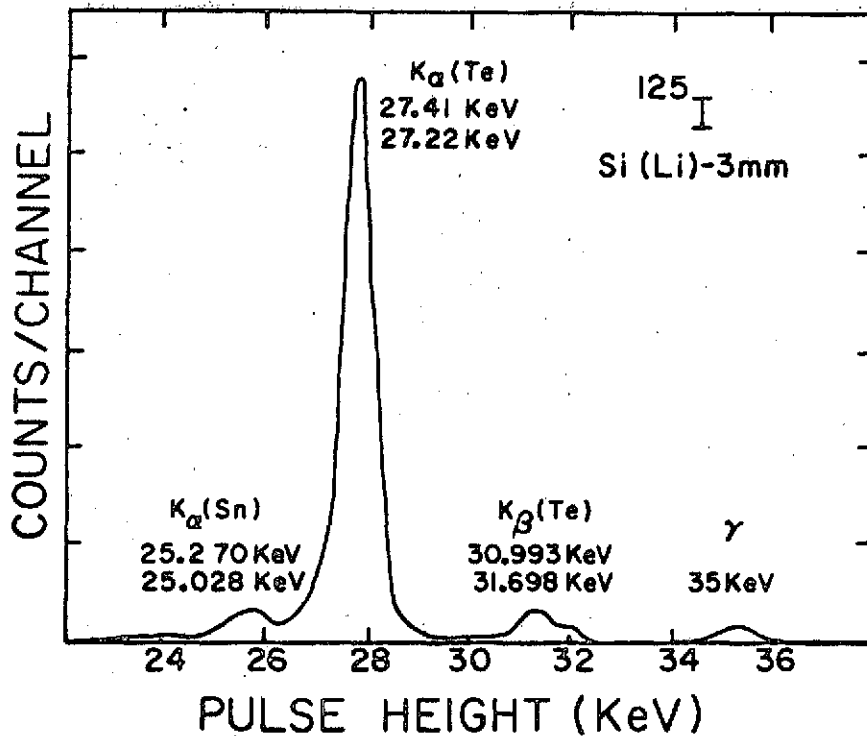

Figure 1: Spectrum of the ^{125}I beam using a Si(Li) x-ray spectrometer. The ^{125}I source had a 0.05 mm tin filter. The Si(Li) detector was 3mm thick.

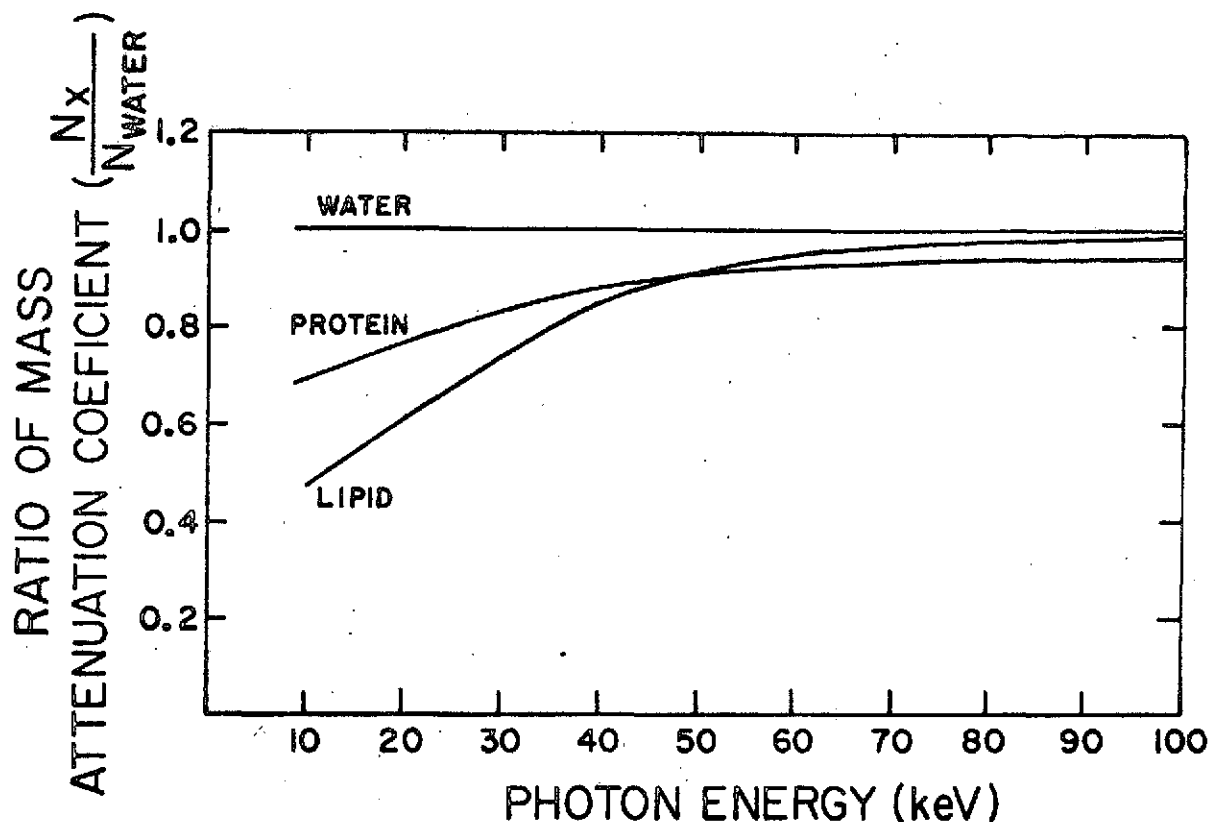**Figure 2:** The ratios of the mass attenuation coefficients of water to lipid and water to protein as a function of photon energy.

METHODS

The measurements to evaluate the effects of scatter were made with a measurement apparatus consisting of

1. The source
2. Collimated detector
3. Electronics.

The intensity of the beam was measured with the collimated NaI(Tl) scintillation detector. The detector assembly acted as a radiation shield to reduce the background. The detector aperture diameter was varied by changing the inserts that had diameters from 1.58 mm to 12.7 mm and a height of 3.5 cm. The assembly could be clamped 9 cm to 19 cm from the source position, bottom of assembly to the source. The integral mounted NaI(Tl) crystal and photomultiplier tube slid into the assembly and was held in place with a ring clamp. The NaI(Tl) crystal was 3 mm thick and 13 mm in diameter with a 0.025 mm thick aluminum window.

The detector was greater than 99% sensitive for the photons from ^{125}I. The electronics used, high voltage supply, amplifier, single channel analyzer, scaler and timer, were components of a gamma-ray spectrometer. The analyzer setting for the ^{125}I beam was a lower level of 21 keV with a window of 14 keV.

The scattered intensity to unattenuated intensity for a particular phantom thickness was estimated from Equation 1.

$$S(A) = R(A) - \lim_{A \to 0} R(A) \tag{1}$$

where $R(A)$ = ratio unattenuated intensity to detected intensity

A = area of circular aperture

The ratio, $R(A)$, has been measured for various methyl methacrylate thicknesses as a function of detector aperture size. Corrections were made for background and count rate loss. The methyl methacrylate rested on the platform 3 cm from the source. Results for 6.9 g/cm^2 of methyl methacrylate are shown in Figure 3. To obtain the limiting value of $R(A)$ the curve shown was fit by hand. An expression for the scattered radiation detected has been derived (Judy, 1971).

$$S(A) = e^{-\mu t/\rho} \ (e^{C\sigma s/\rho^t} - 1) \tag{2}$$

where t = thickness of phantom expressed as mass per unit area traversed

$\sigma s/\rho$ = mass scatter cross-section

C = a function that accounts for the geometry of a particular situation

μ/ρ = mass attenuation coefficient

The product, $C\sigma s/\rho$, was estimated by least squares regression analysis of measurement of $S(A)$ for various phantom thicknesses. This product is called the effective scatter cross-section.
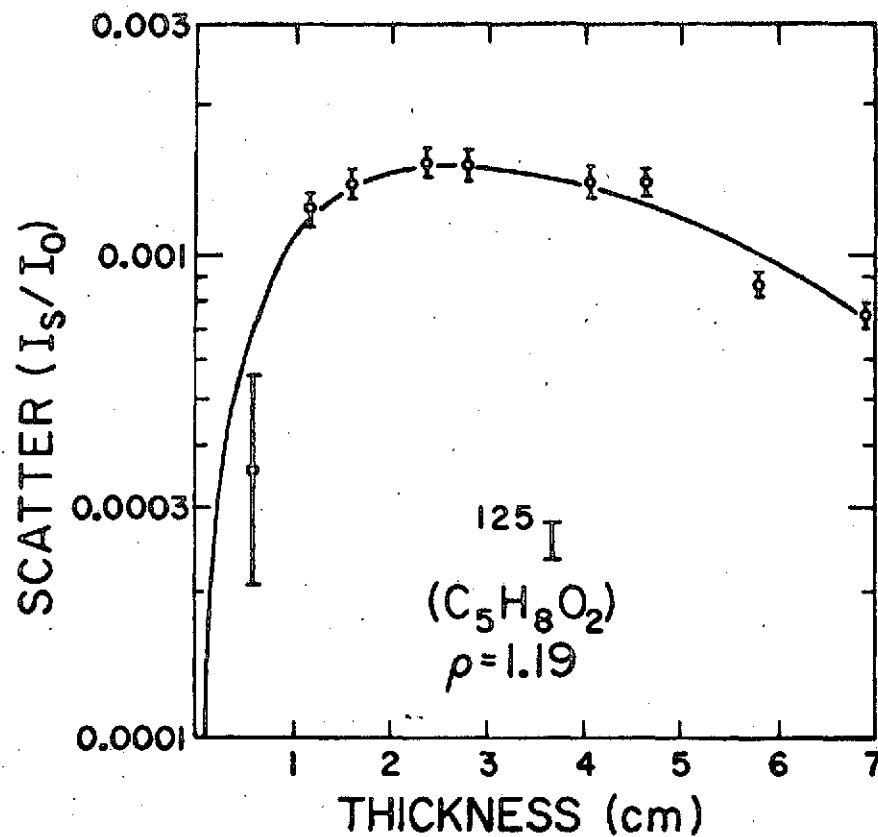
Figure 3: The transmitted intensity of the [125]I
beams by 6.89 g/cm² of methyl methacrylate
as a function of detector aperture area.

RESULTS

The scatter to unattenuated ratio for various thicknesses of methyl
methacrylate is shown in Figure 4 with least squares regression curve
fit to Equation 2. This is for a detector aperture of 6.4 mm. Effective
scatter cross-sections in methyl methacrylate were estimated for various
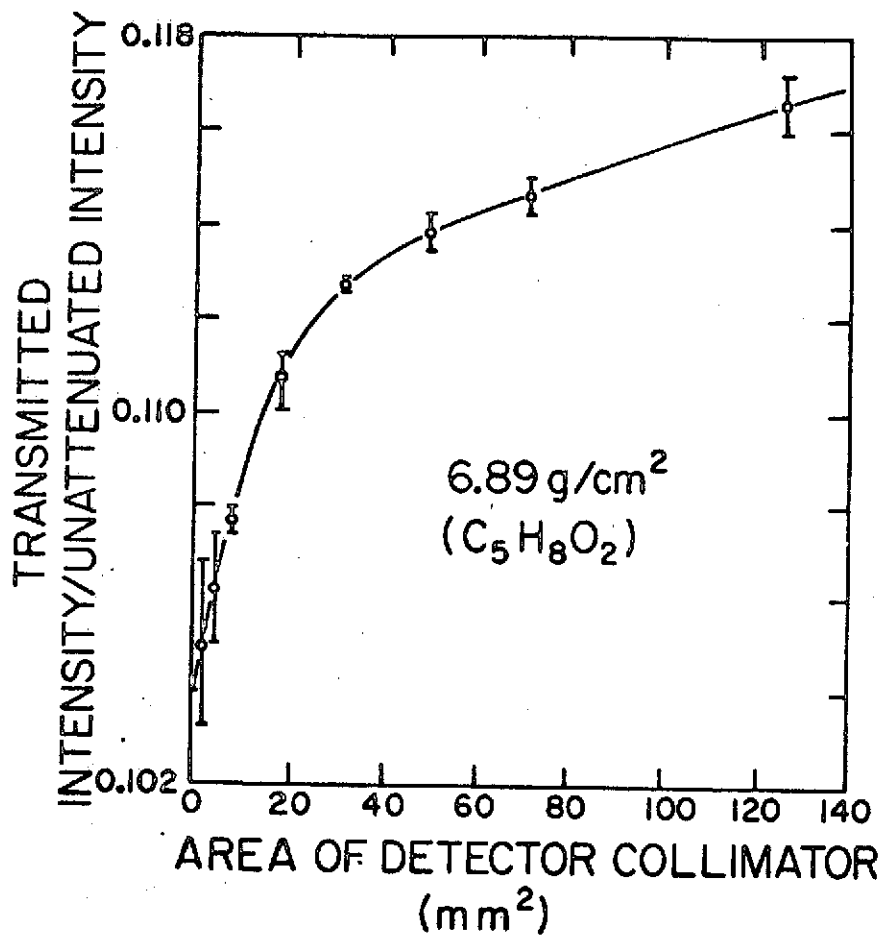detector apertures and are summarized in Table 1.

Figure 4: The scatter detected for the ^{125}I beam as a function of methyl methacrylate thickness. The detector aperture diameter was 6.4 mm. The solid line is the best fit to Equation 2.

Diameter (mm)	$(cm^2/g \times 10^{+3})$
1.59	1.30 ± 0.5
2.38	4.14 ± 0.8
3.18	5.63 ± 0.8
4.76	10.0 ± 1.2
6.35	12.8 ± 0.6
7.94	14.3 ± 1.0
9.52	15.1 ± 1.0
12.7	17.4 ± 0.9

Table 1: Effective scatter cross-sections of methyl methacrylate for ^{125}I beams.

These experimental scatter cross-sections have been compared with the theoretically calculated values (Davisson, 1965) in Figure 5. The calculation includes the incoherent and coherent scattered radiation in the direction between 0 and θ_{max}. There is an uncertainty in the maximum scattering angle θ_{max} for the experimental data that has two sources.

1. The angle the detector views is a function of depth in the attenuator.

2. The beam is diverging.

The error bars in the angle are ranges of the maximum scattering angle possible for each detector aperture. The theoretical values for carbon and oxygen are shown. Methyl methacrylate is 60% carbon, 32% oxygen and 8% hydrogen.
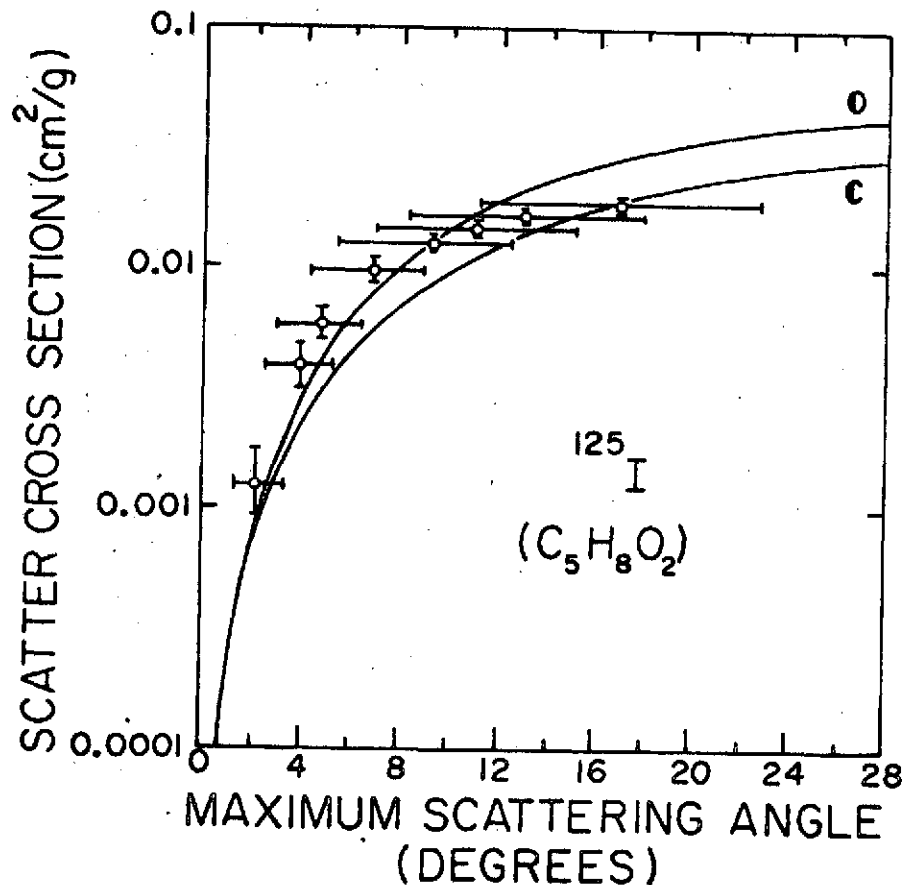

Figure 5: Measured scatter cross-section of methyl methacrylate as a function of maximum scattering angle. The solid lines are the theoretical values for carbon and oxygen (Davisson, 1965).

DISCUSSION AND CONCLUSIONS

The transmission of a substance in geometries chosen to simulate ^{125}I bone absorptiometry has been shown to be described by

$$I_T = I_o e^{-(\mu/\rho + C_1 \sigma_s/\rho) t} \qquad (3)$$

This equation was derived from Equation 2, which was shown to be valid within the limits of the experiment. This indicated the transmission remained exponential, which is all that is required for the formula used in ^{125}I bone absorptiometry. The scatter cross-sections have a slight dependence on the composition of the material increasing as the atomic number increases, $z^{1/3}$, (Hubbell, 1969).

The scatter cross-sections for bone mineral will be slightly larger, but the transmission will remain exponential and the detection of scattered photons should not effect the accuracy of ^{125}I bone absorptiometry.

The accuracy of ^{125}I bone absorptiometry is limited by the uncertainty and variation of soft tissue composition over and in the bone. The magnitude of this error has been estimated to be from 2% (Wooten et al., 1973) to as large as 30% (Zeitz, 1972). In a particular measurement, the error depends on the actual adipose distribution. The instrumental accuracy determined by other physical processes not adequately described by a single exponential formula (i.e. hardening, scatter and finite beam size) can be reduced to less than 2% by calibrating the measurement system with an ash study.

REFERENCES

Cameron, J.R., R.B. Mazess and J.A. Sorenson 1968. Precision and accuracy of bone mineral determination by direct photon absorptiometry. Invest. Radiol. 3: 141-150.

Davisson, C.M. 1965. Private communication.

Hubbell, J.M. 1969. Photon cross-sections, attenuation coefficients from 10 keV to 100 keV. National Bureau of Standards, NSRDS-NBS29. U.S. Department of Commerce, Springfield, Va.

Judy, P.F. 1970. Theoretical accuracy and precision in the photon attenuation measurement of bone mineral. In: J.R. Cameron (ed) Proc. Bone Measurement Conference. U.S. Atomic Energy Comm. Conf. 700515. U.S. Department of Commerce (CFSTI), Springfield, Va.

Judy, P.F. 1971. A Dichromatic Attenuation Technique for the In Vivo Determination of Bone Mineral Content. Ph.D. Thesis, University of Wisconsin, Madison, Wisconsin.

Sandrik, J.M., and P.F. Judy 1973. Effects of the polyenergetic character of the spectrum of ^{125}I on the measurement of bone mineral content. Invest. Radiol. 8: 143-149.

Wooten, W.W., P.F. Judy and M.A. Greenfield 1973. Analysis of the effects of adipose tissue on the absorptiometric measurement of bone mineral mass. Invest. Radiol. 8: 84-89.

Zeitz, L. 1972. Effect of subcutaneous fat on bone mineral content measurements with the "single-energy" photon absorptiometry technique. Acta Radiol. 11: 401-410.

BONE MINERAL CONTENT OF
NORTH ALASKAN ESKIMOS

Richard B. Mazess* and
Warren Mather

ABSTRACT

Direct photon absorptiometry was used to measure
the bone mineral content of forearm bones in Eskimo
natives of the north coast of Alaska. The sample con-
sisted of 217 children, 89 adults, and 107 elderly (over
50 years). Eskimo children had a lower bone mineral con-
tent than United States whites by 5 to 10% but this was
consistent with their smaller body and bone size. Young
Eskimo adults (20 to 39 years) of both sexes were similar
to whites, but after age 40 the Eskimos of both sexes had
a deficit of from 10 to 15% relative to white standards.
Aging bone loss, which occurs in many populations, has
an earlier onset and greater intensity in the Eskimos.
Nutritional factors of high protein, high nitrogen, high
phosphorus, and low calcium intakes may be implicated.

*Reprint available upon request

BONE MINERAL CONTENT IN CANADIAN ESKIMOS

Richard B. Mazess* and Warren E. Mather

ABSTRACT

Bone mineral content was measured using direct photon absorptiometry in the forearm bones of Canadian Eskimos in the northern Foxe Basin. The sample consisted of 177 children, 92 young adults and 66 older adults. Canadian Eskimo children had slightly lower bone mineral (4 to 5%) than Alaskan Eskimo children, and much lower bone mineral (10 to 13% than U.S. Whites), but these group differences were commensurate with the lower weights of the Canadian children. Throughout adulthood Canadian Eskimo bone mineral was almost identical on the average with values for Alaskan Eskimos; the major differences were lower mineral-width ratios in the Canadian Eskimo males over 50 years of age. Thus the Canadian Eskimo-White differences paralleled the relative deficit demonstrated for Alaskan Eskimos in a previous study, with the exception that relative bone loss in elderly males seemed even greater in the Canadian than Alaskan group. Eskimo males had a bone loss of about 10% a decade, and Eskimo females about 15% a decade, beginning in the forties; this was about 5% per decade for both sexes greater than the aging bone loss seen in U.S. Whites, and the onset of the bone loss was a decade sooner in Eskimo males.

*Reprint available upon request

BONE MINERAL CONTENT OF CANADIAN
AND ALASKAN ESKIMOS

Richard B. Mazess

For the Third International Symposium on Circumpolar
Health, Yellowknife, Northwest Territory, Canada

ABSTRACT

Direct photon absorptiometry with ^{125}I was used to
measure the bone mineral content on the limbs of Eskimos
from the north coast of Alaska (Wainwright, Point Hope,
Barrow) and from Canada (Hall Beach and Igloolik). In
Alaska the measurements were made on 413 subjects of
which 217 were children between 5 and 19 years. In
Canada there were 335 subjects of which 117 were children.

U.S. Whites were taller and heavier than Alaskan
Eskimo males and taller than Alaskan Eskimo females; the
Alaskan Eskimos were taller and heavier than their
Canadian kin. Canadian Eskimo children had lower bone
mineral content than Alaskan children who were in turn
lower than U.S. Whites. Both Canadian and Alaskan Eskimo
young adults were similar to U.S. Whites but with aging
both groups showed a relatively large loss of bone com-
pared to Whites. These results in contemporary Eskimo
groups correspond to the high bone loss seen in the
skeletons of the Sadlermiut archeological series. A
chronic high protein diet may be one of the key factors
responsible for the early onset and large magnitude of
aging bone loss in Eskimos.

BONE MINERAL CONTENT IN ALASKAN ESKIMOS

Richard B. Mazess

Department of Radiology (Medical Physics)
University of Wisconsin Hospitals,
Madison, Wisconsin

ABSTRACT

Direct photon absorptiometry with ^{125}I was used to measure the bone mineral content in Eskimo natives of the north coast of Alaska. The sample consisted of 217 children, 89 younger adults, and 107 elderly adults (over 50 years of age). The Eskimo children had a lower (by 5 to 10%) bone mineral content than U.S. Whites, but this was consistent with their smaller body and bone size and did not indicate growth retardation. Young Eskimo adults (20-39 years) of both sexes were similar to comparable groups of U.S. Whites, but after age 40 the Eskimos of both sexes had a bone deficit of from 10 to 15% relative to White standards. Aging bone loss, which occurs in many populations, has an earlier onset and greater magnitude in the Eskimos. Similar findings were observed in Canadian Eskimos and in archeological bones. Of the many pertinent nutritional influences a high protein intake appears to be more important than phosphorus, calcium or vitamin D intakes.

ABSTRACT OF BONE MINERAL WORK DONE IN THE
DEPARTMENT OF POULTRY SCIENCE SINCE FEBRUARY, 1970

Paul C. Miller, Department of Poultry Sciences,
University of Wisconsin, Madison, Wisconsin

ABSTRACT

Bone mineral studies with laying hens have been in four
areas:
(1)   influence of temperature on bone mineralization
(2)   recovery period after a restricted intake of
calcium
(3)   differences in bone formation due to various
levels of calcium in the feed
(4)   effect of various particle sizes of limestone and
oyster shell on bone mass.

The influence of temperature on bone was not demonstrable.
Birds held on low calcium (0.6, 0.9 and 1.5%) from 20 to 24
weeks of age recover their bone mass at 40 weeks of age when
fed a normal 3.0% calcium diet from 24-40 weeks. There was
no difference in bone mass between birds fed 2.3, 3.0 and 4.5%
calcium, but the hens fed 1.5% calcium had bone mass values
significantly lower (0.05 level) than the other three calcium
levels. Neither the source nor the particle size (flour,
pullet, or hen) influenced the bone mineralization.

BODY COMPOSITION MEASUREMENTS USING ^{109}Cd

Norbert Pelc, Department of Radiology
(Medical Physics), University of Wisconsin
Hospitals, Madison, Wisconsin

Introduction

The use of ^{109}Cd as a source for dual photon absorption measurement of body composition has been investigated (Preuss and Schmonsees, 1972; Schmonsees and Preuss, 1971). It appeared that this source would provide more sensitive measurements than the ^{125}I/^{241}Am combination although it could only be applied to locations where the tissue thickness was not very great because of attenuation and hardening of the lower energy beam. We have used this source for measurement of both the soft tissue composition and the bone mineral content of the hand. These measurements may be of particular interest for clinical conditions in which either the bones of the hand are especially involved, for example in renal disease, or in which there are alterations of the fat-lean composition or fluid status, for example in the edema of heart disease. Clinical measurements require high precision. Our present results showed coefficients of variation of 2.5% in the fat fraction and 3.0% in the total soft tissue mass, while the standard deviation of bone mineral content ranged from $\pm$ 0.01 to $\pm$ 0.07 g/cm. With higher activity sources clinical measurement of the hand seems feasible.

Isotope

^{109}Cd decays by electron capture to the .088 MeV level of ^{109}Ag with a half life of 453 days. This metastable state decays to the ground state with a half life of 40 sec emitting four 88 keV γ-rays for every 100 disintegrations (Lederer et al., 1968). Also emitted are the characteristic x-rays of Ag. Table 1 lists these x-ray lines, their energies and their intensities normalized to 100 for $K_{\alpha 2}$.

LINE	ENERGY(keV)	INTENSITY
$K_{\alpha 1}$	21.99	51
$K_{\alpha 2}$	22.16	100
$K_{\beta 1}$	24.9	25
$K_{\beta 2}$	24.5	5

Table 1: Characteristic x-ray lines of Ag
(Lederer et al., 1968).

The ^{109}Cd source for these studies is filtered with .004 inches of Palladium (Pd). The spectrum of the filtered ^{109}Cd source is shown in Figure 1. The ^{109}Cd is filtered for two reasons: 1) to reduce the amount of hardening of the characteristic x-rays, and 2) to optimize the relative energy composition of the beam.
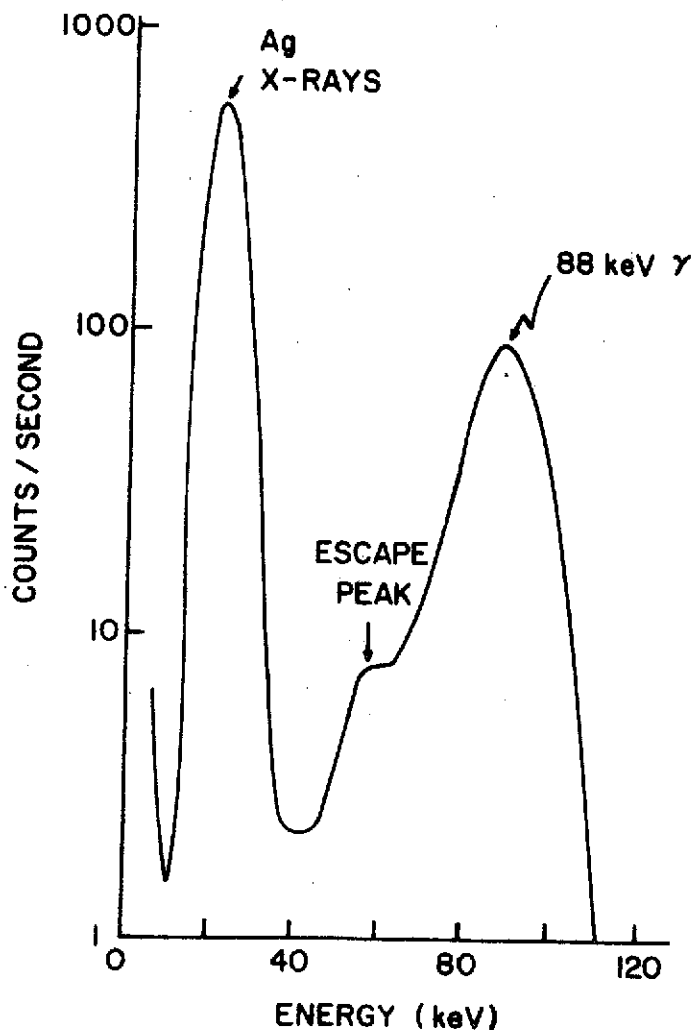

Figure 1: Energy spectrum of the filtered ^{109}Cd source.

When a polyenergetic x-ray beam is attenuated by matter, the effective energy of the beam tends to increase with increasing thickness of the absorber, due to the greater attenuation of the lower energy photons. This effect makes the attenuation coefficient of the absorber a function of the absorber thickness and composition. To make the beam attenuation coefficient independent of the amount of material, the photon beam should be as monoenergetic as possible. This can be done by selective filtration. Palladium (Z = 46) with an absorption edge at 24.35 keV (Lederer et al., 1968) is well-suited to selectively filter the K_β characteristic x-rays of Ag. A 0.1 mm thick PD filter reduces the K_β intensity by a factor of 1000 and the K_α intensity by a factor of 4 (Schmonsees and Preuss, 1971).

The ^{109}Cd beam should also be filtered to optimize the ratio of the relative incident intensities of the two energies, 22 and 88 keV. An optimum ratio can be demonstrated when the variance (σ_{MB}^2) of bone mineral mass (MB) is expressed as a function of the initial intensities (I_{01}, I_{02}) and the attenuated intensities (I_1, I_2).

The variance of the mineral mass is given by ·

$$\sigma_{MB}^2 = \left(\frac{\partial MB}{\partial I_{01}}\right)^2 \sigma_{I_{01}}^2 + \left(\frac{\partial MB}{\partial I_1}\right)^2 \sigma_{I_1}^2 + \left(\frac{\partial MB}{\partial I_{02}}\right)^2 \sigma_{I_{02}}^2 + \left(\frac{\partial MB}{\partial I_2}\right)^2 \sigma_{I_2}^2$$

where, $\sigma_{I_{0i}}^2$ and $\sigma_{I_i}^2$ (i = 1, 2) are the variances for the unattenuated and the attenuated intensities of the i-th beam. Computing the various partial derivatives from the dichromatic equation for bone mineral mass and substituting them into the variance equation, it can be reduced to

$$\sigma_{MB}^2 = C_1^2 \left(\frac{1}{I_{01}} + \frac{1}{I_1}\right) + C_2^2 \left(\frac{1}{I_{02}} + \frac{1}{I_2}\right)$$

where, C_1 and C_2 are constants depending on the attenuation coefficients for bone and soft tissue.

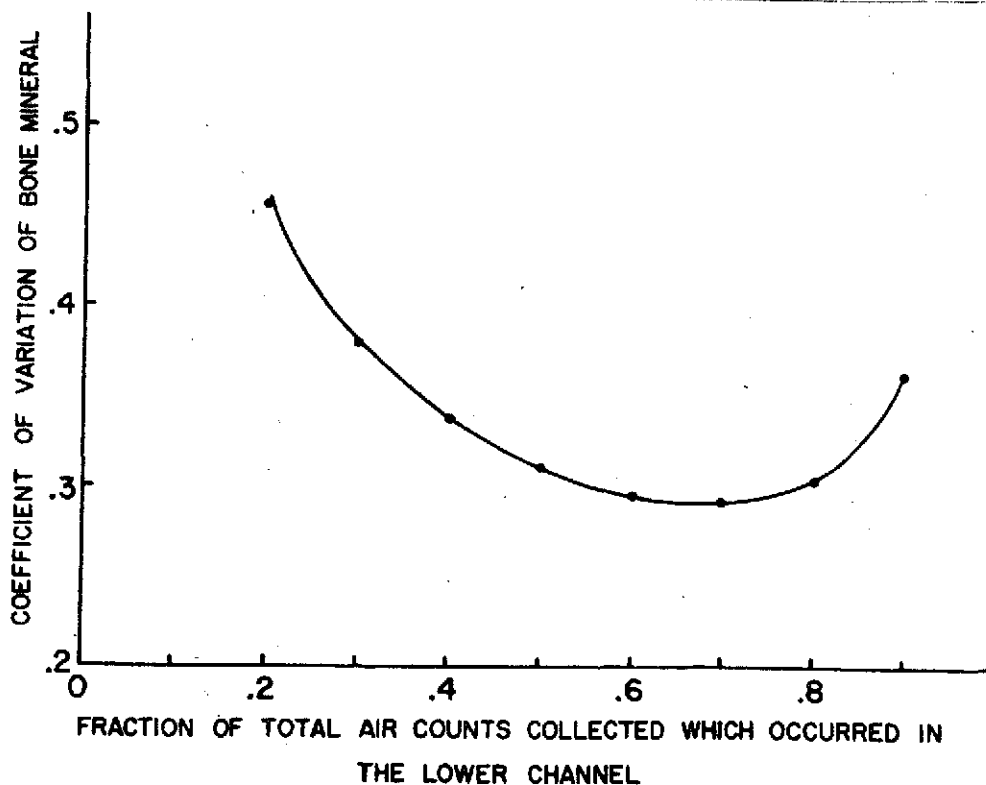FRACTION OF TOTAL AIR COUNTS COLLECTED WHICH OCCURRED IN THE LOWER CHANNEL

Figure 2:   Error in the measurement of bone mineral content as a function of the relative intensity of the two photon energies (22 keV and 88 keV).

The coefficients of variation in bone mineral content were calculated for different fractions of the total incident counts in the low energy channel and plotted in Figure 2. All calculations were done assuming the beam was composed of 22 keV and 88 keV photons, with a total initial intensity $(I_{01} + I_{02})$ of 1600 counts and was attenuated by .45 g/cm^2 of bone mineral and 5 g/cm^2 of soft tissue. The bone mineral content coefficient of variation reached a minimum when about 70% of the initial unattenuated counts were due to 22 keV photons. For the unfiltered ^{109}Cd beam the ratio of the lower energy intensity to the upper energy is 1000:1 (Schmonsees and Preuss, 1971). For the beam filtered by .004 inches of Pd and the .125 inch thick lucite scanning table the ratio was approximately 3:1, or 75% of the total detected air counts were occuring in the low energy channel.

Method

Due to the low activity of the ^{109}Cd source (est. activity 14 mCi), the source had a large exit aperture (0.6 mm diameter) and the detector had a 0.635 mm diameter entrance aperture. The ^{109}Cd source and a NaI(Tℓ) detector were mounted on a rectilinear scanner (Sandrik et al., 1971) at a source-detector distance of 13.5 cm. The scanning speed was set at 1 mm/sec and step lengths were set at 10.73 mm/step. The transmitted counts were collected once a second using the same digital data acquisition equipment previously reported (Judy et al., 1971). With this source-detector geometry and data collection time, the unattenuated counts were 1050 counts in the lower channel and 400 counts in the upper channel.

The three chambers of a bone mineral standard (Witt, 1974) were scanned 3 times one day and 8 times a different day using the rectilinear scanner in the no-step mode. A rectilinear scan of the right hand of a normal adult male was done which covered an area of 150 mm x 120 mm. Also, the midpoint site of the second metacarpals of the same hand was scanned five times with this technique and three times with a calibrated single photon direct readout unit with ^{125}I as the photon source.

A Fortran program was written to analyze the scan data recorded on digital magnetic tapes.

Point measurements with the same geometry but much longer data collection times (several minutes) were performed to ascertain the limitation of low beam intensity.

Results

The total soft tissue, bone mineral content, and the ratio (R) of the soft tissue attenuation coefficient for the low energy to the high energy were calculated for all scans.

Preuss and Schmonsees (1972) have shown that R is approximately, linearly related to the fraction of fat of the soft tissue, and it can be shown that

$$R = \ln(I_{01}/I_1) \ / \ \ln(I_{02}/I_2)$$

where, I_{01}, I_{02} are the unattenuated intensities at the lower and upper energies respectively and I_1 and I_2 are attenuated intensities (Schmonsees and Preuss, 1971).

For the scans of the standard, the coefficient of variation for the total soft tissue mass was 1.5% on the first day and 3% on the second day. The coefficient of variation for the average for each set of scans was less than 0.5%.

The bone mineral content of the three chambers can be measured with a standard deviation ranging from ± 0.01 to ± 0.06 g/cm on each set of scans, where the larger deviations correspond to the larger tubes. The day-to-day precision of the bone mineral content ranged from ± 0.02 to ± 0.03 g/cm.

The value of R for the standard could be measured with a coefficient of variation ranging from 4% to 5% for each set of scans, and a day-to-day coefficient of variation of 2.6%. This corresponds to errors in the fat fraction of 6%.

The scans of the bone standard were also used to calibrate the bone mineral content values for the dual photon scans. Two of the chambers in the standard were built to simulate forearm bones and are larger than those expected in the hand. The calibrated values for the three chambers and the sum of the bone mineral content for the three chambers was plotted as a function of the quantity measured by the dual attenuation technique (Figure 3).
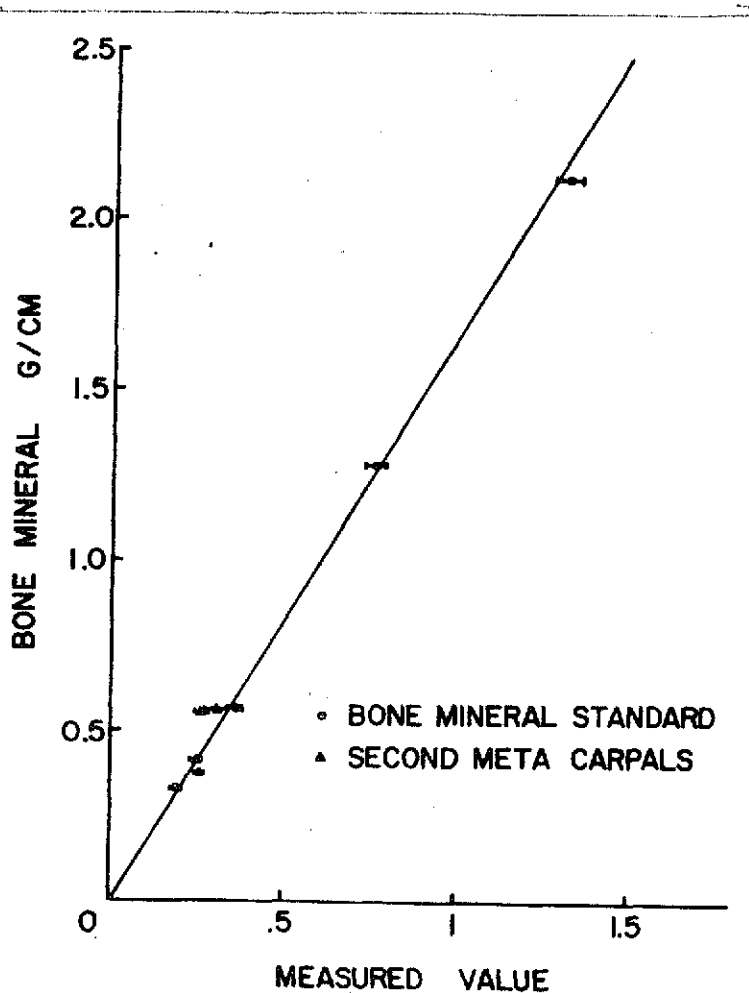

Figure 3: Calibration curve for bone mineral content measured with the dual photon technique using ^{109}Cd.

For the rectilinear scan of the right hand the bone mineral content ranged from 0.35 to 0.6 g/cm. The soft tissue mass ranged from 1 to 3 g/cm in the fingers and from 20 to 30 g/cm in the palm. The percent fat of the soft tissue mass ranged from 6% to 25%.

The coefficient of variation of five repeated linear scans at the midpoint site of the second metacarpals for soft tissue was 3%. The coefficient of variation for R for the same set of scans was 2% corresponding to a 5.7% error in estimating the fat fraction. Bone mineral content values for the second metacarpals ranged from 0.42 to 0.50 g/cm, which agrees with what other investigators have observed (Mazess, 1974). Standard deviations in the bone mineral contents ranged from $\pm$ 0.02 to $\pm$ 0.07 g/cm, the smaller bones have the smaller deviations. The bone mineral content values for these bones and their corresponding values as measured with a single photon direct readout unit are also shown in Figure 3.

To investigate the source of these large variations several point measurements were performed on the R value for oil, water, lucite, and the palm of a right hand. The geometry used was the same as that for the scan measurements but the collection times were increased to accumulate more counts. With about 100,000 counts collected in each channel variations in R were reduced to $\sim 1\%$ corresponding to 2.5% error in the fat fraction estimate. Therefore, to increase the precision of the dual photon scan measurements a much higher activity ^{109}Cd source would be necessary.

Conclusion

The experiments performed indicate that the dual attenuation technique using ^{109}Cd can be used to reproducibly measure bone mineral content, soft tissue mass, and soft tissue composition in vivo.

The basic limitation at the present time is the activity of the ^{109}Cd source. We have shown that errors in fat fraction estimates can be reduced by a factor of 3 or 4 when more counts are collected. Similar improvement in the measurement of other parameters can be expected. With higher activity sources, the aperture sizes could be reduced giving better spacial resolution, or the collection time could be decreased to reduce the total scan time.

References

Judy, P.F., M.G. Ort, K. Kianian and R.B. Mazess 1971. Developments in the dichromatic attenuation technique for the determination of bone mineral content in vivo. USAEC Progress Report COO-1422-97.

Lederer, C.M., J.M. Hollander and I. Perlman 1968. Table of Isotopes John Wiley and Sons, New York, 6th Edition.

Mazess, R.B. 1974. Private communication.

Preuss, L.E. and W. Schmonsees 1972. ^{109}Cd for compositional analysis of soft tissue. Int. J. Appl. Isotopes 23: 9-12.

Sandrik, J.M., R.B. Mazess, C.E. Vought and J.R. Cameron 1971. Rectilinear scanner for determination of bone mineral content. USAEC Progress Report COO-1422-96.

Schmonsees, W.G. and L.E. Preuss 1971. The potential use of Cd^{109} for dual absorption measurements of soft tissue. In: Charles A. Ziegler (ed) Applications of Low Energy X and Gamma Rays. Gorden & Breach Science Publishers, New York.

Witt, R.M. 1974. Bone standards for the intercomparison and calibration of photon absorptiometric bone mineral measuring systems. In: R.B. Mazess (ed) Proc. Intern. Conf. on Bone Mineral Measurement. U.S. Govt. Printing Office, Washington, D.C.

THE EFFECTS OF TEMPORARY PROTEIN DEPRIVATION ON BONE WIDTH AND BONE MINERAL CONTENT IN RHESUS MACAQUES

W. Leutenegger, R. M. Larsen, and Sylvia Bravo

Department of Anthropology, University of Wisconsin, Madison, Wisconsin

A group of infant rhesus macaques were placed for a period of 180 d (from 30-210 d of age) on a low protein diet, which was followed by a period of rehabilitation averaging 1400 d. Deprivation was severe enough to retard weight gain during the experiment and to prohibit normal weight recovery. The protein deprivation did not adversely affect skeletal dimensions, as indicated by width measurements, but did reduce bone mineral content in the rehabilitated animals.

Protein malnutrition retards bone growth (Jha, *et al.*, 1968) and reduces mineral densities (du Boulay, 1972) in primates. Similar bone disturbances have been reported in humans (Jones and Dean, 1959; Gillman and Gillman, 1951), in pigs (Pratt and McCance, 1964), and in rats (McCance and Widdowson, 1962; Dickerson, *et al.*, 1972). The chronological timing and duration of deprivation influence the extent and permanence of bone alterations (Pratt and McCance, 1964).

Normal bone growth and maturation (Kerr, *et al.*, 1972), as well as bone growth in protein deficiency (Kerr, *et al.*, 1973) have been recorded in rhesus macaques. The impact of temporary protein deprivation, followed by a normal diet, on the bone, however, has not been well documented for these animals. The objective of this study was to provide measurements of bone dimension and bone mineral in macaques recovered from temporary protein malnutrition in their first year.

MATERIALS AND METHODS

Seventeen rhesus macaques were selected for a study on temporary protein deprivation. This study was part of a larger research effort considering calorie-protein malnutrition carried out by the Wisconsin Regional Primate Center. These animals were divided into two dietary groups, the dietary regimes of which are presented in Table 1. Control animals (n = 9) were fed foodstuffs which contained 18.2% protein during their first year. The composition of their control diet (Similac—

TABLE 1

DIETARY REGIMES, AGES OF SACRIFICE, AND AVERAGE WEIGHTS AT SACRIFICE OF
CONTROL AND DEPRIVED ANIMALS

.	Dietary Regime (Days)	Age of Sacrifice	Mean Weight at Sacrifice
Control	0-365 days control diet* 365—Purina chow and fruit	1650 ± 314 days	5.45 ± 0.87 kg
Deprived	0-30 days control diet 30-210 days control diet with ¼-½ less protein† 210-365 days control diet 365—Purina chow and fruit	1603 ± 223 days	4.61 ± 0.65 kg

* Control diet is commercially called Similac (Ross Laboratories).
† Ross Laboratories also provided the ½ and ¼ protein deficient formulas.

Ross Laboratories) can be found in Kerr, *et al.* (1969). Deprived animals (n = 8) received the control diet but with only 50% (n = 4) or 25% (n = 4) of the control protein level between 30 and 210 days of age. This deficient protein diet was made isocaloric with lactose. The diet, before and after the deprivation, until one year of age, was the control diet. All animals received daily vitamin supplements (Paladac) during the first year, and returned to a Purina monkey chow and fruit diet after one year. The animals were sacrificed at an average age of 4.5 years, approximately 1400 days after deprivation. Dietary regimes, age at sacrifice and weight at sacrifice are presented in Table 1.

Bone mineral values and bone widths of the humerus and femur were taken from the sacrificed animals. *In vivo* determinations of bone width and bone mineral were possible utilizing direct photon absorptiometry. Description and discussion of the technique can be found elsewhere (Cameron, *et al.,* 1968; Mazess, 1964; Mazess, 1971).

RESULTS

Bone widths and bone mineral values for both groups are presented in Table 2 and Table 3. No significant differences in width dimension occurred between the two groups. The bone mineral contents of the control animals were higher at all three sites on both bones. Significantly greater values were recorded at proximal and midshaft sites of the femur of control animals.

TABLE 2
Mean Bone Widths (cm) at Six Sites of Control and Deprived Rhesus Macaques.

Site	Control Mean	S.D.	Deprived Mean	S.D.	t-value
Humerus					
Proximal	1.034	0.179	1.041	0.224	—0.06
Midshaft	0.899	0.152	0.956	0.182	—0.65
Distal	0.863	0.092	0.855	0.140	0.13
Femur					
Proximal	1.099	0.092	1.103	0.084	—0.08
Midshaft	1.141	0.116	1.102	0.070	0.77
Distal	1.139	0.102	1.172	0.118	—0.59

DISCUSSION

In this study a group of infant rhesus macaques were placed on a low protein diet (4.05 or 9.1% protein) between 30 and 210 days of age, after which they received a normal diet. Deprivation was severe enough to retard weight gain during the experiment and to prohibit normal weight recovery. The protein deprivation did not adversely affect skeletal dimensions, as indicated by width measurements, but did reduce bone mineral values in the rehabilitated animals.

A similar study on rats (Dickerson, *et al.*, 1972) found that protein deprivation had a small but permanent stunting effect on some of the bones (pelvis, hind limb) but not on the forelimb. Comparison of the two studies is difficult, however, since bone width was the only common measurement. The significantly lower bone mineral values in the de-

TABLE 3
Mean Bone Mineral Values (g/cm) at Six Sites of Control and
Deprived Rhesus Macaques

Site	Control Mean	S.D.	Deprived Mean	S.D.	t-value
Humerus					
Proximal	0.610	0.122	0.552	0.084	1.06
Midshaft	0.585	0.130	0.546	0.073	0.69
Distal	0.600	0.105	0.553	0.109	0.85
Femur					
Proximal	0.734	0.070	0.650	0.047	2.69*
Midshaft	0.679	0.098	0.576	0.037	2.62*
Distal	0.629	0.086	0.588	0.091	0.90

* Indicates a significance level of less than 0.02.

PROTEIN DEPRIVATION, BONE MINERALS IN RHESUS

prived animals after an early deprivation and a four year recovery period are of interest. These values suggest that a reduction of bone mineral content may be not completely reversible with respect to the recovery of normal bone mass in some bones.

REFERENCES

CAMERON, J. R., MAZESS, R. B., & SORENSON, J. A. Precision and Accuracy of Bone Mineral Determination by Direct Photon Absorptiometry. *Invest. Radiol.* 3, 141-150, 1968.

DICKERSON, J. W. T., HUGHES, P. S. R., & McANULTY, P. A. The Growth and Development of Rats Given a Low-Protein Diet. *Br. J. Nutr.* 27, 527-536, 1972.

DU BOULAY, G. H., HIME, J. M., & VERITY, P. M. Spondylosis in Captive Wild Animals: A Possible Relationship with Nutritional Osteodystrophy. *Br. J. Radiol.* 45, 841-847, 1972.

GILLMAN, J., & GILLMAN, T. Perspective in Human Malnutrition. Grune, New York, 1951.

JHA, G. J., DEO, M. G., & RAMALINGASWAMI, V. Bone Growth in Protein Deficiency. *Amer. J. Path.* 53, 1111-1123, 1968.

JONES, P. R. M., & DEAN, R. F. A. The Effect of Kwashiorkor on the Development of the Bones of the Knee. *J. Pediat.* 54, 176-184, 1959.

KERR, G. R., SCHEFFLER, G., & WAISMAN, H. A. Growth and Development of Infant *M. mulatta* Fed a Standardized Diet. *Growth* 33, 185-199, 1969.

KERR, G. R., WALLACE, J. H., CHESNEY, C. F., & WAISMAN, H. A. Growth and Development of the Fetal Rhesus Monkey III. Maturation and Linear Growth of the Skull and Appendicular Skeleton. *Growth* 36, 59-76, 1972.

KERR, G. R., WAISMAN, H. A., ALLEN, J. A., WALLACE, J., & SCHEFFLER, G. Malnutrition Studies in *Macaca mulatta* II. The Effect on Organ Size and Skeletal Growth. *Amer. J. Clin. Nutr.* 26, 620-630, 1973.

MAZESS, R. B. Accuracy of Bone Mineral Measurement. *Science* 145, 388-389, 1964.

MAZESS, R. B. Estimation of Bone and Skeletal Weight by Direct Photon Absorptiometry. *Invest. Radiol.* 6, 52-60, 1971.

McCANCE, R. A., & WIDDOWSON, E. M. The Bearing of the Plane of Nutrition on Growth and Endocrine Development. In, F. Gross (ed.) Protein Metabolism, pp. 109-117 (Springer, Berlin, 1962).

PRATT, C. W., & McCANCE, R. A. Severe Undernutrition in Growing and Adult Animals. XIV. The Shafts of the Long Bones in Pigs. *Br. J. Nutr.* 18, 613-624, 1964.

THE EVALUATION OF THE DIRECT READOUT
SYSTEM OF BONE MINERAL CONTENT USING
THE DICHROMATIC ATTENUATION TECHNIQUE

William Kan, Radiology Department
(Medical Physics), University of Wisconsin
Hospitals, Madison, Wisconsin

The analog direct readout system for measuring bone mineral content with the dichromatic attenuation technique (Kan et al., 1973) was examined in terms of precision, accuracy and the effects of soft tissue thickness. The inter-comparison between results obtained from the analog system and those obtained from digital computation were also studied.

Different bone standards as well as normal individuals were scanned with a ^{153}Gd dual photon source which has photons at 44 keV and 100 keV. The preliminary results obtained with this developmental system are described.

Precision of the Analog System

The precision of the analog system was checked by scanning a phantom which simulates the upperarm. This upperarm phantom is composed of an aluminum tube with outside diameter 2.24 cm and wall thickness 0.23 cm embedded in a methyl methacrylate block with round edges and flat sides with approximate dimensions of 5.6 x 7.05 x 8 cm^3. The average value for six consecutive scans of the arm standard was 6.27 (arbitrary units) with standard deviation ± 0.09, coefficient of variation 1.45%.

A similar precision test was performed by scanning the upperarm of a normal adult subject. For the subject measurements the ratio of the soft tissue attenuation coefficients for the lower energy to the upper energy (R) was set at 1.301 which corresponds to an assumed 0.20 fat fraction in the general population. This fat percentage lies between the 15% to 25% range of the percentage of fat in soft itssue of normal males and females (Brozek, 1965; Mazess et al., 1970). The average value for eleven consecutive scans was 2.26 with standard deviation ± 0.04, coefficient of variation 1.81%.

The Computation Accuracy of the Analog System

A three-chambered bone standard whose dimensions and predetermined bone mineral content values represent those of adult male and female radii and an adult female metacarpal (Witt, 1970) was scanned with the analog system to evaluate the accuracy of the analog computation.

Ten consecutive scans on each chamber were recorded. The averages of the ten scans for the three chambers were 0.311, 0.542, 1.14 and all were in arbitrary units.

The three average values from the analog system were plotted against the calibrated mineral content values of the three chambers which are 0.379 g/cm, 0.609 g/cm, 1.273 g/cm, Figure 1. From observation, the three intersections of the corresponding values lie on a straight line. From linear regression analysis the standard error of estimate was calculated to be ± 0.013 g/cm.

Independency of Soft Tissue Thickness

The three-chambered bone standard was again scanned. This time with a different number of 0.593 cm thick lucite blocks added to increase the amount of simulated soft tissue over the bone standard. Since for ^{153}Gd methyl methacrylate has the same attenuation characteristics as soft tissue with 77% fat, for these scans, the R value was set to correspond to a 0.77 fat fraction. The spillover correction was set at 2%. Each chamber was scanned ten times and the averages of the ten recordings corresponding to a different number of additional lucite blocks are listed in Table 1.

Except for the small chamber, the coefficients of variation are about 2%. The reason for the slightly larger coefficient of variation in the small chamber may be due simply to the large fluctuation in counting statistics.

Comparison of Analog and Digital Systems

The results from the analog system were compared with the result from a digital computation by software programming. Instead of converting the data stored in the scaler buffers to analog signals for the analog analysis, the digital data was transferred to magnetic tape for temporary storage. The magnetic tape was later processed by software programs to calculate the bone mineral content by the Madison Academic Computing Center.

The three-chambered phantom was scanned six times with the digital system. The average values for the three chambers were 0.355 g/cm, 0.605 g/cm, and 1.428 g/cm. These average values were plotted against the three average values, 0.207, 0.431 and 1.213, obtained from ten consecutive scans on each chamber by the analog system, Figure 2.

With linear regression applied to the three points in Figure 2, the standard error of estimate was calculated to be ± 0.008. This result indicates that the bone mineral content obtained by the analog system is as accurate as the result obtained from the digital computation with software programming.

References

Brozek, J. 1965. Symposium of the Society for the Study of Human Biology, Vol. 7, Human Body Composition: Approaches and Applications, Pergamon Press, Oxford.

Kan, W.C., C.R. Wilson, R.M. Witt and R.B. Mazess 1973. Direct readout of bone mineral content with dichromatic absorptiometry. USAEC Progress Report COO-1422-147.

Mazess, R.B., J.R. Cameron and J.A. Sorenson 1970. Determining body composition by radiation absorption spectrometry. Nature 228: 771-772.

Witt, R.M., R.B. Mazess and J.R. Cameron 1970. Standardization of bone mineral measurements. In: J.R. Cameron (ed) Proc. Bone Measurement Conference. U.S. Atomic Energy Comm. Conf. 700515. U.S. Dept. of Commerce (CFSTI), Springfield, Va., pp. 303-307.

Layers of Lucite Block (.593 cm per layer)	Total Thickness of "Fat Tissue"	Small Chamber Average Value (n = 10)	Medium Chamber Average Value (n = 10)	Large Chamber Average Value (n = 10)
1	3.133 cm	0.226	0.476	1.249
2	3.726 cm	0.223	0.489	1.259
3	4.319 cm	0.216	0.493	1.282
4	4.912 cm	0.238	0.502	1.278
5				
6	6.098 cm	0.239	0.498	1.290
The Average		0.2284	0.4916	1.272
The Standard Deviation		0.0099	0.01	0.0164
The Coefficient of Variation		4.34%	2.04%	1.29%

Table 1: The bone mineral content of the three-chambered phantom was scanned by the analog system with different thickness of fat tissue equivalent (lucite).
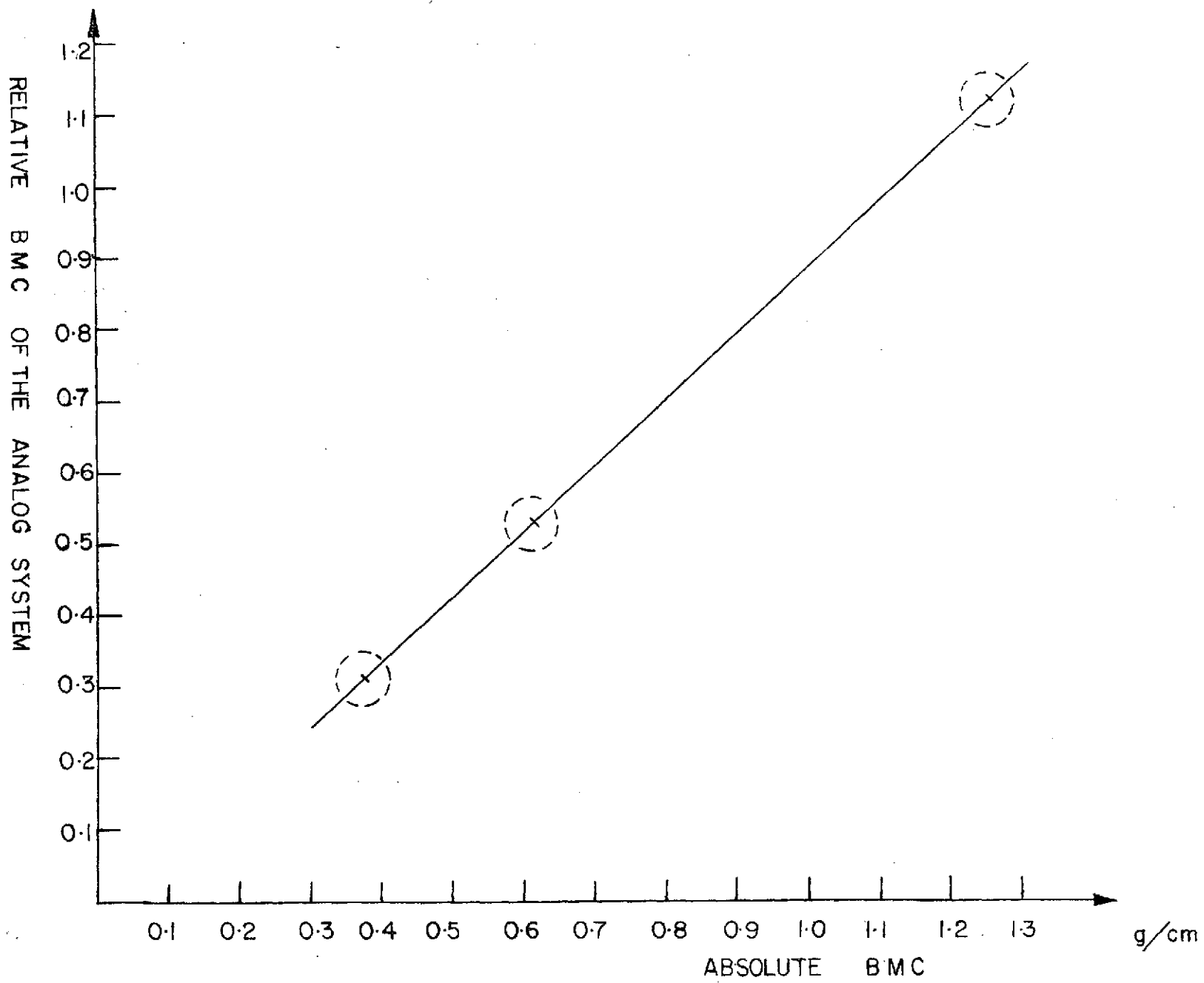
Figure 1: The comparison between the result obtained from the analog system and the actual bone mineral content of the three-chambered bone standard.
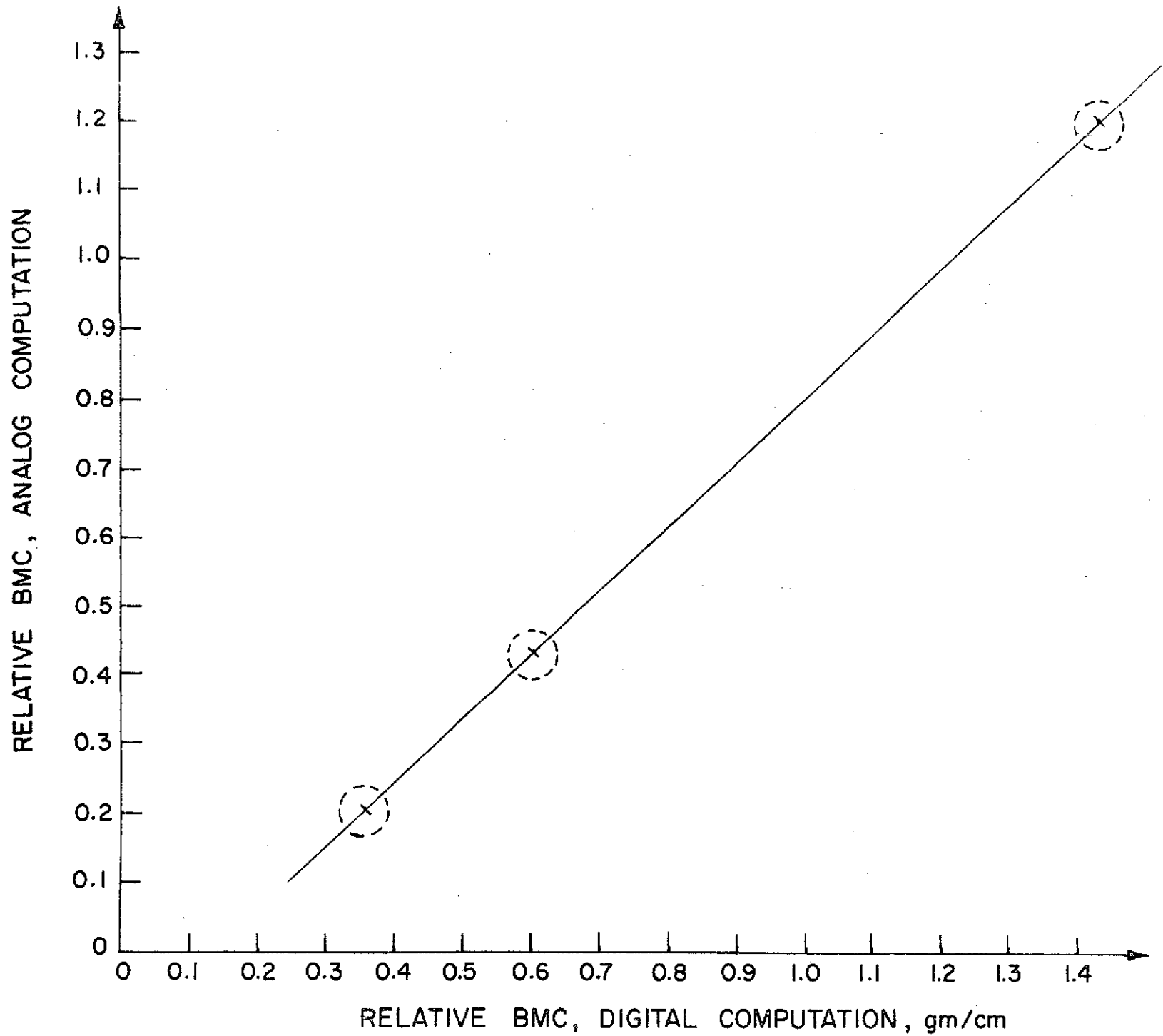
Figure 2:   Comparison of the result from analog system with the
            result from digital computation by software programming.

DUAL PHOTON ABSORPTIOMETRY MEASURING SYSTEMS: CORRECTIONS TO DETECTED PHOTON COUNTS

Robert M. Witt, Radiology Department
(Medical Physics), University of Wisconsin
Hospitals, Madison, Wisconsin

Statement of Problem

For dual photon counting systems with thallium-activated sodium iodide, NaI(Tℓ), detectors the two photon energies are usually separated by pulse height analysis. The amplified and shaped detector pulses are processed by two single channel analyzers, SCA. The two SCA's are composed of four voltage pulse height discriminators with parallel inputs which are set at four increasing voltages to define two pairs of lower level and upper level discriminators. The differences between the lower level and upper level discriminator settings define the window widths. The output of the lower and upper discriminators are connected to an anticoincidence logic circuit so that only those pulses that are contained in the window are passed and counted. The discriminator and anticoincident logic circuits require a finite amount of time to measure the pulse height and make the logical decision. Should another pulse appear during this time period, the SCA would not respond to this pulse and it would be lost by the counting system.

Also in dual photon counting systems the upper energy photon usually contributes some events to the lower energy channel from specific interactions in the NaI(Tℓ) detector so that the lower channel receives events in addition to those due to the low energy photons. The higher energy photons (E $\sim$ 100 keV) can contribute events to the low energy channel from the iodine escape peak and from the single Compton distribution.

Therefore for dual photon counting systems, the counts detected in the lower energy channel must be corrected for count loss due to the deadtime and the upper energy contributions, while only a count loss correction must be made to the upper energy channel counts. If the background event rate is high (> 1 sec^{-1}), it also should be subtracted from the detected counts in each channel. The background counts should be subtracted after the count loss correction for both channels, but before the upper energy contribution correction is made to the low channel.

Count Loss Correction

The count loss characteristics of pulse counting system can be described by two simple models: 1) a non-paralyzable system for which the counter approaches a constant count rate with an increasing incident count rate and 2) a paralyzable system for which the counter count rate increases to a

maximum value with increasing incident count rates and then approaches zero for very high count rates. The observed count rates for paralyzable and non-paralyzable counters can be expressed as functions of the incident (or true) count rates and the characteristic system deadtimes by the following two equations:

Non-paralyzable $\qquad m_i = n_i/(1 + n_i\tau_i)$ $\qquad$ (1a)

Paralyzable $\qquad m_i = n_i e^{-n_i\tau_i} = n_i \exp[-n_i\tau_i]$ $\qquad$ (1b)

where

$\qquad m_i$ = observed average event rate in the i-th channel

$\qquad n_i$ = the true average event rate in the i-th channel

$\qquad \tau_i$ = the characteristic deadtime for the i-th channel

For the following discussion i=1 will signify the low channel and i=2 the high channel.

For the high channel the number of events processed is approximately the same as the number of events detected. For the light load approximation ($n\tau \ll 1$) the true count rate can be estimated for both paralyzable and non-paralyzable counting systems from the following equation:

$$n_2 \simeq m_2/(1 - m_2\tau_2).$$ (2)

As an example, the Surgery Measuring System (Witt, 1974) which is a paralyzable system with an estimated deadtime of 3 µsec, the difference between the actual incident count rate and the estimated count rate is only 1% for an incident count rate of 50,000 sec^{-1}. For non-paralyzable systems the error is negligible (< .001%) even for an incident count rate of 50,000 sec^{-1}.

However, for the low channel the actual number of events processed by the anticoincidence logic is greater than the number of events detected. The count loss in the low channel is determined by the total number of events processed rather than the number of events detected. The number of events processed by the low channel is the sum of the events above the lowest discriminator but below the second discriminator plus all the events above the second discriminator. Since the output above the second discriminator is not monitored, the total number of incident events processed by the low channel is estimated to be the sum of the events in the low channel plus those in the high channel. The true incident event rate for the low channel can be computed from an equation similar to equation 2:

$$n_1' = \frac{m_1'}{1 - m_1'\tau_1}$$ (3)

where

$$n_1' = n_1 + n_2$$

$$m_1' = m_1 + n_2$$

So that after substitution the true average event rate detected in the low channel can be computed from equation 4

$$n_1 = [m_1(1 + n_2\tau_1) + n_2^2\tau_1]/[1 - (m_1 + n_2)\tau_1] \qquad (4)$$

Note that for this computation the observed number of events processed by the low channel has been estimated from the sum of the observed events in the low channel plus the true number of events in the high channel. Thus in the data analysis the count loss errors are corrected for the high channel first.

Upper Energy Contribution Correction

The two principle upper energy contributions to the low energy channel are the iodine escape peak and the single Compton distribution. These upper energy photon contributions to the low energy channel depend upon the crystal dimensions, the source-detector geometry and the energy of the higher photon. Also when the photo peaks are placed in the SCA's windows the correction parameter will depend on the discriminator settings. Since the correction parameter depends on many factors it must be determined empirically for each detector-collimator-SCA combination included in the counting system. The upper energy contribution to the low energy channel can be estimated from the ratio of the counts in the low channel to the counts in the upper channel after all the low energy photons have been attenuated from the low channel.

Escape Peak Ratio

The iodine escape peak contribution is present when using a paired $^{125}I/^{241}Am$ dual photon source. The iodine escape peak appears at approximately 29 keV below the incident 60 keV ^{241}Am photopeak which places it in the ^{125}I energy channel. The attenuated count ratio of the lower to upper channels was measured after attenuating the dual $^{125}I/^{241}Am$ source with 1.37 g/cm^2 of copper which is sufficient to attenuate all the ^{125}I photons. Total attenuation of the ^{125}I photons was verified by noting that the slopes for the Cu attenuation curves were the same for both channels after this much copper attenuation (Pelc, 1973).

The validity of this method to correct the low channel counts for the escape peak contribution has been checked by comparing the ratio of the lower energy to the higher energy attenuation coefficients for water and oil. The measurements were made with the Surgery Measuring System functioning as a dual channel counting system. After correcting the iodine channel counts, for the escape peak contribution, the ratio of the ^{125}I to ^{241}Am attenuation coefficients were 2.09 for water and 1.49 for oil and agree with previous values where the

attenuation coefficients for water and oil were determined with separate ^{125}I and ^{241}Am sources (Mazess, 1970).

The stability of the escape peak correction factor has been checked by measuring the count ratio with 1.37 g/cm^2 of copper attenuating the source during a single day and over a one month period for the same discriminator settings and source-detector geometry. For the measurements made over a single 24 hour period the gain was not adjusted. For the measurements made over the one month period the system gain was adjusted each day to give the same maximum number of counts in the Am energy channel.

The mean escape peak ratio for determinations made over a 24 hour period was 0.1107 with a coefficient of variation of 1.26%. The mean escape peak ratio for 3 determinations made at random times over a one month period was 0.1198 with a coefficient of variation of 1.10%. These variations are about equal to the expected 1% gain stability of the counting system. The difference between the mean values for the escape peak ratios is probably due to different discriminator settings. The single day measurements were made in the laboratory while all the one month period measurements were made after the unit was moved to University Hospitals.

Single Compton Distribution

For ^{153}Gd dual photon sources the 100 keV photons which have undergone a single Compton scattering in the NaI(Tℓ) crystal will contribute counts into the 44 keV channel. The attenuated count ratio, which has been termed the spillover fraction, was measured by attenuating the ^{153}Gd source with aluminum. Typically 18.5 g/cm^2 of aluminum was sufficient to attenuate all the low energy photons and was verified by measuring the same slopes for the aluminum attenuation curves in both energy channels when the source was attenuated with that amount and more of aluminum.

The validity of the spillover correction was checked by noting that the low energy photons were exponentially attenuated by the aluminum when the spillover correction was subtracted from the counts in the low channel. (Madsen, 1974).

Conclusion

The pulse counting portion of photon absorptiometry measuring systems with dual energy photon sources require additional and different corrections than those measuring systems with single energy photon sources. For all dual counting systems the low energy channel requires a count loss correction which depends upon the event rate of both the low and high energy photons. For particular dual counting systems, the corrections for the upper energy photon contributions to the low energy channel which depend upon the NaI(Tℓ) crystal dimensions, the source-detector geometry and the SCA discriminator settings also depends upon the upper photon energy and hence the particular radionuclide chosen as the photon source. Thus for each dual photon source chosen a different combination of correction factors must be applied to the detected count data.

References

Madsen, M. 1974. An _in vivo_ method for the determination of vertebral bone mineral content utilizing ^{153}Gd. USAEC Progress Report COO-1422-181.

Mazess, R.B., J.R. Cameron and J.A. Sorenson 1970. Determining body composition by radiation absorption spectrometry. _Nature_ 228: 771-772.

Pelc, N.J. 1973. Absorptiometry using ^{125}I and ^{241}Am to determine tissue composition _in vivo_. USAEC Progress Report COO-1422-148.

Witt, R.M. 1974. Description of a dual photon absorptiometry system for the determination of body composition _in vivo_. USAEC Progress Report COO-1422-183.

MEASUREMENTS ON CLINICAL STANDARD
USING DIRECT READOUT SYSTEM

Howard Gollup

Department of Radiology (Medical Physics),
University of Wisconsin Hospitals,
Madison, Wisconsin

For routine clinical and field use the operation of the analog direct readout system is evaluated, and the calibration adjusted, using a standard consisting of three annuli filled with a saturated dipotassium hydrogen phosphate solution (Witt et al., 1970). The absorption of this solution approximates that of bone, and the bone mineral content values from scans of this phantom cover the range of bone mineral from forearm to finger bones.

Scans have been made on the dipotassium hydrogen phosphate standard over a 43-month period using a direct readout device in our clinical laboratories. During this period sixteen different ^{125}I sources were used. Generally, measurements of all three annuli were made daily. Often measurements of the middle-sized annulus (or occasionally the large-sized annulus, and very seldom the small-sized annulus) were made after each patient was scanned; hence there are different numbers of scans on each annulus. The means and coefficients of variation over the 43-month period are given in Table 1. There was little systematic change over the 43-month period even though fifteen or sixteen sources were used. For source 70 the width calibration was incorrect and this gave somewhat deviant values at the beginning of this period. The coefficient of variation for bone mineral was between 1-2% for all annuli; highest for the small annulus and lowest for the large annulus. The coefficient of variation for bone width was one-half to one-third that for mineral content. Part of this long-term variation appeared simply to reflect the uncertainties in the last digit of the digital panel meter ($\pm$ 0.01), and this could not be remedied. Differences among sources were not large, and were within the range of experimental error; however, for the first six sources it was necessary to insure that the tin filtration on these sources was identical since the manufacturer (AECL) supplied the sources with filters of varying thickness. This was not necessary for the next nine sources, distributed by Norland Industries. In the last clinical standard update (Gollup, 1973) it seemed that the coefficients of variation for Norland sources 232 through 261 were much higher than the previous AECL sources. Since the last update, however, the later Norland Sources (261 through 409) have shown much smaller coefficients of variation than the Norland sources considered in the last clinical standard update (232 through 261). This may be due in part to the exercise of greater care in positioning of the clinical standard before scanning it.

	Source		Small			Medium			Large	
		N	Min (g/cm)	Width (cm)	N	Min (g/cm)	Width (cm)	N	Min (g/cm)	Width (cm)
Means	70	–	–	–	51	.606	(1.260)	–	–	–
	97	37	.358	.651	92	.602	1.290	37	1.282	1.593
	116	33	.356	.646	107	.598	1.296	33	1.284	1.592
	132	16	.369	.648	54	.608	1.291	16	1.303	1.589
	153	58	.367	.652	226	.608	1.299	58	1.294	1.594
	173	76	.366	.654	302	.605	1.297	76	1.289	1.594
	232	44	.364	.652	106	.604	1.300	44	1.292	1.597
	130	40	.369	.652	106	.613	1.298	40	1.307	1.595
	145	31	.368	.656	66	.608	1.305	31	1.294	1.606
	180	63	.366	.652	108	.607	1.305	63	1.291	1.606
	217	76	.377	.658	115	.619	1.298	97	1.294	1.595
	261	95	.367	.651	121	.609	1.291	105	1.277	1.588
	200	17	.363	.645	21	.602	1.282	18	1.268	1.577
	292	44	.372	.652	58	.619	1.290	51	1.287	1.584
	362	62	.366	.651	82	.609	1.294	66	1.279	1.590
	409	14	.370	.648	19	.617	1.285	14	1.282	1.583
All scans since last update (261-409)		231	.367	.649	301	.611	1.288	253	1.278	1.584
All scans		703	.367	.651	1634	.608	1.295	748	1.288	1.592
CV (%)	70	–	–	–	51	1.25	1.44	–	–	–
	97	37	1.92	1.32	92	1.16	1.16	37	0.90	0.46
	116	33	1.56	0.89	107	1.06	0.59	33	0.81	0.37
	132	16	2.02	0.56	54	1.01	0.60	16	0.89	0.31
	153	58	1.03	0.82	226	0.97	0.54	58	0.74	0.48
	173	76	1.25	0.64	302	1.06	0.47	76	0.88	0.40
	232	44	1.54	0.91	106	0.99	0.47	44	1.15	0.40
	130	40	1.83	1.21	106	1.10	0.66	40	0.61	0.53
	145	31	1.45	1.15	66	1.27	0.71	31	0.86	0.83
	180	63	2.02	1.97	108	1.77	0.16	63	1.64	0.89
	217	76	2.21	2.18	115	1.96	0.95	97	1.42	0.97
	261	95	1.61	1.12	121	1.21	0.66	105	1.06	0.60
	200	17	1.41	0.95	21	1.41	0.52	18	0.89	0.73
	292	44	1.23	0.95	58	1.15	0.64	51	1.01	0.41
	362	62	1.78	1.17	82	1.16	0.65	66	1.34	0.61
	409	14	1.01	0.70	19	1.14	0.64	14	0.82	0.36
All scans		703	2.11	1.35	1634	1.53	0.97	748	1.29	0.76
Among sources		15	1.40	0.53	16	1.00	0.51*	15	0.78	0.49

* N = 15 -- width scans with source 70 not included due to incorrect calibration.

Table 1: Means and coefficients of variation for multiple scans of a three-chambered standard with sixteen different ^{125}I sources over a 43-month period in a clinical laboratory. The differing numbers of scans on on each annulus are due to single-annulus scans made on the standard after each patient was measured.

REFERENCES

Gollup, H. 1973. Measurements on clinical standard using direct readout
system. USAEC Report, COO-1422-144.

Witt, R.M., R.B. Mazess and J.R. Cameron 1970. Standardization of bone
mineral measurements. USAEC Report, COO-1422-70.

A METHOD TO ESTIMATE THE ERROR CAUSED BY ADIPOSE TISSUE IN BONE ABSORPTIOMETRY

Philip F. Judy and John M. Vogel

ABSTRACT

Variation in the amount of adipose tissue has been reported to cause a significant error in the measurement of bone mineral mass. A method has been developed to estimate the magnitude of that error. The bone mineral mass of a site was measured absorptiometrically using ^{125}I (28 keV) and ^{153}Gd (44 keV or 100 keV) source. A linear regression of measurement of bone mineral mass at each photon energy and an experimentally determined factor, K, which related linearly the adipose defect to the magnitude of the error in bone mineral measurement was performed. The adipose defect was defined to be the integral of difference of the mass of adipose tissue in the photon beam during the measurement of the baseline transmission and the transmission through the bone integrated along the scan path. The slope of the regression was the estimate of the adipose defect, while the intercept provided an accurate estimate of bone mineral mass. The factor, K, was determined in the following manner. Polymethyl-methacrylate tubes were filled with soybean oil to simulate adipose tissue. The tubes were placed over a bone mineral reference standard which was developed at the Bone Mineral Laboratory of the University of Wisconsin. The standard and the simulated adipose defect were placed in a water bath and scanned with each source. The scans were repeated with the tubes filled with water. The difference between the two measurements of bone mineral mass was the error caused by the adipose defect.

The method was applied to the rectilinear scan of the os calcis using ^{125}I. The error was estimated on three occasions in six subjects during a bedrest study. The mean error was 1.3 ± 0.5% (SD), when the baseline was estimated from the minimum transmission through the soft tissue alone over a 3-mm interval at the edge of the bone. The mean error was 6 ± 0.5%, when the transmission at both edges of the bone were used to estimate the baseline. No significant variation in the error was observed between individuals or in any single individual during the study.

The results indicate that this method for estimating the error caused by variation in the composition of soft tissue is useful in serial studies. The method is not recommended to correct the error of an individual measurement because it will reduce the precision of the measurement of bone mineral mass.

AN IN VIVO METHOD FOR THE DETERMINATION OF VERTEBRAL
BONE MINERAL CONTENT UTILIZING ^{153}Gd

Mark Madsen, Radiology Department (Medical Physics)
University of Wisconsin Hospitals, Madison, Wisconsin

INTRODUCTION

We have continued development of the dichromatic photon attenuation
technique for the precise determination of vertebral bone mineral in vivo.
Roos et al. (1970) described previously a dichromatic method using the radiations
of ^{137}Cs and ^{241}Am and Jacobson (1970) used a dichromatic method with an x-ray
source. Judy et al. (1972) described a method using the two energies from
^{153}Gd in a manually driven scanner. Our improvements consist of the use of a
high activity, high purity ^{153}Gd source (1.5 Ci), a modified Ohio-Nuclear
rectilinear scanner, and a double delay line amplifier which allows the system
to handle up to 40,000 counts per second with negligible dead time loss. We
have examined the factors related to exponential attenuation of the radiation
from ^{153}Gd, and the technical parameters affecting precision and accuracy of
the measurement. In addition we have measured phantoms, normal subjects and a
few osteoporotic patients.

METHODS

Measuring System Description

The scanner used is a modified Ohio-Nuclear whole body rectilinear scanner
model 54F. A 1.5 Ci ^{153}Gd source is mounted 20 cm below the scanner table top
and a NaI scintillation detector is directly above the source, 30 cm above the
scanner table top. The source is collimated with a circular collimator which
is 2 cm in diameter and is mounted at the table top. The detector is collimated
with a slit collimator; the dimensions of the slit are 3.8 x 1.2 cm. The
collimation was chosen so that the beam width at the vertebrae was approximately
the length of a single vertebra. This tends to defocus the gaps caused by
the intervertebral discs and processes. A slit collimator was used on the
detector because of the limited counting capabilities of the system.

The source and detector move simultaneously in a raster pattern. The scan
length is determined by the positioning of microswitches on the yoke which
supports the drive mechanism of the detector. The scan speed can be varied
from 1 mm/sec up to a speed greater than 10 cm/sec, however, at speeds less
than 5 mm/sec the speed is erratic and varies ± 5%.

The detector used is a NaI(Tℓ) scintillation detector incorporating a
photomultiplier tube. Mounted on the photomultiplier tube is a Tennelec

pre-amp. Pulses from the pre-amp are fed into a Harshaw Na-12D double delay line amplifier with a delay time of 700 nanoseconds. The amplified pulses are simultaneously fed into two single channel analyzers (SCA). The pulses from the SCA are counted by Harshaw NS-30 buffered scalers. The SCA's and scalers are the same as those previously described by Judy et al. (1971). During a scan the number of photons transmitted are sampled at two-second intervals and the data are recorded on 7 track digital magnetic tape. The magnetic tapes are then batch processed by the Madison Academic Computer Center (MACC).

Dosimetry

The exposure at the skin, ovaries, and testicles from ^{153}Gd was determined experimentally. The ^{153}Gd source was positioned over the lumbar vertebrae of a pelvic phantom. Four LiF TLD crystals were placed in the ovarian region and four were placed in the testicular region for a period of 72 hours. The exposure at the skin was determined by positioning 3 LiF TLD crystals at skin level directly over the source for 30 minutes. Four LiF TLD crystals were placed in the ovarian region while the ovaries were directly in the beam for seven hours and 45 minutes. The exposures of the TLD crystals were recorded and averaged for each particular measurement. The total exposure during an actual measurement was calculated assuming 10 passes 25 cm in length over the subject at a scan speed of 2 mm/sec. The results are presented in Table 1.

	Dose Rate (mR/sec)	Total Dose (mR)
Skin	.06	2.0
Ovarian	7×10^{-5}	.09
Testicular	3×10^{-5}	.03

Table 1: Dose to an individual during a normal scan of the lumbar spine.

Calibration of Vertebral Phantom

A calibration experiment was performed on vertebral phantoms. The phantoms were cylindrical plastic bottles 11 cm long and 4.45 cm in diameter. Each of the seven phantoms had a different amount of dipotassium hydrogen phosphate in solution. The densities of the phantoms were determined by the ratio of the weight of the solution to the weight of an equal volume of water. The mass per unit length of dipotassium hydrogen phosphate was then calculated by multiplying the cross-section area of the phantom by the density of the solution minus the density of water. The calculated values ranged from .698 to 7.65 g/cm.

The vertebral phantoms were scanned in 15 cm of water. The mass per unit length was calculated using the dichromatic attenuation technique derived by Judy (1971). The actual mass is plotted as a function of the absorptiometric measurement (Figure 1). The standard error of estimate was 1.2% and the correlation coefficient was .99. The absorptiometric measurement is in

arbitrary units because the attenuation coefficients of the dipotassium hydrogen phosphate used were not measured on this particular measuring system and are not accurate.
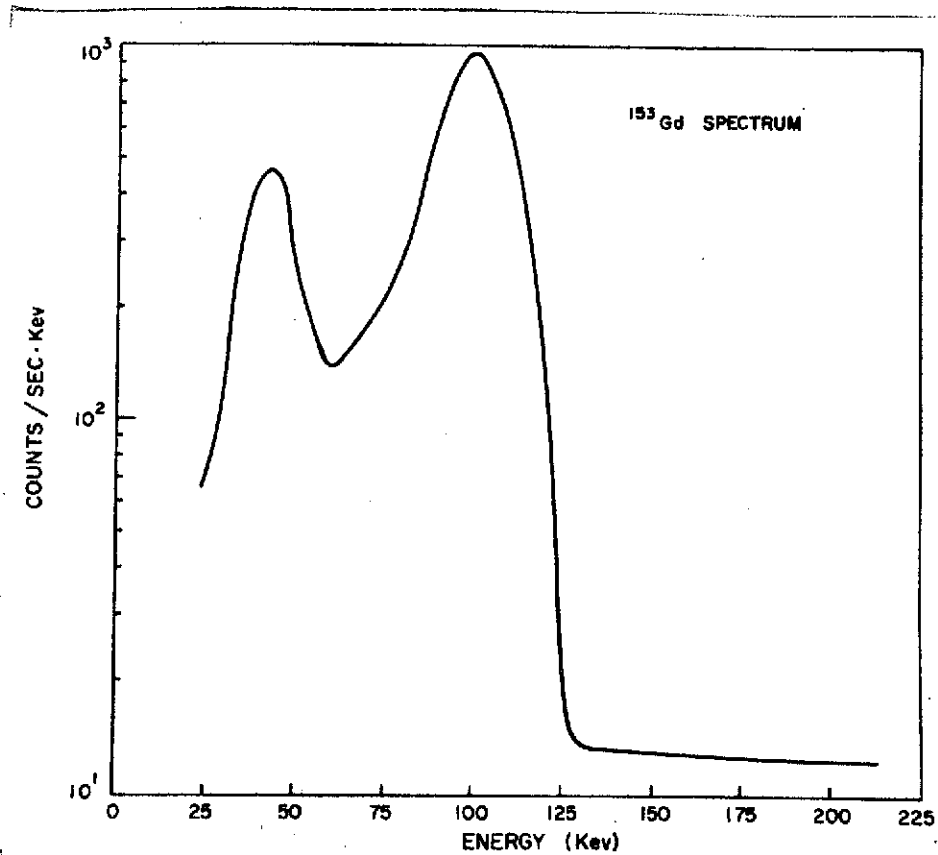

Figure 1: The spectrum of ^{153}Gd with peaks at 44 and 100 keV using NaI(Tℓ) detector.

^{153}Gd Spectrum and Attenuation

The spectrum of ^{153}Gd has been studied. The measurements for the spectrum shown in Figure 2 were made while the beam was filtered through 15 cm of water. Counts were taken at every 3.2 keV with a 3.2 keV window up to 225 keV. The photopeaks were found to be at 43 keV and 100 keV.
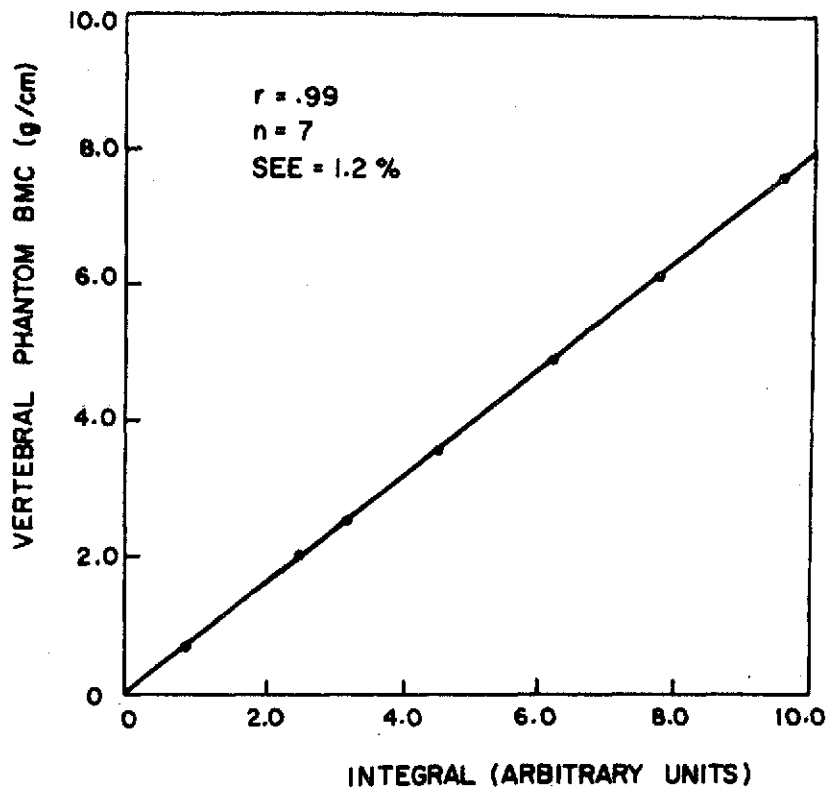
Figure 2: The accuracy of bone mineral determinations on dipotassium hydrogen phosphate standards immersed in a 20-cm water bath using ^{153}Gd.

The attenuation of the 100 keV beam ^{153}Gd is exponential. The counts in the 43 keV channel do not attenuate exponentially. This is due to spillover and detected scatter. Spillover is the result of Compton interactions by the 100 keV photons within the NaI detector in which some of the energy escapes and the detected energy pulses appear in the low energy channel. The magnitude of this effect can be found by selectively filtering the 43 keV photopeak out with aluminum attenuators and measuring the ratio of the counts remaining in the 43 keV channel to the counts in the 100 keV channel. The spillover ratio was found to be 3%. Judy (1971) has shown that detected scatter is a function of tissue thickness and over-all system geometry. It has been found experimentally that the detector scatter in the 43 keV channel can be corrected for by subtracting a constant which varies with tissue thickness from the total detected counts. Tissue thickness can be calculated with an accuracy better than 1% from the attenuation in the 100 keV channel. Thus, the corrected counts in the 43 keV channel can be obtained from the following equation:

$$I_{corr\ 44} = I_{mass\ 44} - S\ (I_{mass\ 100}) - f(t)$$

where

$I_{corr\ 44}$ = corrected intensity of the 43 keV beam

$$I_{mass\ 44} = \text{measured intensity of the 43 keV beam}$$

$$I_{mass\ 100} = \text{measured intensity of the 100 keV beam}$$

$$S = \text{spillover fraction}$$

$$f(t) = \text{linear function of tissue thickness } t$$

Attenuation Coefficients.

The mass attenuation coefficients were measured for water, polystyrene and aluminum. Intensities in the 100 keV and 43 keV channels were recorded as a function of the mass of the attenuators in the beam. The 43 keV channel was corrected for spillover and scatter. Linear regressions were performed on the data. The results are given in Table 2.

Material	Corrected 43 keV Channel	100 keV Channel
Water	.220	.157
Polystyrene	.197	.160
Aluminum	.615	.176

Table 2: Mass Attenuation Coefficients

To demonstrate the validity of the correction factor and the accuracy of the measured attenuation coefficients six point transmission measurements were made over a period of one week. Each measurement consisted of determining the mass per unit area by dichromatic attenuation technique of 0, 1, 2 and 3 aluminum standards which reposed on thicknesses of polystyrene that ranged from 12.7 to 22.9 cm. The mean and standard deviation were calculated for each thickness of polystyrene and are given in Table 3. The calculated mass of aluminum standards is accurate to better than 2% in most of the measurements and is independent of polystyrene thickness.

Thickness Polystyrene(cm)	Actual Mass of Aluminum(g/cm^2)	Calculated Mass of Aluminum $\pm$ SD(g/cm^2)	Coefficient of Variation(%)
	.88	.890 $\pm$ .018	2.0
12.7	1.76	1.759 $\pm$ .033	1.9
	2.64	2.620 $\pm$ .033	1.3
	.88	.895 $\pm$ .015	1.7
15.2	1.76	1.771 $\pm$ .023	1.3
	2.64	2.600 $\pm$ .034	1.3
	.88	.908 $\pm$ .013	1.4
17.8	1.76	1.764 $\pm$ .023	1.3
	2.64	2.601 $\pm$ .056	2.2
	.88	.875 $\pm$ .033	3.8
20.3	1.76	1.728 $\pm$ .023	1.3
	2.64	2.605 $\pm$ .048	1.8
	.88	.880 $\pm$ .031	3.5
22.9	1.76	1.740 $\pm$ .055	3.2
	2.64	2.59 $\pm$ .074	2.9

Table 3: Point Transmission Measurement of Aluminum Standards.

RESULTS

Normals

A 7.5 cm segment of lumbar spine of four individuals was measured four times over a period of a month. The subjects were made to lie supine on the scanner table top. The ^{153}Gd source is positioned above a line joining the tops of the iliac crests. Transmission counts of the 43 keV and 100 keV photons were sampled at two-second intervals and the data was recorded on magnetic tape. The procedure was the same on each of the four days except that the scanning speed was different on the last day.

It was found by measuring the time it took the scanner to travel a specific distance that the speed of the scanner was somewhat erratic and varied by as much as 5%. However, it is possible to correct to an extent differences in measurement due to speed variation by normalizing each individual's measured bone mineral to his bone width. This procedure was used and the results are given in Table 4. The precision of the measurements ranged from .7% to 3.8%.

	Bone Mineral (ARB. Units)	Number	Coefficient of Variation
RW	22.43 ± .34	4	1.5%
RM	22.99 ± .76	4	3.3%
KS	18.35 ± .13	3	.7%
JH	27.92 ± 1.07	4	3.8%

Table 4: Bone mineral of a 7.5 cm section of lumbar spine of four individuals.

The results obtained from this experiment are intended only to demonstrate the precision of the technique. A calibration of measured bone mineral to actual ash weight has not yet been performed on this particular system; P.F. Judy previously found a standard error of estimate of 3% on a similar system (Judy et al., 1972). It should be noted that the comparison of mineral content of a 7.5 cm section of lumbar spine of individuals of different heights and weights may not be biologically meaningful, however, it seems that some normalization would be possible using stature, sitting height or other anthropometric variables.

Patients

Two individuals with suspected osteoporosis were scanned. The first individual was an adult female. She was scanned in a supine position. The results of her scan were normalized to previous scans of normal individuals by comparing the measured value of a vertebral phantom which was used in both scans. Figure 3 shows a plot of the measured bone mineral of the patient and of 2 normal males as a function of position along the spine. The bone mineral was divided by the measured bone width to enable comparisons to be made of different height and weight individuals. The osteoporotic appears to have localized demineralization immediately above the iliac crest.
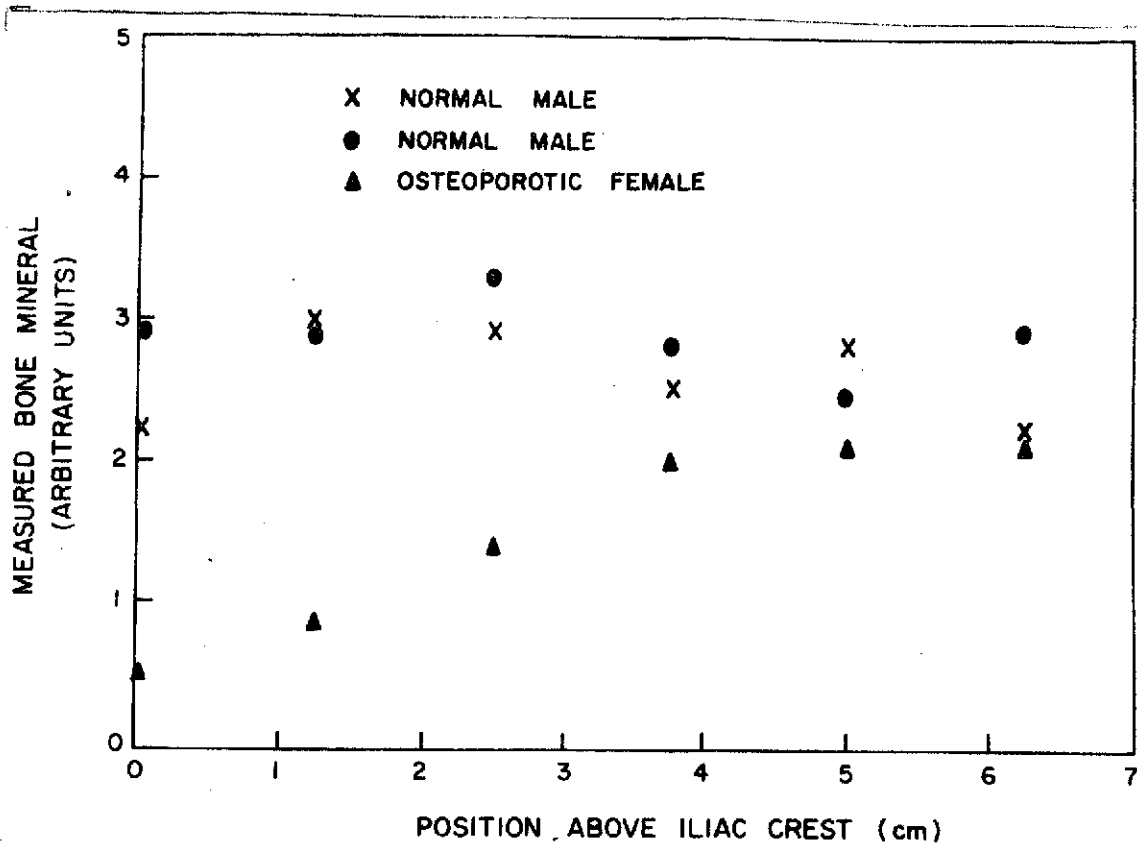
Figure 3: The distribution of measured bone mineral content (adjusted for bone width) in two normal males and in an osteoporotic female. The osteoporotic female appears particularly demineralized in the vertebral area immediately above the iliac crest.

The second individual was an adult male with a history of spontaneous fractures, a condition for which he has been receiving medication. It was not possible for this individual to lie on his back therefore he was scanned in a prone position. The individual was scanned twice over a period of two months. The measured bone mineral was normalized to previous scans of normal individuals as above.

The precision of the total bone mineral for the two measurements was .4%. It did not appear that demineralization was evident in this patient. However, our normative data are limited and with adequate normalization a difference might be apparent. Also there may be a technical problem associated with measuring the spine in a prone position.

CONCLUSION

The precision of the absorptiometric determination of vertebral bone mineral ranged from .7% to 3.8% on normal individuals. At present the accuracy of the measurement in vivo is limited by variations of the scanning speed hence a determination of accuracy e.g. an ash study involving this

system has not been performed. A device is being developed to accurately monitor the position of the scanner throughout an entire scan in order to eliminate any errors due to speed variations. The device consists of an encoder which gives a train of pulses as the shaft of the scanner drive motor rotates. The pulses are counted in up-down counters and the position data are recorded on magnetic tape. After this device is installed and operating an ash study will be done on actual vertebrae to calibrate the system. Measurements will than be performed on a large group of normals and osteo-porotics.

REFERENCES

Jacobson, B. 1970. Bone salt determination by x-ray spectrophotometry. In: J.R. Cameron (ed) Proc. Bone Measurement Conference. U.S. Atomic Energy Comm. Conf. 700515. U.S. Dept. of Commerce (CFSTI), Springfield, Va., pp. 237-242.

Judy, P.F. 1971. A Dichromatic Attenuation Technique for the In Vivo Determination of Bone Mineral Content. Ph.D. Thesis, University of Wisconsin, Madison, Wisconsin.

Judy, P.F., M.G. Ort, K. Kianian and R.B. Mazess 1971. Developments in the dichromatic attenuation technique for the determination of bone mineral content in vivo. USAEC Progress Report COO-1422-97.

Judy, P.F., J.R. Cameron, K.M. Jones and M.G. Ort 1972. Determination of vertebral bone mineral mass by transmission measurements. USAEC Progress Report COO-1422-126.

Roos, B., B. Rosengren and H. Sköldborn 1970. Determination of bone mineral content in lumbar vertebrae by a double gamma-ray technique. In: J.R. Cameron (ed) Proc. Bone Measurement Conference. U.S. Atomic Energy Comm. Conf. 700515. U.S. Dept. of Commerce (CFSTI), Springfield, Va., pp. 243-254.

PRECISION AND ACCURACY OF
PHOTON ABSORPTIOMETRY

James Hanson

Department of Radiology (Medical
Physics), University of Wisconsin
Hospitals, Madison, Wisconsin

Introduction

Measurements of bone mineral with photon absorptiometry must be precise and accurate. Two techniques are commonly used, the single photon technique (SAT) and the dual photon technique (DAT). Theoretical calculations of expected precision have been done for the two techniques (Watt, 1974; Mazess et al., 1974). When using the optimal photon energies, a SAT point measurement is more precise in terms of counting statistics. This is not an absolute limitation of the DAT since its radionuclide activity and the number of measurements can be increased. The accuracy of absorptiometry for bone mineral measurements, when correlated to the ash weights of bone, has been reported (Sorenson and Cameron, 1967). For in vivo measurements of bone mineral, the accuracy is sensitive to the extent of the variations in the composition of the soft tissue.

ACCURACY

SAT – Uniform Soft Tissue Composition

In vivo photon absorptiometry measurements are corrected by a calibration constant derived from measurements made on a calibration standard with known masses. If the tissue equivalent material used in the calibration is different from the in vivo composition then a small inaccuracy is encountered. The problem associated with a non uniform distribution of soft tissue, i.e. a different composition of soft tissue over the bone than that where an I_0^* reading is made, is dealt with later. The assumption that the soft tissue composition is uniform throughout is made now in order to separate two different problems. This inaccuracy is only dependent on the photon energy used and the difference between the composition of the calibration standard and the individual being measured. For longitudinal studies within one institution on an individual, this inaccuracy is not relevant assuming that the individual's soft tissue composition (STC) has not changed. When comparing measured bone mineral results between institutions, this inaccuracy can be reduced by having the same calibration standard at each institution. When comparing different individuals' calibrated bone mineral content within the same institution, the inaccuracy of the comparison will depend on the difference in their STC. The comparison of the ratio of the non calibrated bone mineral content values for the two individuals would be accurate. The elimination of this problem would require

a calibration standard for each individual measured, based on his particular STC. This obviously impractical and not necessary as the inaccuracies are smaller than the errors attributed to precision.

Theory

For the calibraiton, a linear relation is assumed, i.e. true mass of bone mineral = K (calibration constant) x measured bone mineral constant, where the zero order coefficient is assumed to be zero. The calibration standard has a certain STC with a fat fraction, f. When measuring individuals, the use of the calibration constant, K, presupposes that their STC is identical to that of the standard, but this is not true. It is this assumption (that the individual's STC is the same as the standard's) that results in an inaccuracy. The measured bone mineral is

$$m_b = K \ln I_o^*/I \tag{1}$$

where $K = \rho_b/\mu_b\rho_b - \mu_{st}\rho_{st}$.

The mass attenuation coefficient, μ_{st}, and the density, ρ_{st}, are for the calibration standard with a fat fraction of f.

The individual's true STC is a fat fraction of f' so that the actual bone mineral is

$$m_b^* = \frac{\rho_b \ln I_o^*/I}{\mu_b\rho_b - \mu_{st}^*\rho_{st}^*} \tag{2}$$

where μ_{st}^* and ρ_{st}^* are for a STC with a fat fraction of f'. The calibrated bone mineral measurement, m_b, will never equal the actual bone mineral, m_b^*, unless the calibration standard's fat fraction, f, is equal to the individual's fat fraction, f'.

The calibrated mass related to the actual mass by

$$\frac{m_b}{m_b^*} = \frac{\mu_b\rho_b - \mu_{st}^*\rho_{st}^*}{\mu_b\rho_b - [(\mu_{st}^* + (f' - f)(\mu_\ell - \mu_f)(\rho_{st}^* + (f' - f)(\rho_\ell - \rho_f)]} \tag{3}$$

where μ_ℓ and μ_f are mass attenuation coefficients and ρ_ℓ and ρ_f are densities of lean and fat tissue respectively. By weighting the mass attenuation coefficients of lean and fat tissue according to their mass fractions, μ_{st} is related to μ_{st}^*, similiarly, ρ_{st} relates to ρ_{st}^* by the weighted densities of fat and lean tissue.

Equations 1 and 2 are two different ways of finding the bone mineral of the same bone within the same soft tissue.

The only difference comes in the denominator where a value of μ_{st} and ρ_{st} are needed. Equation 2 has the actual values of μ_{st}^* and ρ_{st}^*; Equation 1 has

the values of the calibration standard, μ_{st} and ρ_{st}. If the calibration standard is fatter than the true soft tissue then the denominator of Equation 1 will be larger than that of Equation 2 and m_b will be less than m_b^*.

Calculated Results

Figure 1 shows the absolute error in bone mineral content as a function depending on the STC's fat fraction for the SAT with ^{125}I as the photon source. For the SAT with a uniform distribution of STC, the difference between the measured and the actual bone mineral content is small. The actual bone mineral in Figure 1 is 1.0 g/cm^2 with a uniform thickness of 4.717 cm of soft tissue. The actual STC is 15% fat so that when a calibration standard with a .15 fat fraction is used, the calibrated or apparent bone mineral is equal to the actual bone mineral.
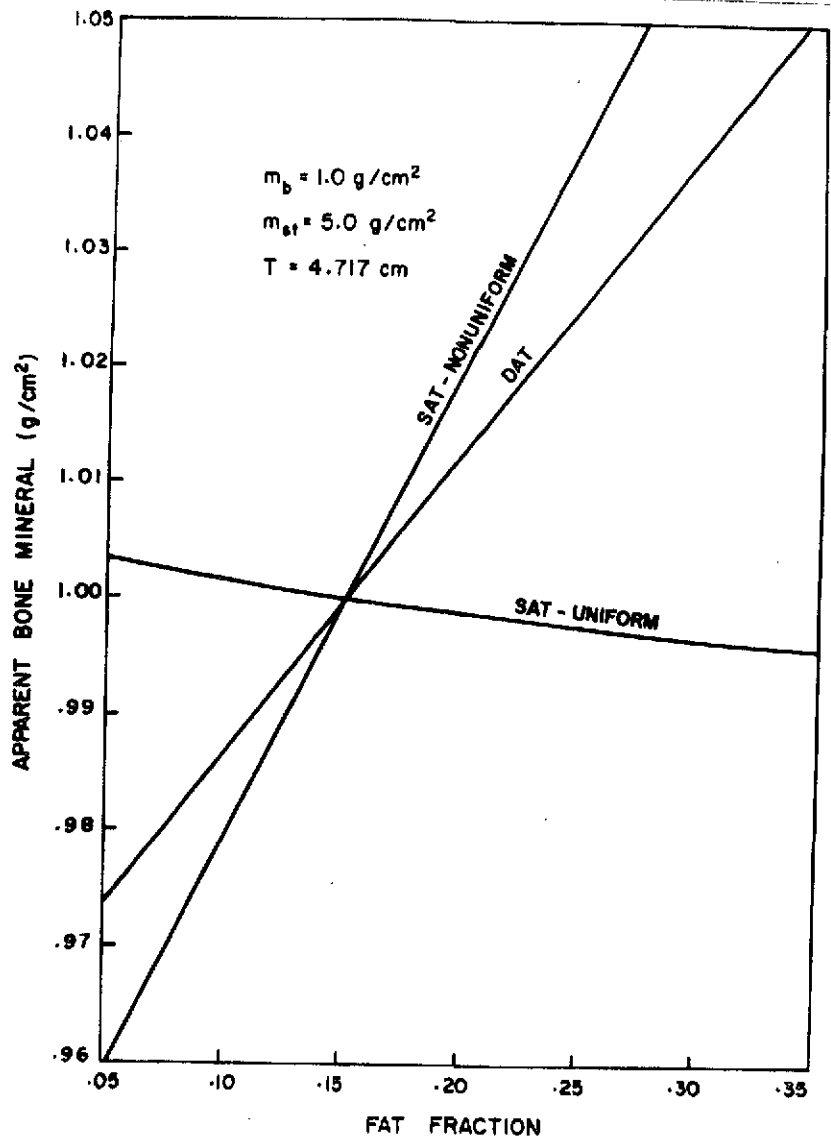

$m_b = 1.0$ g/cm^2

$m_{st} = 5.0$ g/cm^2

$T = 4.717$ cm

SAT - NONUNIFORM

DAT

SAT - UNIFORM

APPARENT BONE MINERAL (g/cm^2)

FAT FRACTION

Figure 1: The deviation from the actual mineral content caused by fat for the SAT with ^{125}I and the DAT with ^{125}I/[241]Am.

If the actual bone mineral is within a STC of 15% fat and the calibration standard is for 35% fat then an inaccuracy of .40% is made in the calibration of the measured value. Over the normal range (5-35% fat) of STC's the maximum error would be .70%. As shown in Equation 3 the error will be dependent on 1) the difference in fat fraction between the individual measured and the calibration standard and 2) the photon energy used.

SAT - Non Uniform STC

When the STC is non uniform (i.e. the fat fraction adjacent to bone is different from that over the bone), the accuracy of a SAT measurement depends on a knowledge of the variation of the STC over the limb. Zeitz (1972) reported 15% variations in SAT measurements with ^{125}I as the photon source depending on the location in the soft tissue mass surrounding the bone of the I_0^* measurement. For accurate SAT measurements, the I_0^*'s must be measured in soft tissue of the same composition as that over the bone. An I_0^* measurement in soft tissue fatter than that over the bone will result in a measured bone mineral greater than the actual bone mineral. Wooten and Judy (1973) have investigated this problem.

Theory

The inaccuracy due to different I_0^* values is expressed as two different bone mineral measurements; one being the actual bone mineral where the I_0^* measurement is made in the soft tissue where the STC is the same as that over the bone; the other being the inaccurate measurement where the I_0^* measurement is made in soft tissue with a composition different from that over the bone. The actual bone mineral is

$$m_b^* = K \ln I_0^{*'}/I \tag{4}$$

where $I_0^{*'} = I_0 \exp(-\mu_{st}^* \rho_{st}^* T)$ and μ_{st}^* and ρ_{st}^* are for the STC over the bone with a fat fraction of f' and T is the thickness in centimeters. The inaccurate bone mineral measurement is

$$m_b = K \ln I_0^*/I \tag{5}$$

where $I_0^* = I_0 \exp(-\mu_{st} \rho_{st} T)$ and μ_{st} and ρ_{st} are for a STC with a fat fraction of f. The calibration constant, K, is from a calibration standard with a STC the same as the actual STC, i.e. the calibration standard has a fat fraction of f'. The calibrated bone mineral measurement relates to the actual bone mineral by

$$m_b = m_b^* + K[-(\mu_{st}^* + \Delta f(\mu_\ell - \mu_f))(\rho_{st}^* + \Delta f(\rho_\ell - \rho_f)T) + \mu_{st}^* \rho_{st}^* T] \tag{6}$$

where $\Delta f = f'-f$ and μ_ℓ and μ_f are the mass attenuation coefficients and ρ_ℓ and ρ_f are the densities of lean and fat tissue respectively, and T is the thickness. The calibration constant, K, has the value of $\rho_b/\mu_b\rho_b - \mu_{st}^*\rho_{st}^*$, which relates to the true STC. If I_0^* is measured in soft tissue of the same composition as that over the bone, then $\Delta f = 0$ and $m_b = m_b^*$. If the I_0^* measurement is made in a STC fatter than that over the bone then m_b is greater than m_b^*.

Calculated Results

Figure 1 shows the absolute error in bone mineral content as a function depending on the composition of the soft tissue where the I_0^* measurement is made for the SAT with ^{125}I as the photon source. The actual bone mineral content is 1.0 g/cm^2 and the STC over the bone is 15% fat. When the I_0^* measurement is made in soft tissue with a fat fraction of .15 then the measured value is equal to the actual value. The limb being measured is viewed as a bone covered with a constant thickness of soft tissue which has different composition at different positions along side of the bone. If the I_0^* measurement is made in STC with a fat fraction of .35 then the measured bone mineral content is 1.08 g/cm^2. Over the normal range of STC (5-35% fat), the maximum error shown in Figure 1 would be 12%.

DAT - Uniform STC

The dual photon absorptiometry technique (DAT) has an inaccuracy which depends on a knowledge of the STC over the bone. An accurate solution of a DAT measurement requires knowing accurately the mass attenuation coefficients ($\mu_{st,1}$ and $\mu_{st,2}$) of the soft tissue at both photon energies. If the values of $\mu_{st,1}$ and $\mu_{st,2}$ used in solving a point DAT measurement are different from the true values for the soft tissue over the bone, then the measured bone mineral is inaccurate. This inaccuracy is significant.

Since the DAT can be used to measure soft tissue composition (Preuss and Schmonsees, 1972; Mazess et al., 1970), this inaccuracy can be reduced when measurements of the soft tissue composition adjacent to the bone are used to estimate the composition over the bone. For an uniform soft tissue distribution, this inaccuracy is reduced to the variation that occurs for measurements of the soft tissue composition. Accurate measurements of STC at any point adjacent to the bone will represent the composition over the bone.

Theory

The mass of bone mineral for the DAT is expressed as

$$m_{bm} = \frac{\mu_{st,2} \ln\left(\frac{I_{0,1}}{I_1}\right) - \mu_{st,1} \ln\left(\frac{I_{0,2}}{I_2}\right)}{\mu_{st,2}\mu_{bm,1} - \mu_{st,1}\mu_{bm,2}} \qquad (7)$$

where the only measured values are $I_{0,K}$ and I_K which are the unattenuated and attenuated intensities of the Kth photon energy respectively. The subscripts 1 and 2 denote the photon energy. Accurate values of the mass attenuation coefficients of soft tissue must be known. If the actual STC is uniform and has a fat fraction of f' or mass attenuation coefficients of $\mu_{st,1}^*$ and $\mu_{st,2}^*$ then the actual bone mineral is

$$m_{bm}^* = \frac{\mu_{st,2}^* \ln\left(\frac{I_{0,1}}{I_1}\right) - \mu_{st,1}^* \ln\left(\frac{I_{0,2}}{I_2}\right)}{\mu_{st,2}^*\mu_{bm,1} - \mu_{st,1}^*\mu_{bm,1}} \qquad (8)$$

Equation 7 can be considered as the inaccurate measurement where the transmittance is the same as Equation 8 and the STC is inaccurately assumed to have a fat fraction of f with mass attenuation coefficients of $\mu_{st,1}$ and $\mu_{st,2}$. Equation 7 can be expressed in terms of differences in fat fractions between the actual and assumed value $(f' - f)$ and the actual parameters

$$m_{bm} = \frac{(\mu_{st,2}^* + K_2)\ln\left(\frac{I_{0,1}}{I_1}\right) - (\mu_{st,1}^* + K_1)\ln\left(\frac{I_{0,2}}{I_2}\right)}{D + (\mu_{bm,1}K_2 - \mu_{bm,2}K_1)} \qquad (9)$$

where $D = \mu_{st,2}^*\mu_{bm,1} - \mu_{st,1}^*\mu_{bm,2}$ and $K_1 = (f' - f)(\mu_{\ell,1} - \mu_{f,1})$ and $K_2 = (f' - f)(\mu_{\ell,2} - \mu_{f,2})$ where μ_ℓ and μ_f are the mass attenuation coefficients of fat and lean tissue at the photon energy denoted by the numeric subscript. If the assumed values of $\mu_{st,1}$ and $\mu_{st,2}$ are for a STC fatter than the actual values, i.e. $f > f'$, then the measured bone mineral is greater than the actual bone mineral.

As an alternate approach, the mass of bone mineral can be expressed in terms of the ratio of $\mu_{st,1}/\mu_{st,2}$, R;

$$m_{bm} = \frac{1}{\mu_{bm,1} - \mu_{bm,2}R}\left[\ln\left(\frac{I_{0,1}}{I_1}\right) - R\ln\left(\frac{I_{0,2}}{I_2}\right)\right] \qquad (10)$$

Values of R are determined by solving Equation 10 for R when the photon beams intercept only soft itssue, i.e. $m_{bm} = 0$, so that

$$R = \frac{\ln\ I_{0,1}/I_1}{\ln\ I_{0,2}/I_2} \qquad (11)$$

For the case of uniform STC, accurate measurements of the mass of bone mineral are made by using Equation 10 and having measured R in the soft tissue.

Calculated Results

Figure 1 shows the absolute error in bone mineral as a function depending on the STC's fat fraction for the DAT with the dual source of $^{125}I/^{241}Am$. The actual bone mineral is 1.0 g/cm^2 in a STC of 15% fat. If the measured bone mineral is calculated with assumed values of $\mu_{st,1}$ and $\mu_{st,2}$ of a STC different than that of the actual STC, then the measured bone mineral is inaccurate. Referring to Figure 1, if the STC is assumed to be 35% fat, and mass attenuation coefficients for this are used, then the measured bone mineral will be 1.05 g/cm^2. The maximum error over the normal range of STC's (5-35% fat) is 7.8%.

DAT - Non Uniform STC

For a non uniform STC the uncertainty is the same as with a uniform STC but it becomes variable, depending on the position over the bone and the degree of non uniformity. Using Equations 10 and 11 the accuracy for non uniform STC is determined by the ability of an averaged R measurement adjacent to the bone to accurately represent the soft tissue composition over the bone.

PRECISION

SAT

The precision, or reproducibility, of the SAT has been reported by Judy (1970). The precision of a point measurement is related to counting statistics, photon energies and the amount of bone and soft tissue being measured. For a given amount of bone and soft tissue there is an optimal photon energy. The basic model (Judy, 1970) has been used to express the expected precision of a point measurement of bone mineral in various amounts of bone and soft tissue for different photon energies.

Theory

The mass of bone mineral for the SAT is

$$m_b = K \ln I_o^*/I \tag{12}$$

where $K = \rho_b/\mu_b\rho_b - \mu_{st}\rho_{st}$. The precision of Equation 12 only depends on counting statistics.

For the general case $X = f(u,v)$ the variance of x is given by

$$\sigma_x^2 = \left(\frac{\partial x}{\partial u}\right)^2 \sigma_u^2 + \left(\frac{\partial x}{\partial v}\right)^2 \sigma_v^2 \tag{13}$$

where u and v are uncorrelated parameters.

The expected precision for determining the bone mineral mass from Equation 12 is from the propagation of errors expression given by

$$\sigma_{m_b}^2 = \left(\frac{\partial m_b}{\partial I_o^*}\right)^2 \sigma_{I_o^*}^2 + \left(\frac{\partial m_b}{\partial I}\right)^2 \sigma_I^2 . \tag{14}$$

This is the expected variance of bone mineral as a function of counting statistics where the variance of I_o^* and I are determined by Poisson statistics. The assumption that in a clinical situation repeated I_o^* measurements are made allows the removal of variations due to I_o^* so that

$$\sigma_{m_b}^2 = \frac{K^2}{I}$$

where $\sigma_I^2 = I$. The relative error function, REF, adopted by Judy is

$$REF = \frac{\sqrt{\sigma_{m_b}^2}}{m_b} \cdot \sqrt{I_o} = \frac{K}{m_b} \sqrt{\frac{I_o}{I}} \tag{15}$$

which provides a comparative index independent of count rate.

The precision, or reproducibility, of the DAT has been investigated by Judy (1970), Wooton (1971), Watt (1973) and Hanson (1973). The precision of a point measurement is related to counting statistics, photon energies and the amount of tissue being measured. For a given amount of bone and soft tissue there is an optimal photon energy pair. The expected precision of a point DAT measurement has been expressed for various amounts of bone and soft tissue for different pairs of photon energies.

Theory

The mass of bone mineral, m_{bm}, can be expressed in terms of the attenuation coefficients and the natural logarithm of the ratio of initial to transmitted counts

$$m_{bm} = \frac{\ln\left(\frac{I_{0,1}}{I_1}\right)\mu_{st,2} - \ln\left(\frac{I_{0,2}}{I_2}\right)\mu_{st,1}}{\mu_{bm,1}\mu_{st,2} - \mu_{bm,2}\mu_{st,1}} \tag{16}$$

The assumption that the compositions of bone mineral and soft tissue are invariant makes the attenuation coefficients in Equation 16 constant. With constant values of attenuation coefficients the precision of Equation 16 only depends on counting statistics.

For the general case of $X = f(u,v)$ the variance of x is given by

$$\sigma_x^2 = \left(\frac{\partial x}{\partial u}\right)^2 \sigma_u^2 + \left(\frac{\partial x}{\partial v}\right)^2 \sigma_v^2 \tag{17}$$

where u and v are uncorrelated variables.

The expected precision for determining the bone mineral mass from Equation 16 is from the propagation of errors expression given by

$$\sigma_{m_{bm}}^2 = \left(\frac{\partial m_{bm}}{\partial T_1}\right)^2 \sigma_{T_1}^2 + \left(\frac{\partial m_{bm}}{\partial T_2}\right)^2 \sigma_{I_K}^2 \tag{18}$$

This is the expected variance of bone mineral as a function of counting statistics where T_1 and T_2 are $\ln(I_{0,1}/I_1)$ and $\ln(I_{0,2}/I_2)$ respectively. The variances of T_1 and T_2 are determined by Poisson statistics and are given by

$$\sigma_{T_K}^2 = \left(\frac{\partial T_K}{\partial I_{0,K}}\right)^2 \sigma_{I_{0,K}}^2 + \left(\frac{\partial T_K}{\partial I_K}\right)^2 \sigma_{I_K}^2 \tag{19}$$

where the subscript K denotes the general case.

Equation 4 reduces to

$$\sigma_{T_K}^2 = \frac{1}{I_{0,K}} + \frac{1}{I_K}$$

Since $\sigma_I^2 = I$. Solving Equation 18 in terms of initial intensities, attenuation coefficients, and mass of bone mineral and soft tissue allows the prediction of the expected precision for a given amount of bone mineral and soft tissue for any pair of photon energies.

The expected precision is expressed by the relative error function, REF, which is

$$REF = \frac{\sqrt{\sigma_{m_{bm}}^2}}{m_{bm}} \cdot \sqrt{I_o}$$

where both initial intensities are equal to I_o.

Results

Figure 2 shows the REF for the SAT and DAT as a function of increasing bone and soft tissue for different radionuclides. The REF is nearly always lower for the SAT than DAT; at least for this particular combination where the soft tissue mass is five times the mass of bone. For certain anatomical sites there is an optimal technique. The SAT with ^{125}I has the lowest error for thin section (i.e. forearms); for larger section (i.e. upperarms) the SAT with ^{241}Am is optimal. For the DAT ^{109}Cd is optimal for fingers; $^{125}I/^{241}Am$ and ^{133}Xe are optimal for radius and ulna; and ^{153}Gd is optimal for larger bones.

Conclusion

The precision of a bone mineral measurement made at different anatomical sites can be optimized by selecting the proper technique. The requirement for constant soft tissue thickness puts a physical limitation on the SAT. The DAT is suboptimal to the SAT at all tissue thicknesses. However, the suboptimal conditions of the DAT is not an absolute limitation which can be remedied by using sources of higher activity or by otherwise increasing the counts collected. In establishing an optimal condition accuracy must be considered. The DAT will more accurately predict bone mineral content than the SAT since variations in the bone mineral content which result from monitoring I_o^* at different soft tissue locations will be greater than variation in bone mineral content associated with the estimation of the soft tissue composition over the bone from the estimated tissue composition adjacent to the bone.
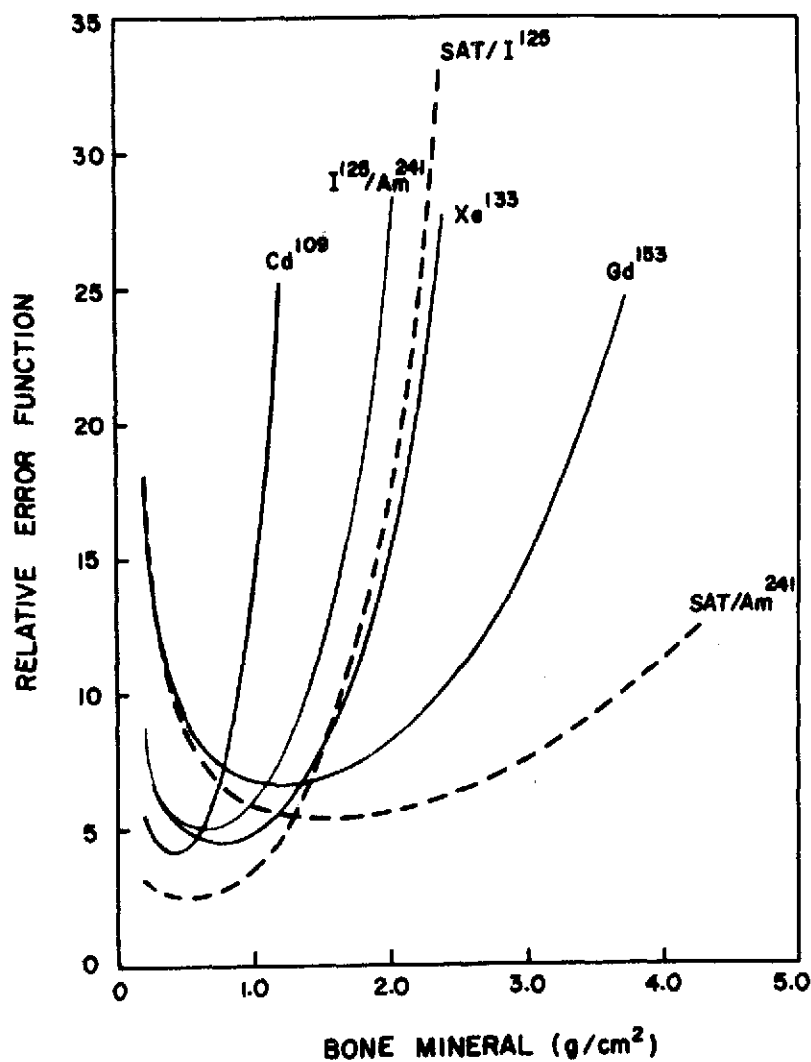
Figure 2: The relative error function for four dual photon sources (solid lines) and two single photon sources (dashed lines).

References

Hanson, J.A. (in press). Analysis of ^{153}Gd and of ^{125}I/^{241}Am sources. In: R.B. Mazess (ed) Proc. Intern. Conf. on Bone Mineral Measurement, U.S. Govt. Printing Office, Washington, D.C.

Judy, P.F. 1970. Theoretical accuracy and precision in the photon attenuation measurement of bone. In: J.R. Cameron (ed) Proc. Bone Measurement Conference. U.S. Atomic Energy Comm. Conf. 700515. U.S. Dept. of Commerce (CFSTI), Springfield, Va.

Judy, P.F. 1971. A Dichromatic Attenuation Technique for the In Vivo Determination of Bone Mineral Content. Ph.D. Thesis in Radiological Sciences, University of Wisconsin, Madison, Wisconsin.

Mazess, R.B., J.R. Cameron and J.A. Sorenson 1970. Determining body composition by radiation absorption spectrometry. Nature 228: 771-772.

Mazess, R.B., C.R. Wilson, J. Hanson, W. Kan, M. Madsen, N. Pelc and R. Witt 1974. Progress in dual photon absorptiometry of bone. In: Symposium on Bone Mineral Determinations, Stockholm/Studsvik.

Preuss, L.E. and W. Schmonsees 1972. ^{109}Cd for compositional analysis of soft tissue. Int. J. Appl. Radiation Isotopes 23: 9-12.

Sorenson, J.A. and J.R. Cameron 1967. A reliable in vivo measurement of bone mineral content. J. Bone Joint Surg. 49(A): 481.

Watt, D.E. (in press). Optimum photon energies for the measurement of bone mineral and fat fractions. Brit. J. Radiol.

Wooten, W.W. 1971. Bone Densitometry: The Two Photon Technique and Fat Content of the Bone. M.S. Thesis, University of California, Los Angeles, California.

Wooten, W.W., P.F. Judy, and M.A. Greenfield 1973. Analysis of the effects of adipose tissue on the absorptiometric measurement of bone mineral mass. Invest. Radiol. 8: 84-87.

Zeitz, L. 1972. Effect of subcutaneous fat on bone mineral content measurement with the "single-energy" photon absorptiometry technique. Acta Radiologica 11: 401-410.

DESCRIPTION OF A DUAL PHOTON ABSORPTIOMETRY
SYSTEM FOR THE DETERMINATION
OF BODY COMPOSITION IN VIVO

Robert M. Witt

Department of Radiology (Medical Physics),
University of Wisconsin Hospitals, Madison,
Wisconsin

Introduction

Dual photon absorptiometry technique has been applied to the determination of percentage of fat (Sorenson and Cameron, 1964; Schmonsees and Preuss, 1971), fluid shifts (Mazess, 1970) and body composition (Mazess et al., 1970; Mazess 1972). In cooperation with the Department of Surgery, a dual photon absorptiometry system was designed to be used in hospital rooms, the Trauma and Life Support Center (TLC) and in the isolation burn ward for the measurement of body fluid changes in patients. The total system is composed of commercial and custom design components. The system can be divided into various major sections; the radiation detector and collimator including the detector high voltage supply; the digital counting and data acquisition section; and the mechanical scanner and support arm including the scanner control circuitry, Figure 1. The dual photon source is described in a separate report (Witt and Hanson, 1974).

Radiation Detector-Collimator Assembly

The radiation detector and collimator assembly for the clinical system for measuring body composition is composed of commercial components enclosed in a custom designed housing. The radiation detector is a 3 mm thick x 1 cm diameter sodium iodine thallimum activated crystal (NaI(Tℓ)) enclosed in a moisture tight crystal housing with a .025 mm thick aluminum entrance window (Harshaw Type M10HE3M). This thickness detector with a detection efficiency greater than 99% at both 30 keV and 60 keV is suitable for detecting the low energy photons emitted from the combined $^{125}I/^{241}Am$ source.

The scintillation pulses from the crystal are detected by 1.92 cm diameter x 10.00 cm long photomultiplier tube with an integral potted voltage divider (RCA Type 4516/2B). The voltage divider which was designed for operating the cathode at negative high voltage was modified to operate with the cathode at ground and the anode at a positive high voltage (V_{max} = 1500 VDC). The shield from the anode lead which was normally connected to the tube housing was removed so that the housing could be grounded in common with the cathode and the crystal housing.

A layer of silicone grease (Dow Corning 200, viscosity 600,000 cs.) optically couples the crystal housing light pipe to the photomultiplier tube (PMT) photocathode glass entrance window. To maintain pressure on the two

surfaces the PMT and crystal housing are spring loaded into a 17.8 cm long x
2.8 cm diameter integral detector housing and collimator. The brass collimator
is 3.6 cm long with a maximum aperture of 1.27 cm and press fits into the
tubular housing. The collimator is threaded and four different inserts with
hole diameters of 3 mm, 4.8 mm, 6 mm and 8 mm can be screwed into it to deduce
the aperture size.

A mini-box attached to the voltage divider end of the detector tube housing
contains the PMT pulse coupling network and provides the mounting surfaces for
the BNC signal and the MHV high voltage connectors. The pulse coupling network
is a standard design and was potted in silicone rubber to minimize voltage
breakdown between the components.

The detector high voltage supply contained in a 2 width NIM module (Nuclear
Data Model ND-537) has a maximum output voltage of 2250 VDC and a maximum
current of 1 mA. The voltage can be adjusted in increments of 250 volts and
the added 10-turn potentiometer allows precise continuous adjustment over each
250 VDC step. The high voltage normally applied to the detector is about
+ 900 VDC and the voltage divider network current is 100 µA.

A typical spectrum of the dual source for this custom assembled detector,
Figure 2, had a FWHM resolution of 38% for the low energy channel and 23% for
the high energy channel. One should recall that the ^{241}Am spectrum from a
NaI(Tℓ) detector has an iodine escape peak which occurs for approximately 15% of
the detected photons and should be subtracted from the events under the ^{125}I
total energy peak. A detailed discussion of the ^{241}Am induced iodine escape
peak for this system appears as a separate report (Witt, 1974).

Digital Counting and Data Acquisition Section

The digital counting and data acquisition section also consists of a combi-
nation of custom designed and built components plus commercial components. All
data counting and acquisition components are contained in NIM standard modules
(NIM, 1969), and are powered by a 90 VA NIM standard relay rack mounted power
bin. The magnetic tape recorder which is mounted on drawer slides also fits in
a standard 19 inch relay rack. The NIM power bin and the tape recorder are
mounted in a 43 cm x 56 cm x 80 cm high relay cabinet (Bud heavy duty Model
CR 1737) which is mounted on four 7.5 cm swivel casters. The cabinet is quite
portable and can be easily moved to hospital rooms and the TLC unit by one person.

Pulse Counting Section

For this description the pulse counting section will be considered to begin
after the voltage pulse generated by the pulse coupling network of the PMT. The
pulse counting section which has been described in more detail in previous reports
(Sitzman et al., 1971, Witt et al., 1972) is composed of an amplifier which shapes
and amplifies the detector pulses; two single channel analyzers (SCA) which
select only certain amplitude voltage pulses; two buffered scalers which count
the pulses from the SCA's; a 100 kHz presetable timer and two logic control cir-
cuits which allow the counting system to accummulate counts for a fixed period of
time. All of the above components plus a + 5 VDC regulated power supply are
contained in a three width NIM module.

Deadtime

Since the deadtime of the pulse counting system previously has been estimated to be large ($\sim$5 μsec)(Witt, 1972), the deadtime was again measured for the total system (detector-to-SCA's). The estimated deadtime was determined in two ways: 1) by the attenuation of the source method; and 2) by modeling the system as a paralyzable counter. The attenuation method gave estimated deadtimes for the two channels of 2.8 μsec and 2.5 μsec. Assuming the system was paralyzable or self-prolonging, at the point of the maximum measured count rate (m_{max}) the deadtime (τ) can be computed from the following equation (Goldanskii et al., 1962)

$$\tau = \frac{1}{e} \cdot \frac{1}{m_{max}}$$

The high incident count rates ($\sim$300,000 counts/sec) necessary for this method were achieved by placing a high activity ^{125}I source (200 mCi) within 6 cm of the entrance aperture of the detector collimator and attenuating the photon beam with copper attenuators .0584 cm thick. The count rate was plotted as a function of the number of attenuators and m_{max} was estimated from the peak of the curve. The maximum detected count rate was about 120,000 counts/sec which implies a deadtime of 3.1 μsec. Both methods of estimating the system deadtime gave comparable results and verifies that the system can be modeled as a paralyzable counter.

Data Acquisition Section

The data acquisition section of the system which has been previously described (Judy et al., 1971) consists of a digital 7-track magnetic tape recorder, a magnetic tape interface, and a parametric data module which allows the entry of code data onto the magnetic tape.

Improvements and Modifications

During the past year the additional commercial components were added to the pulse counting system to make a complete data counting acquisition system. The total system was checked by generating magnetic tapes to see if the custom built dual channel system met design specifications. The total system performed as designed with all data being transferred correctly from the buffers to the magnetic tape. However, it was discovered that the new interface generated BCD coded data which was not equivalent to the original interface. The new magnetic tapes were not compatible with the Madison Academic Computing Center (MACC) Univac 1108 or the newly acquired 1110, and required a computer hardware character translation. The combination of discovering the necessity of a tape translation plus the MACC acquiring the new computer model which lacked hardware translation, delayed final testing of the new unit for the Department of Surgery.

To further make the system equivalent to the commercial system the timer board was redesigned and upgraded from a 60 Hz time base to a 100 kHz crystal time base, Figure 3. As previously described (Witt et al., 1972), the asynchronous start of the timer and scalers causes a maximum error of one clock pulse for

each START operation. The 100 kHz time base reduces this timer error from 0.16 msec to 10 µsec per preset time period.

A last modification was a change in the method to control the overall gain of the system. Normally the amplifier is operated at a fixed gain setting, and the fine adjustment of the PMT high voltage supply controls the system gain. To make the control more sensitive the original 1-turn potentiometer was replaced by an equivalent 10-turn one.

Scanner Assembly and Control Module

Scanner Mechanism

The mechanical scanner for the system is the one that was under construction last year (Heinner et al., 1973). The mechanism as designed has a 18 cm long scan path whose limits are defined by two mechanical stops which activate micro-switches which provide a logic signal to the Scan Control Module. The scanner carriage is drived by a rack (Boston Gear Y64) and a gear (Boston Gear Y64-112) which is mounted on a 115VAC synchronous reversible motor (Hurst Type CA). The carriage moves at 2.327 mm/sec and the scan-to-scan speed variation is ± .5%, and is independent of angle the mechanisms makes with the horizontal place for angles less than 30 degrees.

Subject Limb Platform

The scan mechanism was fitted with a 335 mm x 455 mm x 12.2 mm thick lucite platform. The platform is adjustable and can be moved ± 46.5 mm to either side of the scan path. The platform locks in position by tighting a single handle.

Reach Arm

To adopt the scanner for use as a clinical machine to measure patients in hospital beds and in the TLC unit, the scanner mechanism was mounted on an adjustable reach arm. The reach arm is a modified dental lamp arm which is pivot mounted to the side of the equipment cabinet. The scanner can rotate 180 degress at the end of the arm and the arm can rotate ᴧ120 degress at the cabinet mounting bracket. The limb platform can be raised from a height of 62 cm above the floor to a height of 120 cm above the floor.

Subject Positioning

Two-point Position Marker. A two-point position marker aids the positioning of the subject's limb on the scanning table. The markers were fabricated from two 300 mm long steel engineering scales. The two scales independently slide past each other perpendicular to the scan path in a housing whose zero index remains fix with respect to the scan path. The positions recorded are the distances the end markers of the two scales are located from the scan path. The total distance between the end markers can range from a minimum of 82.5 mm to a maximum of 563.5 mm.

External Anatomical Sites. To position a subject's limb, either the forearm, the arm or the leg, for scanning the length of the limb is measured between two external anatomical sites on the bone and the scan site is selected by taking a fixed fraction of the length. The limb then is placed on the scan platform with the scan site aligned with the scan path and the position markers are moved until they are align with the external bone markers. The two positions are then recorded for subsequent measurements.

For the forearm the limb length is the distance between ulnar styloid process and the olecranon and scan site is the point 1/3 the length measured from the distal end of the ulnus. For the arm the limb length is the distance between the ulnar olecranon and the greater tuberosity of the humerus measured along the posterior of the arm. The scan site is located at the midpoint of the measured length. For the upper limb the anterior of the arm or forearm are placed on the scan platform so that they are perpendicular to the line defined by the scan path. For the lower limb the scan site of the leg is located at a point where the calf muscle mass becomes large (about the middle of the leg) and the distance recorded is measured from the lateral malleolus of the fibula to the scan site. The posterior of the leg is placed on the scan platform perpendicular to the scan path and the gastrocnemius muscle is spread so that an equal amount lies on either side of the tibia.

Subject Radiation Exposure

The radiation exposure rate at the surface of the skin for a dual photon source with a 50 mCi ^{125}I source capsule and a 45 mCi ^{241}Am source capsule was measured with LiF dosimeters (Cameron et al., 1964). The exposure rate at 4.5 mm below the source was 0.13 mR/sec. The total exposure to the limb depends upon its width and the scan speed. For a scan speed of 2.3 mm/sec and typical limb widths of 100 mm for the forearm and 130 mm for the upperarm, the exposures for each scan are 5.7 mR and 7.4 mR respectively. The radiation exposure is confined to a narrow stripe (4 mm wide) on the limb scanned and should be compared to the recommended maximum exposure of 7500 mR per year to the extremities.

Scanner Control Module

A relay control logic circuit was designed and constructed to provide a degree of automatic control over the mechanical scanner and data recording system. The circuit consists of a motor control circuit, a end-of-scan marker circuit and a + 28 VDC filtered relay power supply. The logic circuit design utilizes standard low voltage relay control logic, Figure 4. The motor control circuits are based on those supplied by the manufacturer and reverse the direction of the motor and apply a dynamic D.C. brake whenever the motor is stopped. All components were mounted on a double-sided, vector-type printed circuit board. The circuit board was mounted on standoffs in a 2-width NIM module with the motor power and logic signal connectors mounted on the rear panel; and the power switch, mode selection and control push button switches mounted on the front panel. The entire module obtains its power by a independent A.C. line cord and utilizes no power from the NIM power bin.

The module can be operated in two modes, MANUAL or AUTOMATIC, which are selected by a front panel toggle switch. In the MANUAL MODE the logic pulses from limit switches stops the scan motor, reverses its direction and restarts the scan motor. In the AUTOMATIC MODE the logic signal from the limit switches stops the scan motor, reverses it direction and activates a 3-sec time delay relay. During the 3 second delay a code is written on the magnetic tape signifying the end of a scan, and the scan motor remains stopped. After the time delay elapses the code signal is terminated and power is reapplied to the scan motor. A pair of FORWARD and REVERSE pushbutton switches can override the limit switches causing the identical sequence of control operations. A pair of START-STOP pushbuttons can override the control signals except for the time delay relay which only remains activated for 3 seconds after initiation and then returns to the normal condition.

References

Cameron, J.R., D. Zimmerman, G. Kenney, R. Buch, R. Bland and R. Grant 1964. Thermoluminescent radiation dosimetry utilizing LiF. Health Phys. 10: 25-29.

Goldanskii, V.I., A.V. Kutsenko and M.I. Podgoretskii 1962. Counting Statistics of Nuclear Particles. Hindustan Publishing Corp., Delhi, India.

Hennies, D.A., R.B. Mazess and C.R. Wilson 1973. A compact scanner for measurement of bone mineral content and soft-tissue composition. USAEC Progress Report COO-1422-146.

Judy, P.F., M.G. Ort, K. Kianian and R.B. Mazess 1971. Developments in the dichromatic attenuation technique for the determination of bone mineral content in vivo. USAEC Progress Report COO-1422-97.

Mazess, R.B. 1972. Prediction of body composition from absorptiometric limb scans. USAEC Progress Report COO-1422-122.

Mazess, R.B. 1970. Tissue changes following venous occlusion using photon absorptiometry. USAEC Progress Report COO-1422-76.

Mazess, R.B., J.R. Cameron and J.A. Sorenson 1970. Determining body composition by radiation absorption spectrometry. Nature 228: 771-772.

NIM 1969. Standard Nuclear Instrument Modules. USAEC Report TID-20893 (Rev. 3).

Preuss, L.E. and L.T. Kosnik 1969. Simultaneous analysis of tissue components by x and gamma rays using ^{109}Cd. Journal of Nuclear Medicine 10: 366.

Schmonsees, W.G. and L.E. Preuss 1971. The potential use of ^{109}Cd for dual absorption measurements of soft tissue. In: C.A. Ziegler (ed) Applications of Low Energy X- and Gamma Rays. Gordon and Breach Science Publishers, New York.

Sitzman, J.C., C. Vought and R.B. Mazess 1971. Preliminary report on a dual photon bone mineral measuring instrument. USAEC Progress Report COO-1422-98.

Sorenson, J.A. and J.R. Cameron 1964. Body composition determination by differential absorption of monochromatic x rays. In: *Proc. of Sym. on Low-Energy X- and Gamma Sources and Applications*, AEC Report ORNL-IIC-5, pp. 277-289.

Witt, R.M. 1974. Dual photon absorptiometry measuring systems: corrections to detected photon counts. USAEC Progress Report COO-1422-178.

Witt, R.M., C.E. Vought and R.B. Mazess 1972. Improved version of the dual-channel system to measure bone mineral content. USAEC Progress Report COO-1422-118.

Witt, R.M. and J. Hanson 1974. $^{125}I/^{241}Am$ dual source holder. USAEC Progress Report Holder COO-1422-184.
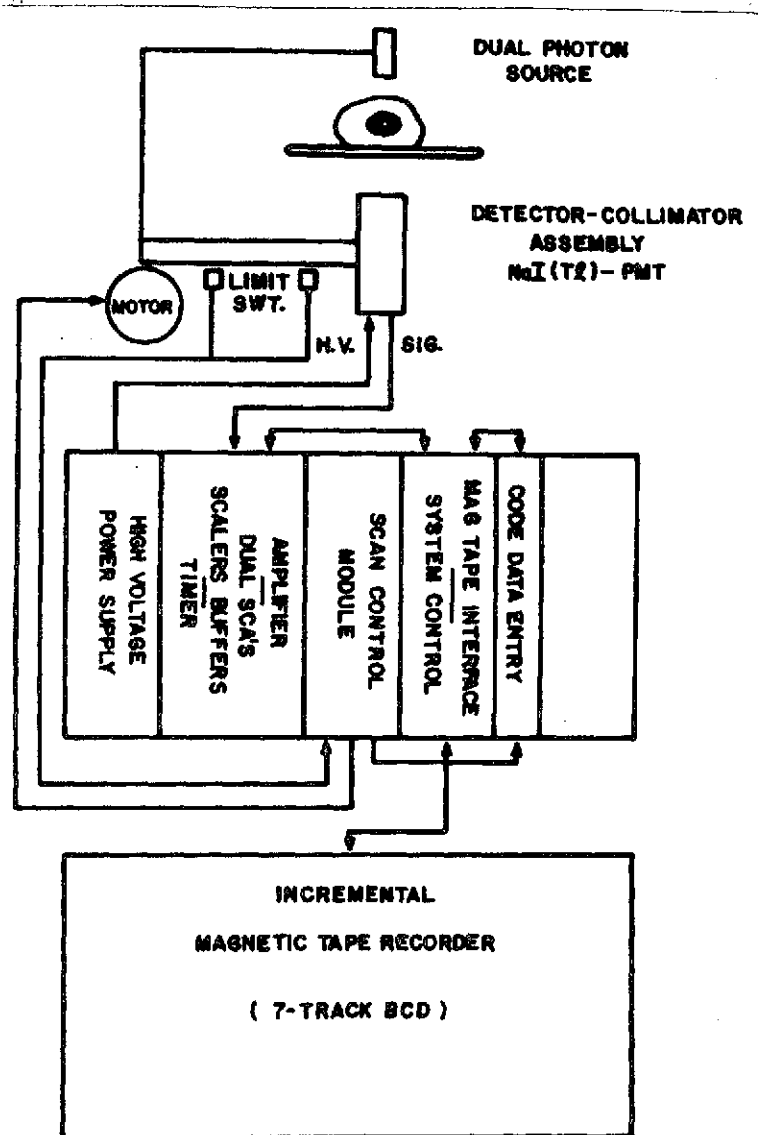
Figure 1: A schematic diagram of the various components which compose the dual photon absorptiometry system for the determination of body composition *in vivo*.
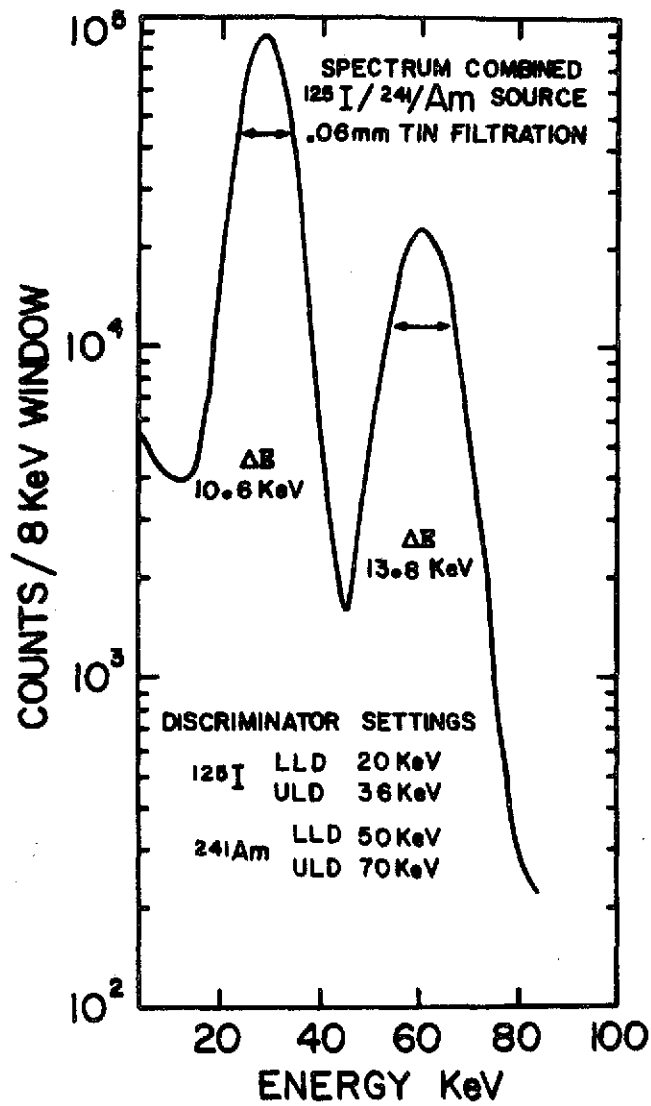
Figure 2: A spectrum of the combined $^{125}I/^{241}Am$ dual photon source made with a 1 cm x 3 mm thick NaI(Tℓ) scintillation crystal detector with the pulse height analyzer window set at 8 keV.

Figure 3: Circuit diagram of a 100 kHz timer with a selectable preset stop and the START-STOP flip-flop controlled by logic signals from the internal Address Control Board.

Figure 4: Circuit diagram of the Scanner Control Module including the relay logic circuit, motor control circuit, and end-of-scan logic signal to the parametric data module.

$^{125}I/^{241}Am$ DUAL SOURCE HOLDER

Robert M. Witt and James Hanson

Department of Radiology (Medical
Physics), University of Wisconsin
Hospitals, Madison, Wisconsin

A new $^{125}I/^{241}Am$ dual source holder was designed and constructed with the active volumes of the source capsules congruent (Figure 1). The holder was machined from brass and the capsules' cavities were designed to contain Union Carbide ^{125}I capsules and Amersham/Searle ^{241}Am capsules (Type X-102). The americium capsule loads from the bottom and the iodine capsule loads from the side. The 0.06 mm thick tin filter loads from the top of the holder and is held in place by a bushing.

The shape of the active volume of the americium capsule is a sphere 3 mm in diameter and the shape of the active volume of the iodine capsule is a disc approximately 2 mm in diameter and 0.4 mm thick. When the iodine capsule is loaded on its side, the disc shaped active volume also is on its side. To make the centers of the active volumes congruent the iodine capsule is placed so that the center of the disc lies over the center of the spherical americium volume.

The congruence of the two active volumes was verified by measuring the differential edge response of the combined sources (Judy, 1971)(Figure 2). For the prototype holder the centers of the active volumes determined from the peak of the differential edge response were separated by 0.15 mm. For the Surgery Scanning System with a linear scan speed of 2.3 mm/sec this separation represents about 1.6% of a data interval.

Advantages of the new holder design are 1) the same tissue mass simultaneously attenuates both sources and eliminates the need to shift the transmission count data arrays (Pelc, 1973); and 2) the source and detector collimation apertures are smaller improving the detection geometry.

A disadvantage of the new holder design is the reduction of the intensity of the americium source. The iodine capsule which lies above the americium source capsule reduces the americium intensity about 6.5%. The addition of the 0.06 mm tin filter reduces the americium intensity by 22.5% for a total reduction of about 25%. To compensate for the reduction of the effective activity of the ^{241}Am source, a new custom built source has been ordered (Amersham/Searle) which will have 60 mCi (nominal activity) loaded into the 3 mm diameter spherical volume.

References

Judy, P.F. 1971. A Dichromatic Attenuation Technique for the In Vivo Determination of Bone Mineral Content. Ph.D. Thesis, University of Wisconsin, Madison, Wisconsin.

Pelc, N.J.   1973.   Absorptiometry using ^{125}I and ^{241}Am to determine tissue composition in vivo.   USAEC Progress Report COO-1422-148.
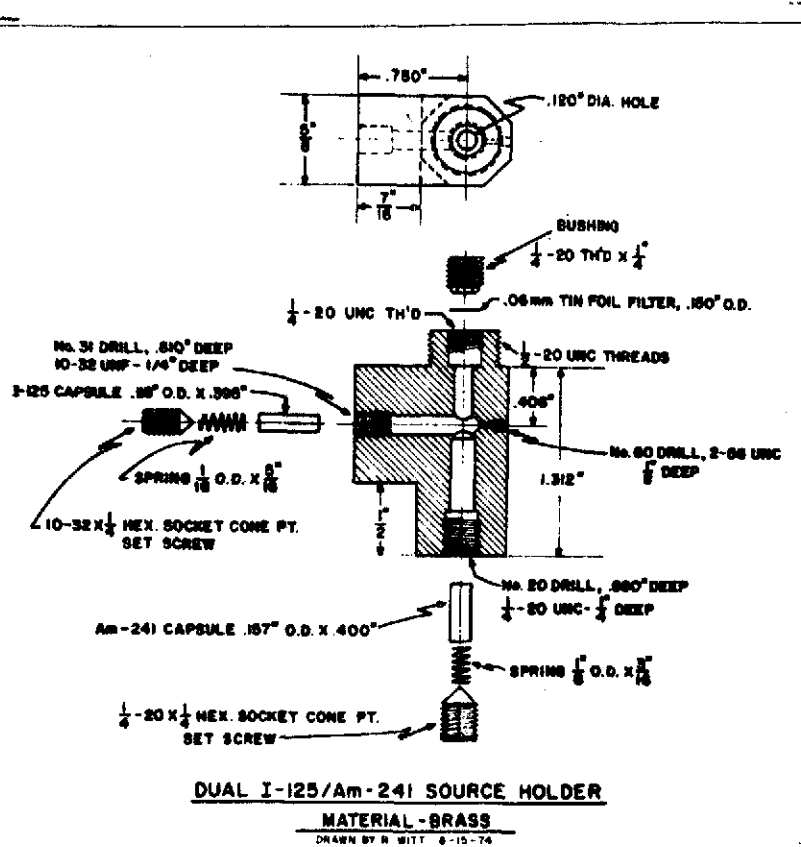

Figure 1:   Drawing of the dual photon source holder designed to hold the active volumes of the ^{125}I and ^{241}Am source capsules congruently.
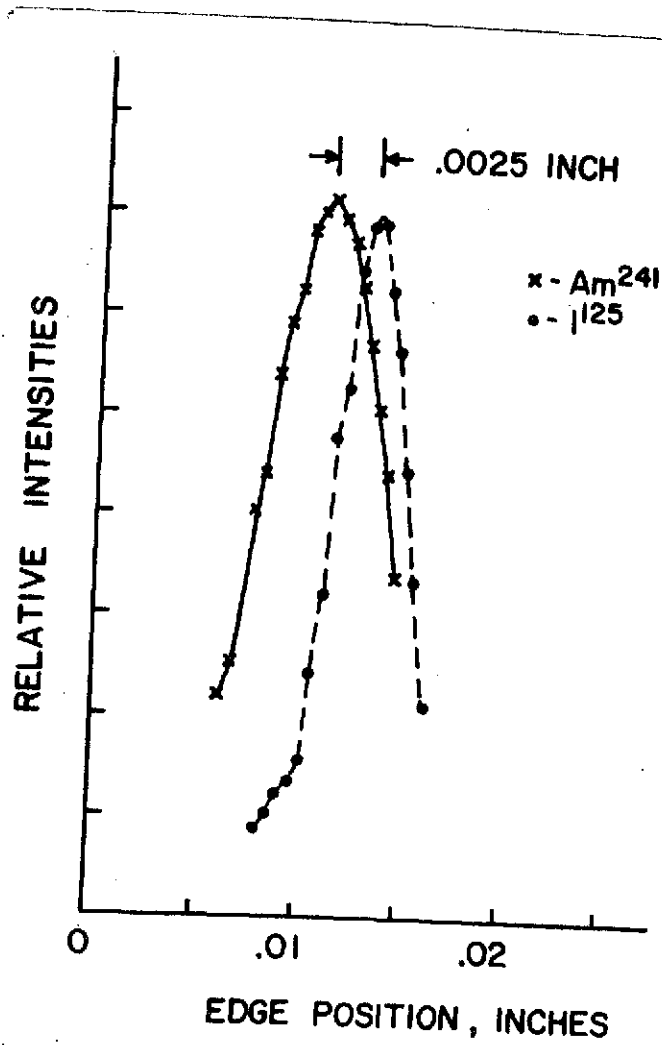
Figure 2: The differential edge response of the combined $^{125}I/^{241}Am$ photon source to determine the separation of the active volumes of the source capsules.